UNIVERSITEIT VAN PRETORIA
UNIVERSITY OF PRETORIA
YUNIBESITHI YA PRETORIA

Development of electrochemical sensing techniques for the determination of activity-composition relations in liquid alloys and slags at 1873 K

by

Jacobus Marthinus Andreas Geldenhuis

Submitted in fulfilment of the requirements for the degree

Philosophiae Doctor

in

Metallurgical Engineering

in the Faculty of Engineering, University of Pretoria, Pretoria,
Republic of South Africa

October 1991

© University of Pretoria

UNIVERSITEIT VAN PRETORIA
UNIVERSITY OF PRETORIA
YUNIBESITHI YA PRETORIA

SYNOPSIS

A plug-type oxygen probe containing a magnesia stabilized solid zirconia electrolyte rod, was developed. This oxygen sensor was evaluated in the Fe-Cr-O system at 1873 K by determining the Raoultian chromium and Henrian oxygen activities of an Fe-Cr alloy which was in equilibrium with pure Cr_2O_3 and a Cr_2O_3-saturated liquid slag respectively. However, the slag reacted with the oxygen probe and therefore, a crucible assembly was developed to prevent direct contact between the slag and the oxygen sensor. The results obtained with this crucible assembly proved that no interaction between the oxygen probe and slag occurred and that the smaller slag/metal interface did not effect equilibrium between the slag and the metal.

The Raoultian chromium activities of the Fe-Cr alloy containing 5 to 25 % chromium determined in this study, deviate negatively from ideal Raoultian behaviour. The oxygen and chromium activities were used to determine the standard free energy change for the formation of solid Cr_2O_3 from the elements at 1873 K, and the value obtained is in good agreement with existing data. Evidently, the plug-type oxygen probes and the redesigned crucible assembly can be used to determine the oxygen activity of an Fe-Cr alloy, in equilibrium with a liquid slag at 1873 K, accurately and reliably. Therefore, these measurements were extended to the determination of the activity of MnO in (MgO-SiO_2-MnO)-slags.

The chemical composition of the equilibrium phases pertaining in (MgO-SiO_2-MnO)-slags saturated with (MnO-MgO) solid solutions and in contact with manganese metal, were determined by microprobe analyses. These results together with the known activity-composition relations of (MnO-MgO) solid solutions at 1873 K, were used to determine the activity of MnO in the slag. This method proved to be reliable and the MnO activities so obtained, could serve as a check for activities determined with the electrochemical technique. Furthermore, the same method could be used for

© University of Pretoria

UNIVERSITEIT VAN PRETORIA
UNIVERSITY OF PRETORIA
YUNIBESITHI YA PRETORIA

the determination of the high temperature phase constitution of the slag when the oxygen potential of the slag/metal system is determined by electrochemical means.

In the course of the determination of the oxygen potential of (MgO-SiO_2-MnO)-slags at 1873 K by means of electrochemical oxygen probes, the magnesia stabilized zirconia solid electrolytes reacted with manganese metal and vapour which had a detrimental influence on the accuracy and reliability of the EMF (electromotive force) measurements. Accordingly, it was illustrated that zirconia solid electrolytes are not suitable for application in slag/metal systems containing manganese metal at 1873 K. Previous workers have shown that thoria solid electrolytes are not attacked by manganese metal at these high temperatures and should consequently be used with the crucible assembly developed in this study, for the determination of activities in (MgO-SiO_2-MnO)-slags at 1873 K.

© University of Pretoria

UNIVERSITEIT VAN PRETORIA
UNIVERSITY OF PRETORIA
YUNIBESITHI YA PRETORIA

SAMEVATTING

'n Prop-tipe suurstofsensor is ontwikkel waarin 'n magnesia-gestabiliseerde sirkonia vastestofelektrolietstafie as sleutelkomponent gebruik word om suurstofpotensiale te meet. Hierdie suurstofsensor is geëvalueer deur die Raoultiese chroom- en die Henriaanse suurstofaktiwiteit in 'n Fe-Cr-legering te bepaal, in die spesiale gevalle waar die legering by 1873 K onderskeidelik in ewewig was met suiwer Cr_2O_3 en 'n Cr_2O_3-versadigde slak. Die Cr_2O_3-versadigde slak het egter met die suurstofsensor gereageer en gevolglik moes 'n kroesopstelling ontwerp word wat verhoed dat die suurstofsensor met die slak in aanraking kom. Uit die resultate wat met hierdie kroesopstelling verkry is, blyk dit duidelik dat geen interaksie tussen die sensor en die slak plaasvind nie. Die kleiner slak/metaalreaksie-intervlak het ook nie die ewewig tussen die slak en die metaal beïnvloed nie.

Die gemete chroomaktiwiteite in 'n Fe-Cr-legering, waarvan die chroomkonsentrasie tussen 5 en 25% gewissel het, toon 'n negatiewe afwyking van ideale Raoultiese gedrag. Die suurstof- en chroomaktiwiteite is gebruik om die standaard vrye-energieverandering vir die vorming van Cr_2O_3 in die vastetoestand by 1873 K te bepaal, en goeie ooreengestemming met reeds gepubliseerde waardes is verkry. Die resultate wat met hierdie studie verkry is, is genoegsame bewys dat die prop-tipe suurstofsensor en die kroesopstelling wat ontwikkel is, met vertroue aangewend kan word om die suurstofpotensiaal in 'n Fe-Cr-legering, wat in ewewig met 'n vloeibare slak by 1873 K is, akkuraat te bepaal. Hierdie tegniek is gevolglik uitgebrei ten einde die aktiwiteit van MnO in die slaksisteem $MnO\text{-}SiO_2\text{-}MgO$ te bepaal.

Die chemiese samestelling van die ewewigsfases van ($MnO\text{-}SiO_2\text{-}MgO$)-slakke wat met (MnO-MgO)-vaste oplossings by 1873 K versadig is en wat in ewewig is met mangaan metaal, is met behulp van 'n mikrosonde bepaal. Die mikrosonde-analise is gedoen op monsters wat so vinnig van die reaksietemperatuur na

© University of Pretoria

UNIVERSITEIT VAN PRETORIA
UNIVERSITY OF PRETORIA
YUNIBESITHI YA PRETORIA

kamertemperatuur afgeblus is, dat die ewewigsfases by die hoë temperatuur behoue gebly het. Hierdie resultate, tesame met die bekende MnO aktiwiteite van die (MnO-MgO)-vaste oplossings wat in ewewig met die slak is, is gebruik om die aktiwiteit van MnO in die slak te bepaal. Hierdie aktiwiteite stem goed ooreen met resultate wat deur vorige navorsers verkry is en gevolglik is daar voldoende bewys dat die tegniek betroubaar en akkuraat is, en daarom ook aangewend kan word om die samestellling van die ewewigsfases in ander slak/metaalsisteme by 1873 K te bepaal. Die MnO-aktiwiteite wat op hierdie wyse bepaal is, kon ook dien as 'n kontrole vir die aktiwiteite wat met behulp van elektrochemiese metings in soortgelyke slaksisteme gemaak is.

Tydens die bepaling van die suurstofpotensiaal by 1873 K in (MnO-MgO-SiO_2)-slakke met behulp van elektrochemiese suurstofsensors, reageer die mangaan metaal wat in ewewig met die (MnO-SiO_2-MgO)-slak is, met die magnesia-gestabiliseerde sirkonia-vastestofelektroliet en beïnvloed die betroubaarheid en akkuraatheid van hierdie EMK (elektromotoriese krag) metings nadelig. Sirkonia-vastestofelektroliete is gevolglik nie geskik vir toepassing in slak/metaalsisteme wat mangaanmetaal by 1873 K bevat nie. Vorige navorsers het egter aangetoon dat toria-basis vastestof-elektroliete nie met mangaan metaal reageer by temperature so hoog as 1823 K nie, en behoort tesame met die kroesopstelling wat in hierdie studie ontwikkel is, gebruik te kan word vir die bepaling van MnO-aktiwiteite in silikaatslakke by 1873 K.

© University of Pretoria

UNIVERSITEIT VAN PRETORIA
UNIVERSITY OF PRETORIA
YUNIBESITHI YA PRETORIA

ACKNOWLEDGMENTS

The author wishes to express his sincere appreciation to the following:

* His advisor, Professor R.J. Dippenaar, for his rigorous guidance, genuine interest and continuous encouragement in the course of this study. His untiring patience is gratefully acknowledged.
* Professor Dr.-Ing. D. Janke of the Max Planck Institüt für Eisenforschung for his valuable clues and discussions regarding experimental techniques at high temperatures, and for offering his service as external examiner.
* Professor M. Iwase of the Kyoto University, Japan, who also performed the task of being external examiner.
* His employer, The Iron and Steel Corporation of South Africa (Iscor Ltd.) for supporting this research and for the opportunity to devote his time entirely to the project.
* The Council for Mineral Technology (Mintek) for providing financial support for this research.
* The University of Pretoria for provision of the laboratory facilities.
* Dr. E.B. Pretorius for constructive discussions and encouragement at a critical stage in this project.
* The Analytical Chemistry Section of Iscor Ltd., headed by Dr. A.J. van Wyk, for carrying out chemical analyses on a multitude of metal samples, and to Dr. J.M. van Wyk for carrying out analyses for the total oxygen content of the metal samples.
* Dr. J. Smuts for his assistance with the SEM analyses of all the slag samples.
* Mr. J.P. van der Merwe for the preparation of the Fe-Cr and Fe-Mn master alloys.
* Mr. S.D. McCollough for his assistance with the quenching experiments.
* Dr. W.H. van Niekerk, a fellow postgraduate student, for fruitful discussions.
* Mr. C.J. van der Westhuizen, an undergraduate student, for general assistance in the laboratory.
* To his late parents, for their love, for being parents, educators and friends, and for all the innumerable ways in which they had contributed to his life and well-being.
* Finally, to his wife, Charloom, for her love, continuous moral support, assistance and mothering his children, Ruan and Ezelle, throughout this study.

© University of Pretoria

UNIVERSITEIT VAN PRETORIA
UNIVERSITY OF PRETORIA
YUNIBESITHI YA PRETORIA

TABLE OF CONTENTS

Page

© University of Pretoria

UNIVERSITEIT VAN PRETORIA
UNIVERSITY OF PRETORIA
YUNIBESITHI YA PRETORIA

Page

© University of Pretoria

UNIVERSITEIT VAN PRETORIA
UNIVERSITY OF PRETORIA
YUNIBESITHI YA PRETORIA

LIST OF FIGURES

Page

Chapter 2

Chapter 3

© University of Pretoria

UNIVERSITEIT VAN PRETORIA
UNIVERSITY OF PRETORIA
YUNIBESITHI YA PRETORIA

Page

© University of Pretoria

UNIVERSITEIT VAN PRETORIA
UNIVERSITY OF PRETORIA
YUNIBESITHI YA PRETORIA

Page

© University of Pretoria

UNIVERSITEIT VAN PRETORIA
UNIVERSITY OF PRETORIA
YUNIBESITHI YA PRETORIA

Page

© University of Pretoria

UNIVERSITEIT VAN PRETORIA
UNIVERSITY OF PRETORIA
YUNIBESITHI YA PRETORIA

LIST OF TABLES

Page

Chapter 3

© University of Pretoria

UNIVERSITEIT VAN PRETORIA
UNIVERSITY OF PRETORIA
YUNIBESITHI YA PRETORIA

Page

Chapter 4

© University of Pretoria

UNIVERSITEIT VAN PRETORIA
UNIVERSITY OF PRETORIA
YUNIBESITHI YA PRETORIA

© University of Pretoria

UNIVERSITEIT VAN PRETORIA
UNIVERSITY OF PRETORIA
YUNIBESITHI YA PRETORIA

LIST OF SYMBOLS

a_i^R	Raoultian activity of component i
γ_i	Raoultian activity coefficient of component i
γ_i^0	Raoultian activity coefficient of component i when $X_i \rightarrow 0$
e_i^j	First order Raoultian interaction coefficient of component j on component i
ρ_i^j	Second order Raoultian interaction coefficients of component j on component i
$\rho_i^{j,k}$	Raoultian cross-product second-order term
X_i	Mole fraction of component i
a_i^H	Henrian activity of component i
f_i	Henrian activity coefficient of component i
e_i^j	First order Henrian interaction coefficient of component j on component i
r_i^j	Second order Henrian interaction coefficient of component j on component i
$r_i^{j,k}$	Henrian cross-product second-order term.
%i	Weight per cent of component i
E	Electromotive force
F	Faraday constant
ΔG°	Standard free energy change
P_{O2}	Partial pressure of oxygen
P_e	A measure of the n-type electronic conduction of a solid electrolyte, defined as the partial pressure of oxygen at which $t_{ion} = 0.5$
R	Gas constant
t_{ion}	Ionic transport number
T	Absolute temperature
< >	Solid
[ ]	Gas
( )	Liquid

© University of Pretoria

UNIVERSITEIT VAN PRETORIA
UNIVERSITY OF PRETORIA
YUNIBESITHI YA PRETORIA

CHAPTER 1

INTRODUCTION

The increasing demand for high alloy and stainless steels world wide, has put great emphasis on the optimization of the applicable production processes to reduce production costs. The price of nickel has increased dramatically over the past few years[1] resulting in an increased price of nickel-chromium stainless steels. This is just one of the factors that has aroused interest in the increased production of manganese containing stainless steels, for instance the SAE 200 series, in which nickel is partly replaced by relatively inexpensive manganese. Manganese ore is freely available on the local market and, with the exciting prospect of the availability of a direct steelmaking route to produce manganese-containing stainless steel, a fundamental knowledge of the activity of manganese oxide in the liquid slag during the smelting stages of the process is required. It is important to quantify the thermodynamic behaviour of the manganese oxide in the slag because this knowledge is required to minimize manganese losses to the slag and to optimize the slag composition. However, there is very little information available in the literature on the thermodynamic properties of this system, and there is consequently much incentive to determine the activity of manganese oxide in the applicable slag systems.

Conventionally, the gas-slag equilibrium technique has been used successfully for the determination of metal-oxide activities in several slag systems in the temperature range 1673 to 1923 K[2][3][4][5][6]. For instance, Pretorius[2] determined the CrO-activity in a (CrO-SiO_2-CaO)-slag at 1773 K. A platinum crucible contained the slag which was equilibrated with a mixture of (CO_2+H_2) gas of known oxygen potential. Equilibrium between the slag, gas and metal is established through the reaction:

© University of Pretoria

$$x\langle \underline{Cr} \rangle_{Pt} + \tfrac{1}{2}[O_2] = (Cr_xO)_{slag}. \qquad [1.1]$$

At equilibrium, the chromium content of the platinum crucible is fixed by the oxygen potential of the gas and the chromium oxide in the slag. The chromium oxide activity was determined by Pretorius[2] as a function of slag composition by the subsequent chemical analysis of the chromium content of the platinum crucible and the chromic oxide content of the slag.

Equilibrium between the gas and slag phases is typically attained after periods varying from 12 to 48 hours when the gas-slag equilibrium technique is used[2][3][4][5][6]. Consequently, it is imperative that the flow rates of the different gases are accurately controlled to ensure that the oxygen potential of the gas is constant and known throughout the equilibration period. However, slags containing volatile components can not be studied by this technique, since the evolution of gases from the slag will change the oxygen potential of the system. Furthermore, the composition of the slag will continuously change as a function of time due to the evaporation of the volatile components.

In recent years however, increasing use has been made of electrochemical methods to determine the oxygen potentials of slag/metal systems. In contrast to the gas-slag equilibrium technique, an inert gas is used as protection gas and the oxygen potential of the melt is fixed by the reaction between slag and metal. In this technique, equilibrium between slag and metal is typically attained after reaction periods varying between 30 and 60 minutes[7][8][9][10] and the oxygen potential of the slag/metal system is determined by means of an electrochemical oxygen concentration cell. Such an electrochemical cell can be expressed as:

$$(P_{O_2})_{ref} \;/\; solid\ electrolyte \;/\; (P_{O_2})_{slag}\ , \qquad [1.2]$$

and is usually comprised of a reference electrode of known oxygen potential, a solid electrolyte tube, for instance magnesia stabilized zirconia, and a liquid slag or metal

© University of Pretoria

electrode of which the oxygen potential has to be determined. However, the type of solid electrolytes available on the market usually exhibit excessive electronic conduction when used in high-temperature slag-metal systems, where a very low oxygen potential prevails[11][12][13][14] Examples of such systems are the Cr/CrO and Mn/MnO systems. Should an attempt be made to determine the oxygen potential in these systems by electrochemical means, polarization at one or both electrodes may occur which will effect the accuracy and reliability of the measurements.

Another difficulty in the use of the electrochemical technique, is that the electrical conductivity of slags is usually too low to ensure proper electrical contact between the slag and the oxygen sensor. Therefore, a metal in the liquid state and in equilibrium with the slag, is required to ensure proper electrical contact with the oxygen probe. This implies that the crucible (oxide or metal) which serves as container for the liquid slag and liquid metal, should be inert with respect to both the slag and the metal. Previous workers have shown that this requirement is easily accomplished at temperatures up to 1673 K[8][9][10][15]. For instance, Van Wijngaarden and Dippenaar[15] determined the FeO-activity of (FeO-SiO_2-CaO-CaF_2)-slags at 1673 K. An Fe crucible contained pure silver metal and the slag, both phases in the liquid state. Since Fe and Ag are immiscible at 1673 K, the oxygen activity of the silver, in equilibrium with the FeO-containing slag, was determined and the FeO activity in the slag calculated accordingly.

However, at 1873 K there is virtually no metal which satisfy the requirements to serve as an inert container for the slag and the metal in the liquid state. In most instances, metal crucibles of which the melting point is well above 1873 K, will react with the liquid metal thereby lowering the melting point. Therefore, oxide crucibles with melting points well above 1873 K have to be used to contain the metal and the slag. Because most slags react chemically with oxides at these

© University of Pretoria

temperatures, the oxide crucible tends to dissolve and consequently, slags are saturated with the oxide used as crucible material. Furthermore, the slag could react chemically with the oxygen probe, resulting in erroneous measurements. However, should these experimental limitations be overcome, the electrochemical technique can be used to determine the thermodynamic behaviour of several slag/metal systems at temperatures up to 1873 K.

The main objective of this study was to develop the electrochemical technique to the extent that the MnO-activity of different slags in the ternary MgO-SiO_2-MnO system, can be measured reliably. In principal, it is possible to determine the influence of volatile components on the thermodynamic behaviour of MnO in the slag, something which is virtually impossible to do with the gas- slag equilibrium technique. However, it was imperative that the accuracy and reliability of the technique be established before the measurement of the MnO- activities in the MgO-SiO_2-MnO ternary system could be attempted and before more complex systems containing volatile components, could be studied. It is furthermore essential that the electrical characteristics of the solid electrolyte which serves as a key component in the oxygen sensor, should be known accurately. A technique was developed in a previous study by which the electrical characteristics of solid electrolytes could be determined and these characteristics were established for a number of electrolytes, including the magnesia stabilized zirconia solid electrolytes used in this study[16][17][18].

In the present study, polarization effects at one or both electrodes were minimized by developing a plug-type oxygen sensor. The plug-type oxygen probe was evaluated by determining the Henrian oxygen activity and Raoultian chromium activity of an Fe-Cr alloy in equilibrium with pure Cr_2O_3 or a Cr_2O_3-saturated slag at 1873 K, as a function of the chromium content (5% to 25% Cr). Since previous researchers have already determined the Cr activity in Fe-Cr alloys, the results of

© University of Pretoria

this study could be compared to those previously obtained[19][20] as a check on the accuracy and reliability of the plug-type probe. However, the corrosive Cr_2O_3-saturated slag in the liquid state reacted with the oxygen probe resulting in erroneous measurements. It was consequently necessary to develop a crucible assembly which prevented direct contact between the slag and the oxygen probe before reliable oxygen activity measurements could be made. This type of assembly was also used in the final phase of the study, of which the objective was to determine the MnO activity of (MgO-SiO_2-MnO)-slags saturated with (MnO-MgO) solid solutions and manganese metal at 1873 K.

In the course of the final phase of this study, a third method was employed for the determination of the activity of MnO in these silicate slags. Because the slag phase was in equilibrium with a (MnO-MgO) solid solution of which the activity-composition relationship is known, the activity of MnO could be calculated from the relationship

$$(a_{MnO})_{slag} = (a_{MnO})_{solid\ sol.} \qquad [1.3]$$

where $(a_{MnO})_{slag}$ and $(a_{MnO})_{solid\ sol.}$ are the activities of MnO in the slag and solid solution phases, respectively. This partially molten slag-solid solution phase system was equilibrated with pure manganese metal ($a_{Mn}=1$). The activities of the manganese oxide determined by this experimental technique where the slag was in equilibrium with Mn metal as well as with (MnO-MgO) solid solutions, were compared to the experimental findings of previous researchers who used the gas-slag-metal equilibrium technique in which the oxygen partial pressure was fixed and the a_{Mn} in the alloy known.

This experimental technique could very elegantly be utilized to determine the feasibility and accuracy of the electrochemical measuring technique. The partial pressure of oxygen determined by employing electrochemical oxygen probes, could

© University of Pretoria

be compared to that calculated with this method, since the melts are in equilibrium with Mn and the activity of MnO in the melts is known. Should it be possible to verify the ability of electrochemical probes to determine the oxygen potential in these Mn/MnO/MgO silicate slag systems accurately, the electrochemical technique could easily be expanded to melts where the activity of MnO is not known.

© University of Pretoria

UNIVERSITEIT VAN PRETORIA
UNIVERSITY OF PRETORIA
YUNIBESITHI YA PRETORIA

CHAPTER 2

BACKGROUND

In 1984 a research program was initiated in the pyrometallurgy research group at the University of Pretoria in which the electrochemical technique was extensively used, for example to determine the iron oxide activities of iron- and steelmaking slags[10][15]. From these studies it was evident that the limiting factors of the technique should be carefully dealt with when it is used for the determination of the oxygen activity of high-temperature slag/metal systems. Because this technique has not previously been employed in liquid slags at temperatures higher than 1823 K, the aim of the present study was to use and further develop the electrochemical technique for the determination of the MnO activity in MnO-containing liquid slags at 1873 K. Accordingly, the fundamental aspects inherent to the electrochemical technique and the MnO activities of different MnO-containing liquid slags determined previously, are discussed below.

2.1 Fundamental Aspects of the Electrochemical Measuring Technique

In 1933, Wagner[21] developed a differential equation which described the relationship between the electromotive force and the oxygen potential of an electrochemical cell containing a solid electrolyte which exhibited mixed ionic and electronic conduction. The oxygen potentials at the two electrodes μ' and μ'' respectively, are related to the electromotive force (E) as follows:

$$E = \frac{1}{zF} \int_{\mu_{O_2}}^{\mu_{O_2}''} t_{ion} \cdot d\mu_{O_2} \qquad [2.1]$$

where z is the number of electrons required to ionize an oxygen molecule according to the reaction:

© University of Pretoria

$$O_2 + 4e^- \rightleftharpoons 2O^{2-} \qquad [2.2]$$

F is the Faraday constant and t_{ion} is the ionic transport number. The oxygen potential, μ_{O2}, can be expressed as:

$$\mu_{O_2} = \mu^\circ_{O_2} + RT\ln P_{O_2} \qquad [2.3]$$

Since the standard chemical potential, μ°_{O2}, of both electrodes are the same, equation [2.1] simplifies to the following when the solid electrolyte exhibits pure ionic conduction ($t_{ion} = 1$):

$$E = \frac{RT}{4F} \ln \frac{P_{O_2}''}{P_{O_2}'} \qquad [2.4]$$

where T is the absolute temperature, R is the gas constant and P_{O_2}' and P_{O_2}'' are the partial pressures of oxygen at the two electrodes respectively. It is important to emphasize that equation [2.4], often referred to as the Nernst equation, is valid only when the solid electrolyte exhibits pure ionic conduction. However, it is well known[11][12][13][14] that zirconia solid electrolytes exhibit mixed ionic and n-type electronic conduction when used at high temperatures and low oxygen potentials. Since the ionic transport number, t_{ion}, is a function of the oxygen partial pressure, different values for t_{ion} are applicable when the same solid electrolyte is used in systems of different partial pressures of oxygen. Therefore, it is important to define a parameter which describes the electrical characteristics of a solid electrolyte irrespective of the partial pressure of oxygen. Schmalzried[22][23] carefully analyzed the Wagner equation (equation [2.1]) and defined the value P_e of a solid electrolyte as the partial pressure of oxygen at which t_{ion} equals 0.5. In mathematical terms, this statement may be expressed as follows:

© University of Pretoria

$$t_{ion} = \frac{1}{1 + \left(\frac{P_{O_2}}{P_e}\right)^{-\frac{1}{4}}} \qquad [2.5]$$

Substitution of equation [2.5] into equation [2.1], yields the following expression:

$$E = \frac{RT}{F}\ln\left[\frac{(P_{O_2}'')^{\frac{1}{4}} + (P_e)^{\frac{1}{4}}}{(P_{O_2}')^{\frac{1}{4}} + (P_e)^{\frac{1}{4}}}\right] \qquad [2.6]$$

It is important to establish the sensitivity of the cell potential (EMF) to variations in the P_e-value of the solid electrolyte. As an example, the following electrochemical cell may be considered:

$$(+)\ Mo\ /\ (Fe\text{-}Cr)_{alloy}\ /\ solid\ electrolyte\ /\ (Cr+Cr_2O_3)_{ref}\ /\ Mo\ (-) \qquad [2.7]$$

The EMF of the cell was calculated as a function of the Cr activity in an Fe-Cr alloy at 1873 K for three different P_e-values of the solid electrolyte. These calculations are shown in *Figure 2.1*. For the purpose of this calculation it was assumed that the Fe-Cr alloy is in equilibrium with pure Cr_2O_3, and the standard free energy change, ΔG° for the reaction $2<Cr> + 3/2O_2 \rightleftharpoons <Cr_2O_3>$, is -651704 J/mol at 1873 K. The reference electrode consists of a mixture of pure ($Cr+Cr_2O_3$) powder with an equilibrium partial oxygen pressure at 1873 K[24] of 7.6×10^{-13} atm.

It follows from *Figure 2.1*, that if the true chromium activity of the alloy is for example 0.4, cell [2.7] will yield an EMF reading of 38 mV if the P_e-value of the electrolyte is 10^{-14} atm. If this cell potential is used for the calculation of the activity in the same alloy but using a P_e-value of 10^{-16} atm., an activity of 0.48 is obtained. This represents an error of 20% in the activity value. Evidently, the P_e-value of a solid electrolyte used in an oxygen concentration cell, should be known accurately if accurate and reliable measurements are to be made when the solid electrolyte

© University of Pretoria

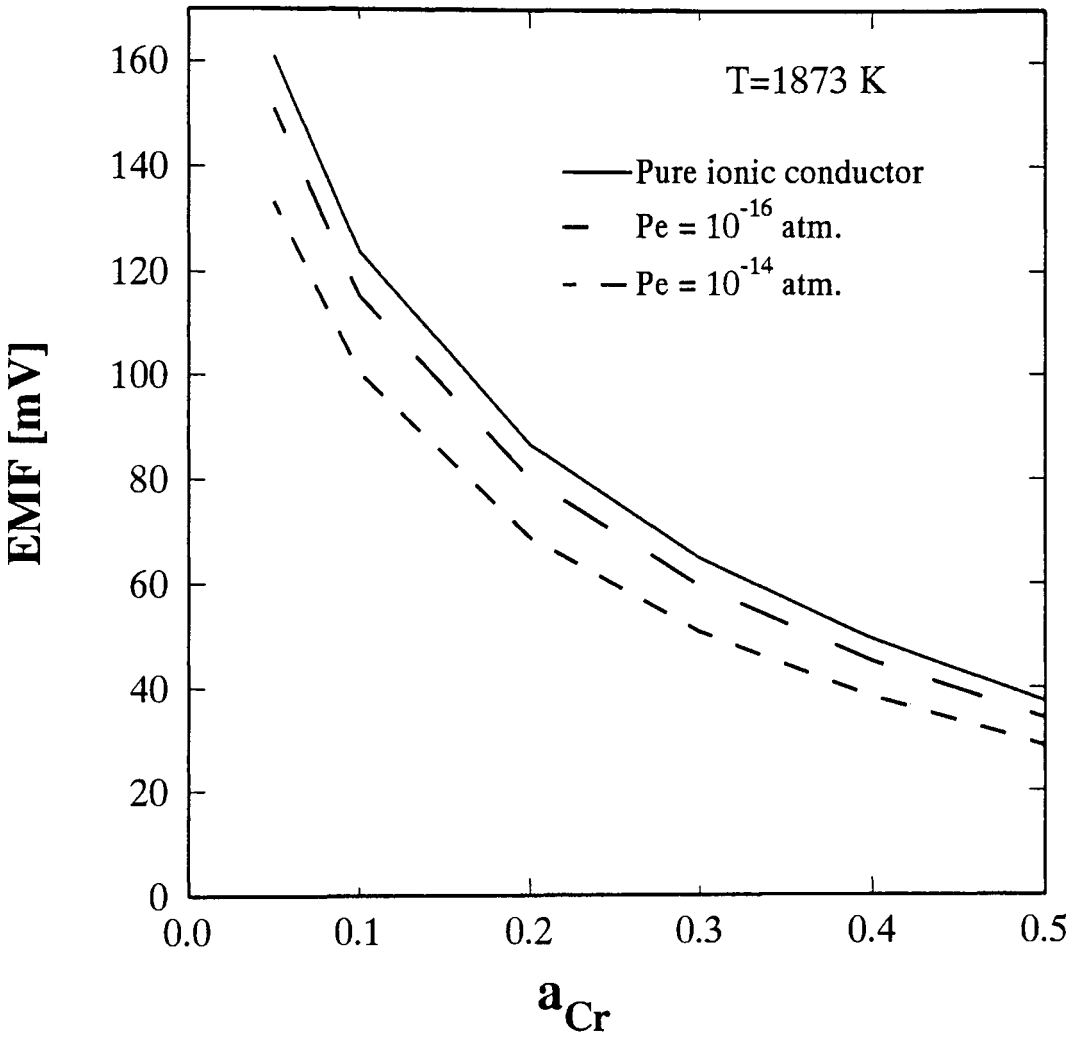

Figure 2.1 - *Calculated cell potentials of cell [2.7] as a function of the chromium activity at 1873 K for different P_e-values of the solid electrolyte*

© University of Pretoria

exhibits mixed ionic and electronic conduction ($t_{ion} < 0.99$).

2.1.1 Limitations of the Electrochemical Technique

Although the solid electrolyte measuring technique has become an appropriate tool to control oxygen levels in steel melts, or to determine the oxygen potential of high temperature slag metal systems, due account has to be taken of various sources of error especially at low oxygen activities and high temperatures. In the previous paragraph, it was shown that the P_e-value of the solid electrolyte should be known accurately, but erroneous EMF values may also be obtained as a result of the following:[12]

a) transportation of oxygen ions will occur when the solid electrolyte displays some electronic conductivity and this will cause polarization
b) chemical interaction between the solid electrolyte and the liquid metal/slag when the probe is immersed into the melt, will cause the electrical characteristics of the sensor to change
c) the use of inaccurate thermochemical data for the different reactions occurring in the slag/metal system studied will cause inaccuracy in the activities calculated from the measured EMF values
e) transportation of gaseous oxygen through pores and micro cracks in the electrolyte material will cause polarization
f) insufficient knowledge of the thermoelectric voltage generated between two different contact leads to the two electrodes, will cause erroneous oxygen potentials to be calculated.

Error sources a) and b) are of utmost importance and are discussed in more detail below.

© University of Pretoria

2.1.1.1 Polarization

Polarization at one or both electrodes of an electrochemical cell containing a solid electrolyte, is a direct result of electronic conduction which occurs when the ionic transport number, $t_{ion} < 0.99$. To illustrate the extent of ionic conduction, the ionic transport number is shown in *Figure 2.2* as a function of the oxygen partial pressure at 1873 K for solid electrolytes with different P_e-values, calculated by equation [2.5]. Also shown in this figure, is the range of the partial pressure of oxygen in the Mn/MnO system when the MnO activity in the slag, in equilibrium with pure Mn, varies between 0.1 and 1.0. For a solid electrolyte with a P_e-value of 10^{-18} atm., t_{ion} varies between 0.85 and 0.95 compared to a variation between 0.3 and 0.55 for a solid electrolyte with a P_e-value of 10^{-14} atm., when used in the Mn/MnO system. Although both these electrolytes exhibit mixed ionic and n-type electronic conduction, the electrolyte with a P_e-value of 10^{-18} atm. clearly exhibits almost complete ionic conduction whereas a significant amount of electronic conduction will occur in the electrolyte with a P_e-value of 10^{-14} atm. When electronic conduction occurs, the electrochemical cell is partially short-circuited because electrons migrate from the electrode with the lower oxygen potential to the electrode with the higher oxygen potential and oxygen ions migrate in the opposite direction, as illustrated schematically in *Figure 2.3*. Consequently, if the rate of oxygen transfer through the electrolyte is higher than the rate at which oxygen is supplied or adsorbed at either electrode, an oxygen concentration gradient develops within the electrode. Under these circumstances, the electromotive force between the two electrode/electrolyte interfaces diminishes as a function of time and such a measured EMF is not a true representation of the oxygen potential difference between the electrodes on either side of the solid electrolyte. The difference in oxygen potentials across the solid electrolyte is related to the thermodynamic driving force for oxygen ions to migrate, but when actual migration occurs, the thermodynamic driving force diminishes, *i.e.* polarization occurs.

© University of Pretoria

UNIVERSITEIT VAN PRETORIA
UNIVERSITY OF PRETORIA
YUNIBESITHI YA PRETORIA

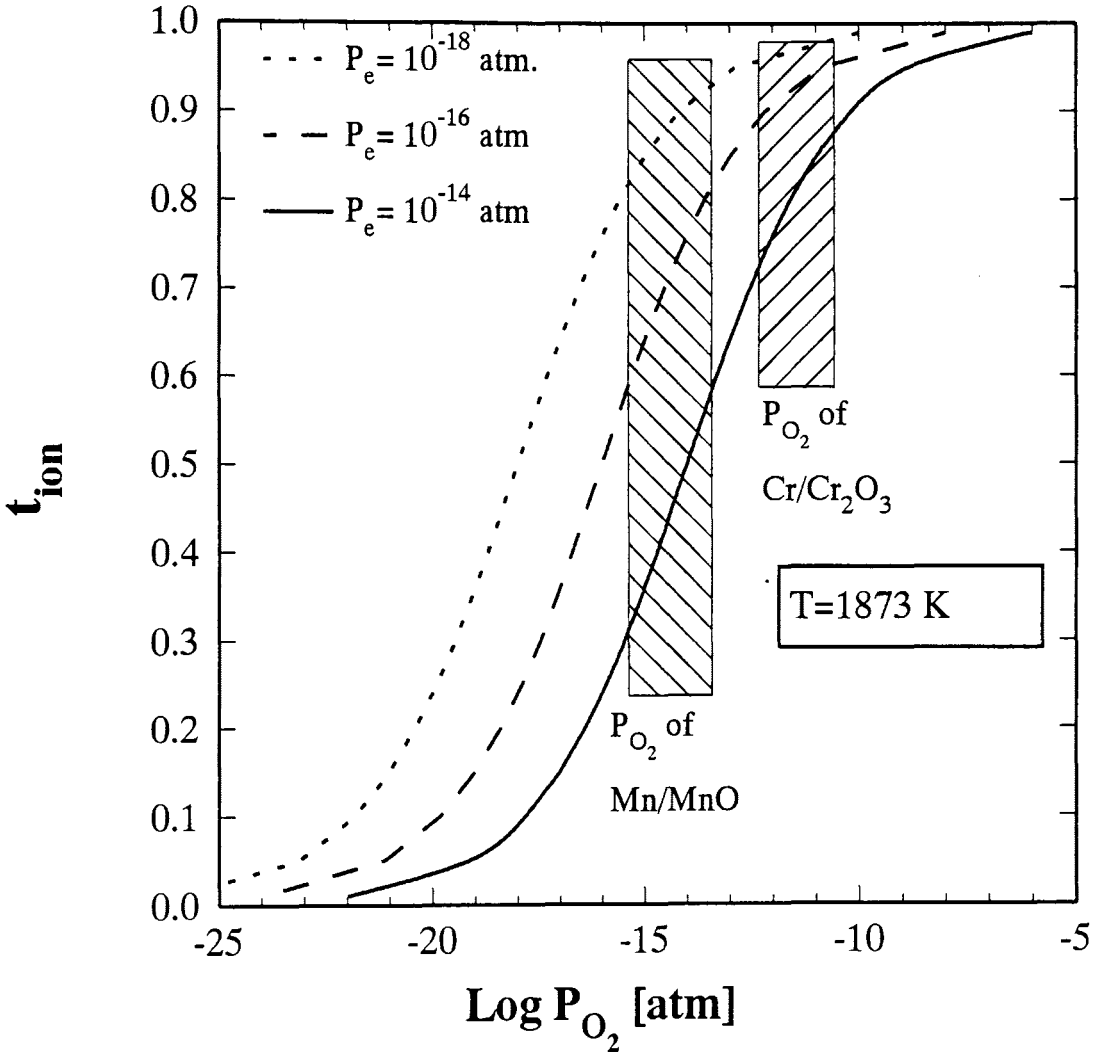

Figure 2.2 - *Relationship between the partial pressure of oxygen and the ionic transport number (t_{ion}) of solid electrolytes with different P_e-values at 1873 K*

© University of Pretoria

UNIVERSITEIT VAN PRETORIA
UNIVERSITY OF PRETORIA
YUNIBESITHI YA PRETORIA

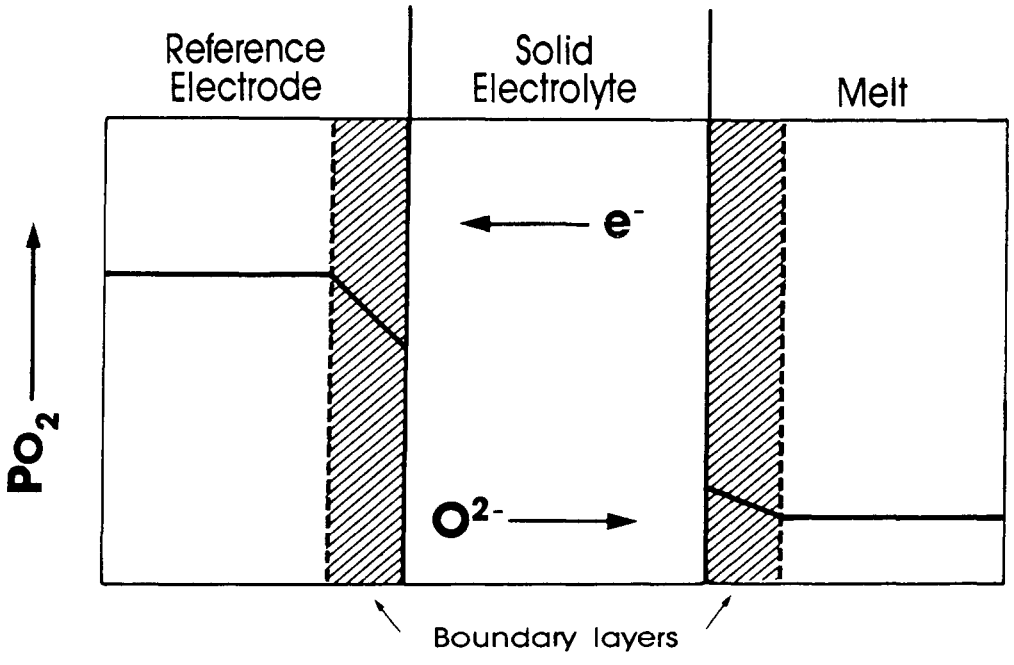

Figure 2.3 - *Schematic representation of polarization at the electrode-electrolyte interfaces of an oxygen probe of which* $t_{ion} < 0.99$.

© University of Pretoria

It is consequently of great importance that polarization effects at one or both electrodes be avoided or at the very least minimized by minimizing the transfer of oxygen ions through the electrolyte, if successful measurements are to be made. In principle, this goal can be accomplished in one of the following ways[12]:

i) Ideally the solid electrolyte to be used should possess a P_e-value which is low enough to ensure that $t_{ion} > 0.99$ (*Figure 2.2*). Because this is not always possible, the P_e-value of the solid electrolyte used should be as low as possible.

ii) The oxygen partial pressure of the reference electrode chosen for the electrochemical cell should be as close as possible to that of the melt so as to lower the oxygen gradient across the electrolyte.

iii) The thickness of the solid electrolyte should be increased, thereby lowering the oxygen gradient across the solid electrolyte.

Stabilized zirconia has in the past been used successfully to measure the oxygen potential in steel and various slag systems. However, the P_e-values of zirconia solid electrolytes at 1873 K are in the range of 10^{-14} atm. and attempts have been made to render these electrolytes useful by a careful selection of a suitable reference electrode and by increasing the thickness of the electrolyte between the electrodes. Janke[25] developed an oxygen sensor which he termed a plug-type oxygen probe, for the continuous measurement of the oxygen potential in liquid steel. Such a probe is schematically illustrated in *Figure 2.4*. Stabilized zirconia powder was sintered at elevated temperatures into a thin-walled alumina tube (outer diameter 4mm and inner diameter 3mm). The thickness of the solid electrolyte plug was between 10mm and 20mm and an iridium wire served as the electrical contact lead to a Cr/Cr_2O_3 reference electrode. The electromotive force (EMF) measured with this probe in pure iron at 1873 K was compared to the EMF obtained by a conventional commercial oxygen probe containing a solid electrolyte tube. A constant EMF signal which

© University of Pretoria

UNIVERSITEIT VAN PRETORIA
UNIVERSITY OF PRETORIA
YUNIBESITHI YA PRETORIA

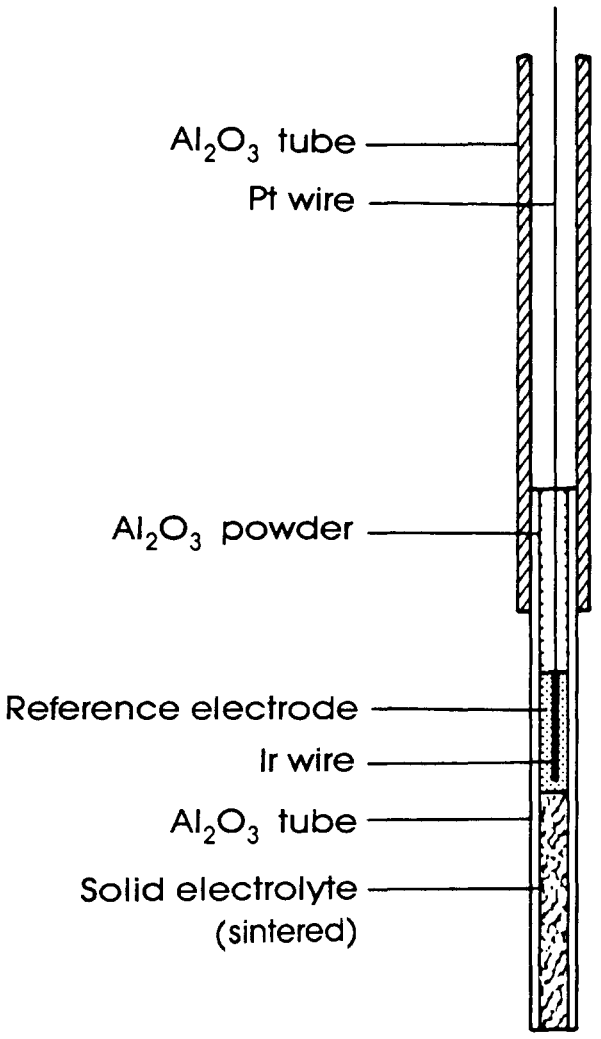

Figure 2.4 - *Schematic illustration of the plug-type oxygen probe introduced by Janke*[25]

© University of Pretoria

lasted for up to two hours, was recorded with the plug-type probe. By comparison, the EMF plateau recorded by a tubular sensor lasted for only a few seconds and then changed continuously as a result of polarization at one or both electrodes. These experiments by Janke proved conclusively that polarization was minimized in the plug-type design of his oxygen probe, indicating that oxygen transfer through the solid electrolyte is minimized by increasing the thickness of the solid electrolyte. Heinz *et.al*[26] used this plug-type design of an oxygen probe to determine the oxygen activity in Cr-containing Fe and Ni-based melts at 1823, 1873 and 1923 K. Since polarization was minimized, stable EMF plateaus were recorded.

2.1.1.2 Slag Attack

Zirconia solid electrolytes, stabilized with MgO, CaO or Y_2O_3 are frequently used in electrochemical oxygen concentration cells. When these oxygen probes are in contact with liquid slags at high temperatures, these solid electrolytes tend to dissolve. However, previous studies[8][9][10][15], have shown that MgO stabilized zirconia electrolytes can be used successfully in Fe_xO-containing slags at 1673 K, when the solid electrolyte is in direct contact with the slag.

An extensive literature search was conducted to establish whether previous attempts have been made to determine the oxygen potential of liquid slags at 1873 K by electrochemical means, but no reports of such measurements could be found. Because the electrochemical technique offers certain decided advantages in determining the oxygen potential in liquid slag/metal systems, it is probable that such attempts have been made but may have failed because of the corrosiveness of liquid slags at temperatures above 1723 K.The solid electrolytes contained in oxygen probes, are attacked chemically by the corrosive liquid slags at these high temperatures, resulting in erroneous EMF measurements. This problem can be overcome by designing the crucible assembly so as to prevent direct contact between

© University of Pretoria

UNIVERSITEIT VAN PRETORIA
UNIVERSITY OF PRETORIA
YUNIBESITHI YA PRETORIA

the corrosive slag and the oxygen probe. However, Oishi *et.al.*[27] reported that if such type of crucible assembly is used, periods of up to 10 hours at 1673 are required before equilibrium between slag and metal is attained.

2.1.2 Analysis of the EMF Recording

The determination of the oxygen activity of any slag/metal system with an oxygen probe, is based on the correct interpretation of the EMF signal which is generated as a result of the difference in oxygen potential at the two electrodes. It is therefore of the utmost importance that EMF recordings should be analyzed accurately and reliably.

2.1.2.1 EMF Plateau

Three examples of recorder outputs (EMF vs time) of electrochemical oxygen probes dipped into an Fe-Cr alloy at 1873 K, are schematically illustrated in *Figure 2.5*. When the plug-type oxygen probe containing a MgO stabilized zirconia rod is dipped into the melt, a stable EMF is attained after a period of approximately 1 to 2 minutes (curve 1). This period is determined by the type and size of the solid electrolyte contained in the probe, the type of reference electrode used, the temperature at which the measurement is made and the manner in which the oxygen probe is lowered into the melt. When the oxygen sensor is attacked chemically by the slag or liquid metal, the electrodes are short-circuited and the measurement should be discarded (curve 2). An EMF signal which changes as a function of time without attaining a stable value, indicates that polarization effects are dominant (curve 3), and is typically obtained when a tubular zirconia oxygen probe (wall thickness 1mm) is dipped into an Fe-Cr alloy at 1873 K.

© University of Pretoria

UNIVERSITEIT VAN PRETORIA
UNIVERSITY OF PRETORIA
YUNIBESITHI YA PRETORIA

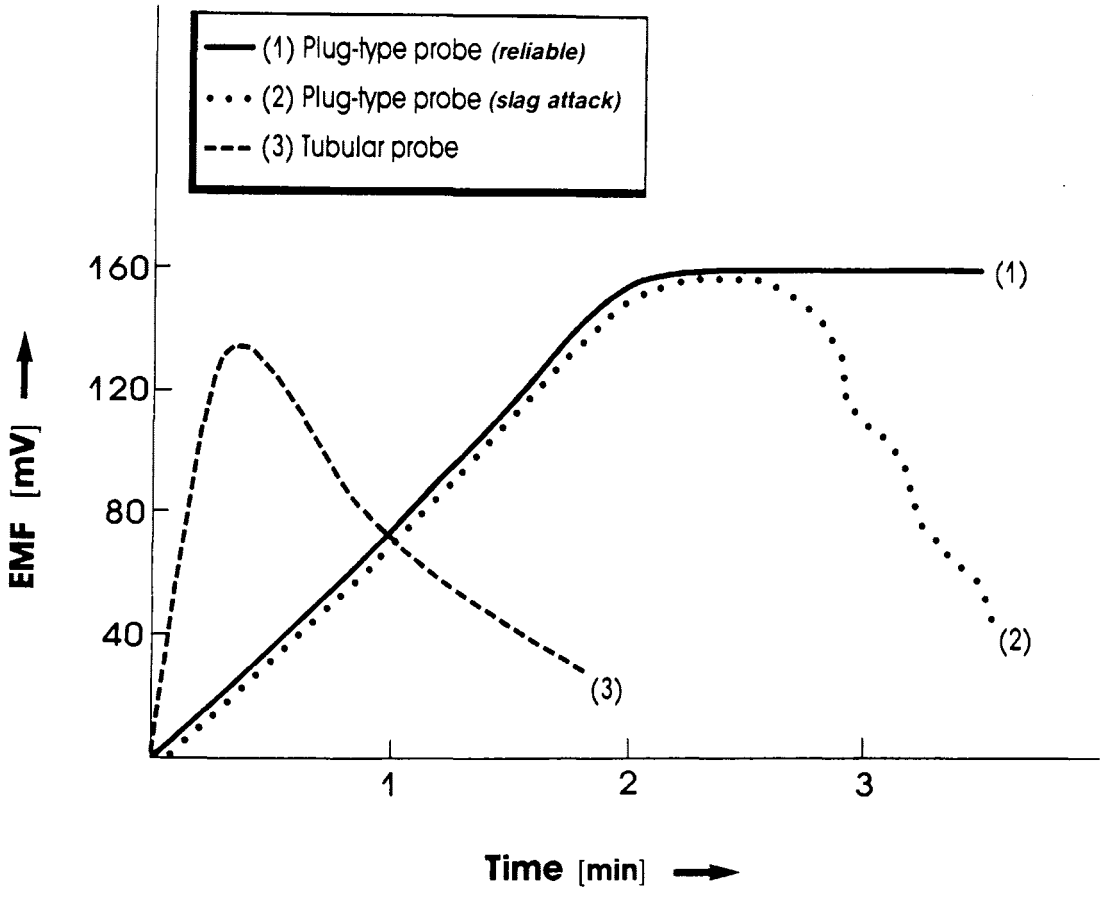

Figure 2.5 - *Schematic representation of EMF recordings of different oxygen sensors at 1873 K.*

© University of Pretoria

2.1.2.2 Cell Resistance

It is very important to ensure that the oxygen probe as well as the electrical contact lead make proper electrical contact with the melt during an oxygen activity measurement. If, for instance, the wire that serves as electrical contact lead is not dipped properly into the melt, an additional resistance is generated in the measuring circuit influencing the EMF signal adversely. That the electrical circuit functions properly can be very easily determined by measuring the electrical resistance of the electrochemical cell in the following manner: A direct current of 1 mA is applied to the oxygen probe while the cell potential is registered simultaneously so that the cell resistance can be calculated. When a probe or contact lead do not make proper electrical contact, the electrical resistance is usually one or two orders of magnitude higher than average, typically 300 ohm as against 20 ohm for a cell making proper electrical contact. Therefore, a relatively low cell resistance is an indication of a proper and reliable measuring circuit.

2.2 Previous Work

The thermodynamic behaviour of MnO in slags at temperatures above 1773 K, was studied mainly in the period 1950 to 1970. The work was aimed at the production of ferromanganese in the blast furnace and concentrated on the determination of the manganese partition ratio between slag and metal. Only limited data are available in the literature regarding the activity of MnO in these slag systems.

Stukel and Cocubinsky[28] studied the partition of manganese between carbon saturated iron and a (MnO-SiO_2-CaO)-slag at temperatures between 1723 and 1823 K. Their most important conclusion was that the partitioning of manganese between slag and metal ($[Mn]_{slag}/(\underline{Mn})_{Fe}$) decreased with an increase in temperature and an increase in basicity (CaO/SiO_2) respectively. Turkdogan[29] used these results to

© University of Pretoria

UNIVERSITEIT VAN PRETORIA
UNIVERSITY OF PRETORIA
YUNIBESITHI YA PRETORIA

calculate the MnO activity in the ($MnO-CaO-SiO_2-Al_2O_3$) system, of which the MnO content was less than 10%. In this analysis, Turkdogan assumed ideal Henrian behaviour of Mn in the carbon saturated liquid iron. These calculations indicated that for a given $CaO:SiO_2$ ratio, the activity coefficient of MnO (γ_{MnO}) decreased with an increase in Al_2O_3 content of the slag.

Abraham *et al.*[3] used the gas-slag equilibrium technique to determine the activity of MnO in ($MnO-SiO_2-CaO$)- and ($MnO-SiO_2-CaO-Al_2O_3$)-slags at 1773 K and 1923 K respectively. The important conclusion of this study was that at both temperatures, the addition of CaO to the ($MnO-SiO_2-CaO$)-slag increased the activity coefficient of MnO, γ_{MnO}. The activity of MnO in the ($MnO-SiO_2-CaO-Al_2O_3$)-slag differed significantly from those calculated by Turkdogan, but Abraham *et al.* could not explain these differences.

Mehta and Richardson[4] also used the gas-slag equilibrium technique to determine the activity of MnO in the ternary systems ($MnO-SiO_2-CaO$), ($MnO-SiO_2-MgO$), ($MnO-BaO-SiO_2$), ($MnO-CaO-Al_2O_3$) and the quaternary system ($MnO-SiO_2-CaO-Al_2O_3$) in the temperature range 1773 to 1923 K. They have shown that in the ternary systems, the BaO is more effective in raising the activity coefficient of MnO than either MgO or CaO. The MnO-activity measured in the ($MnO-SiO_2-CaO-Al_2O_3$)-slag was in good agreement with that determined by Abraham *et al*[3]. The amphoteric nature of Al_2O_3 was evident since in the vicinity of 60% SiO_2, the substitution of CaO with Al_2O_3 had no effect on the activity coefficient of MnO, indicating that Al_2O_3 acted as a base. In the region where SiO_2 was less than 30%, the substitution of CaO with Al_2O_3 lowered γ_{MnO}, indicating that Al_2O_3 acted as an acid in these slags.

Tsai[6] determined activity-composition relations in (MnO-MgO) solid solutions at 1773 and 1873 K respectively. He has shown that the activity of MnO in these solid

1638980
1638978

© University of Pretoria

solutions deviate positively from ideal Raoultian behaviour in this temperature range. Furthermore, the activity coefficient of MnO is slightly higher at 1773 K as against 1873 K.

Simeonov and Sano[30], studied the manganese equilibrium distribution between lime-based slags containing MnO, BaO, Na_2O and CaF_2 and carbon saturated iron in the temperature range 1523 to 1623 K. They found that the equilibrium manganese distribution between slag and metal decreased with the addition of Na_2O, BaO and CaF_2 to (CaO-SiO_2-MnO)-slags, respectively. However, the effect of CaF_2 and Na_2O on the activity of MnO in these slags at 1873 K have not been determined as yet. With the exciting prospect of a direct steelmaking route to produce manganese containing stainless steel, it is evident that a great need exists to determine the thermodynamic behaviour of MnO in these slags, especially at temperatures of 1873 K and higher.

© University of Pretoria

UNIVERSITEIT VAN PRETORIA
UNIVERSITY OF PRETORIA
YUNIBESITHI YA PRETORIA

CHAPTER 3

ACTIVITY MEASUREMENTS IN THE Fe-Cr-O SYSTEM AT 1873 K

3.1 Introduction

It has become common practice to use magnesia-stabilized zirconia solid electrolyte tubes in commercial oxygen probes for the determination of the oxygen content of liquid steel. However, it is well known that these solid electrolyte tubes exhibit excessive electronic conduction when applied to high-temperature slag-metal systems where a very low oxygen potential prevails, as for instance, in the Mn/MnO system. Consequently, polarization at one or both electrodes has a detrimental effect on the accuracy and reliability of these measurements as discussed in *par. 2.1.1.1.* In this study, polarization effects were minimized by developing a probe similar in design to that introduced by Janke[25]. It was intended to use this probe to determine activities at 1873 K in the Mn/MnO system, of which the oxygen potential is very low, and therefore the accuracy and reliability of this type of oxygen sensor had to be evaluated. For this purpose, attention was focused on the Fe-Cr-O system: the oxygen activity of the Fe-Cr-O system is of the same order as that of the Mn/MnO system at 1873 K and the Fe-Cr-O system has been studied by previous investigators. Therefore, oxygen activity measurements were made in the Fe-Cr-O system to verify the accuracy and reliability of the newly developed probe.

The oxygen activity measurements in the Fe-Cr-O system were divided into three experimentally discernible studies: Initially the Fe-Cr alloy was contained in alumina crucibles coated with a thin layer of Cr_2O_3 and with a layer of solid Cr_2O_3 on top of the alloy. Following this, a pure Cr_2O_3 crucible was used and the activities of chromium in the same Fe-Cr alloys were re-assessed. In the third study, pure Cr_2O_3 crucibles were used but the molten alloy was equilibrated with a partially liquid,

© University of Pretoria

Cr_2O_3-saturated, lime-silica slag. However, the liquid slag chemically attacked the oxygen probe and it was necessary to modify the cell design to prevent this attack, in order to make reliable oxygen measurements. The development of this cell design was fairly successful and the oxygen activities determined were verified by comparing it to those of previous workers.

3.2 Design of the Plug-type Oxygen Probe

The wall thickness of the zirconia solid electrolyte tubes which are usually encountered in commercial oxygen sensors and electrochemical cells used for research purposes is of the order of 1mm. When these electrolyte tubes are used for the determination of the oxygen activity in slag-metal systems at low oxygen potentials, the oxygen gradient over the solid electrolyte is relatively high and the electrical cell resistance is low. Consequently, oxygen ions migrate from the electrode of higher oxygen potential to the electrode of lower oxygen potential under open-circuit conditions and electrons migrate in the opposite direction. This nett transfer of ions and electrons results in polarization at one or both electrodes which, in turn, decrease the accuracy of the oxygen potential measurements. Polarization can be minimized by the use of a solid electrolyte with very low n-type electronic conductivity. For example, the n-type electronic conductivity of yttria-stabilized thoria solid electrolytes, is low enough to minimize polarization at either electrode. However, it was impossible to obtain thoria solid electrolytes for this study and moreover, experimentation with radio-active material is extremely difficult in a university laboratory.

An alternative approach to solving the problem of polarization is to redesign the probe containing the zirconia solid electrolyte in such a way that the ionic cell resistance is increased. Janke[25] has shown in a convincing manner that this approach can be used successfully (*par. 2.1.1.1)*. The oxygen probe developed along similar lines in the present study, consisted essentially of a 9 mol% magnesia-stabilized zirconia solid electrolyte rod, supplied by Nippon Kagaku Togyo, Japan, which

© University of Pretoria

UNIVERSITEIT VAN PRETORIA
UNIVERSITY OF PRETORIA
YUNIBESITHI YA PRETORIA

was cemented into an alumina tube of which the wall thickness was 0.5mm. The inner diameter of the alumina tube was 3.95±0.05mm, and each zirconia rod, with an outside diameter 4mm, was ground to fit tightly into the alumina tube. Alumina cement consisting of pure Al_2O_3 powder and a waterglass binder, was used to attach the rod to the tube as shown schematically in *Figure 3.1*. The length of the zirconia solid electrolyte rod, *i.e.* the length of the conduction path for oxygen ions, is 10mm and this dimension should be compared to a wall thickness of 1mm of the electrolyte tube. Consequently, the electrical cell resistance of the plug type probe is much higher than that of a tubular sensor, which is also schematically shown in *Figure 3.1*. Molybdenum wire of 3mm diameter, served as electrical contact to the reference electrode. The $Cr:Cr_2O_3$ ratio in the reference electrode was 3:1 on the basis of mass.

The P_e-value of the 9 mol% magnesia-stabilized zirconia solid electrolyte tubes was measured as a function of temperature in an earlier study and can be expressed as[17]:

$$\log P_e = 22.77 - \frac{67956}{T} \qquad [3.1]$$

where T and P_e are expressed in kelvin and atmosphere respectively. The chemical composition of these tubes and the 9 mol% magnesia- stabilized zirconia rods used in the plug type oxygen sensor, are summarized in *Table 3.1*. It is evident that the chemical compositions of the solid electrolyte rod and tube are very similar. Microprobe analyses indicated that the phase compositions of both types of electrolytes were almost identical. Therefore, the P_e-values of the solid electrolyte rods and tubes ought to be the same, and equation [3.1] was used to calculate the applicable P_e-value of the solid electrolyte rods used in the plug-type oxygen probes.

These probes were evaluated by determining the oxygen activity in the Fe-Cr-O system at 1873 K.

© University of Pretoria

UNIVERSITEIT VAN PRETORIA
UNIVERSITY OF PRETORIA
YUNIBESITHI YA PRETORIA

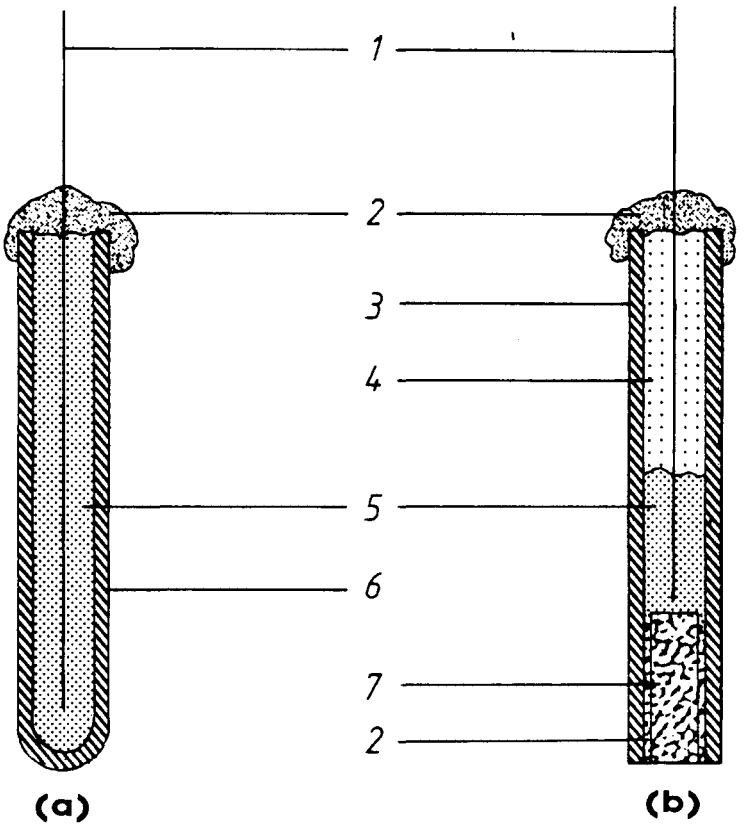

1. Molybdenum wire	5. Reference powder
2. Alumina cement	6. Solid electrolyte tube
3. Alumina tube	7. Solid electrolyte rod
4. Alumina powder	

Figure 3.1 - *Schematic representation of (a) a tubular oxygen probe (b) the plug type oxygen probe used in this study*

© University of Pretoria

Table 3.1 - *Chemical composition of the 9 mol% magnesia-stabilized zirconia solid electrolytes supplied by Nippon Kagaku Togyo.*

Type	%MgO	%CaO	%SiO_2	Al_2O_3	%TiO_2	Fe_2O_3	%K_2O
Tube	3.1	0.3	0.6	1.3	0.1	0.1	tr
Rod	3.0	0.3	0.3	0.6	tr	0.1	tr

tr trace element

3.3 Experimental Aspects

The activity measurements were performed in three experimentally discernable studies as mentioned earlier: In the first experiments Cr_2O_3-coated Al_2O_3 crucibles were used to contain the Fe-Cr alloy in equilibrium with pure solid Cr_2O_3. Following these experiments, Cr_2O_3 crucibles were used and finally, the Fe-Cr alloy was equilibrated with a partially liquid slag contained in a Cr_2O_3 crucible. The experimental details pertaining to the different crucible assemblies, are discussed separately.

3.3.1 Al_2O_3 crucibles Coated with Cr_2O_3

3.3.1.1 Apparatus

The experimental apparatus, illustrated schematically in *Figure 3.2*, consisted essentially of a purification train for the argon gas and a vertical Super-Kanthal furnace containing two alumina reaction tubes. The furnace was equipped with a proportional-integral derivative (PID) controller and the purification train consisted

© University of Pretoria

UNIVERSITEIT VAN PRETORIA
UNIVERSITY OF PRETORIA
YUNIBESITHI YA PRETORIA

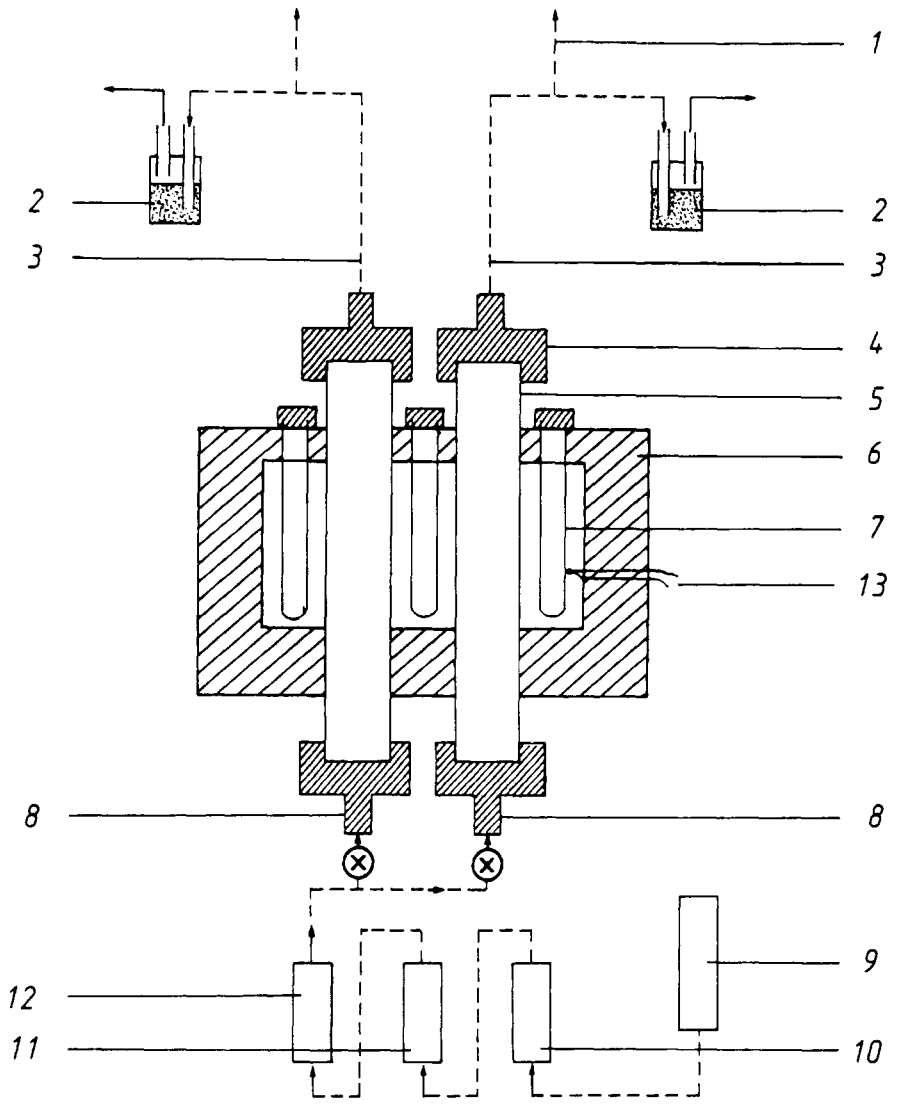

1. To Vacuum pump	8. Gas inlets
2. Oil	9. Argon gas
3. Gas outlets	10. Silica gel
4. Water cooled brass lid	11. Magnesium perchlorate
5. Alumina reaction tubes	12. Phosphorus pentoxide
6. Twin tube furnace	13. Thermocouple
7. Super kanthal elements	

Figure 3.2 - *Schematic representation of the experimental apparatus*

© University of Pretoria

of silica gel, magnesium perchlorate and phosphorous pentoxide. A vacuum pump was connected to the gas line. A digital electrometer with an input impedance of 10^{14} ohm coupled to a chart recorder with an accuracy of approximately 0.25 mV was used to measure the electromotive force (EMF) of the electrochemical cell.

The reaction tube and crucible assembly are shown in more detail in *Figure 3.3*. A cylindrical alumina crucible (outside diameter 42mm, inside diameter 38mm and height 60mm) was coated with a thin layer of chromium oxide on its inside surface as follows: Pure Cr_2O_3-powder and water were mixed and the slurry was painted onto the crucible. It was dried at 80 °C and this procedure was repeated at least three times before it was sintered at 1400 °C for two hours. This Cr_2O_3-coated Al_2O_3-crucible contained the Fe-Cr alloy and chromium oxide (Cr_2O_3). The assembly was placed on an alumina pedestal in the constant-temperature heat zone of the furnace, the temperature of the furnace being controlled by a Pt-6%Rh/Pt-30%Rh thermocouple, which was located next to one of the elements. The temperature of the crucible assembly was measured with a Pt/Pt-10%Rh thermocouple placed adjacent to the cell arrangement. The temperature-measuring circuit was calibrated against the melting point of palladium, and the overall error in the temperature measurements was found to be less than 3 °C. A molybdenum wire (0.9mm diameter) served as the electrical contact to the melt.

© University of Pretoria

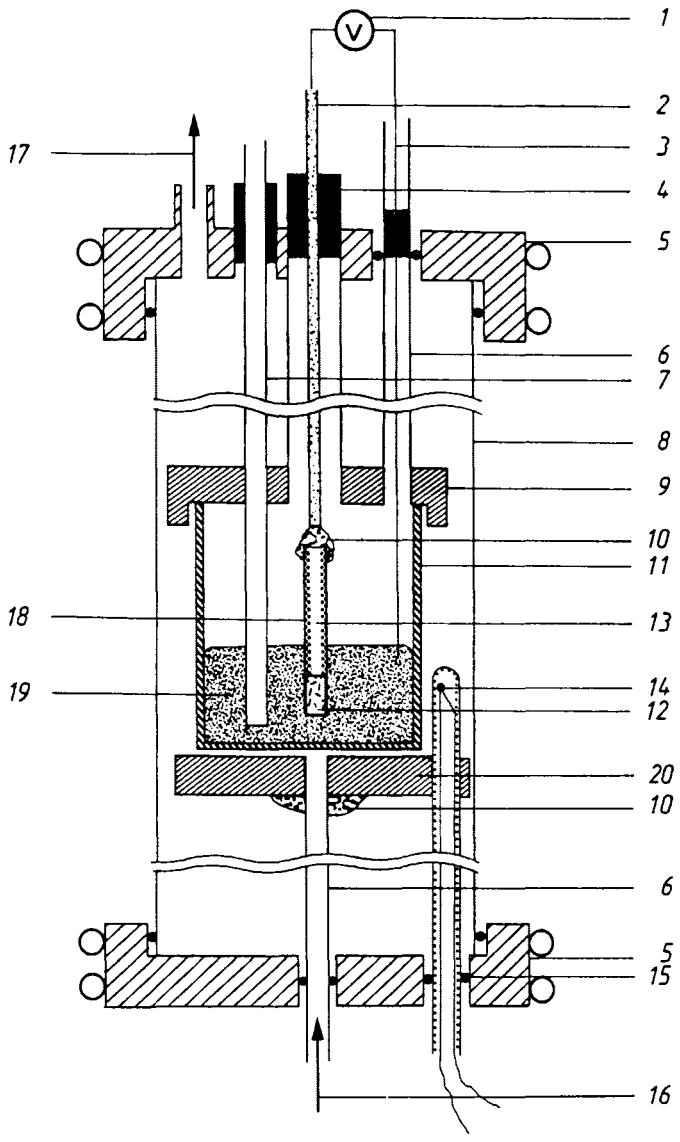

1.	Electrometer	11.	Cr_2O_3 crucible
2.	Mo-rod	12.	ZrO_2 electrolyte
3.	Mo-wire	13.	(Cr + Cr_2O_3) reference electrode
4.	Rubber stoppers	14.	Thermocouple (Pt/Pt-10%Rh)
5.	Watercooled brass lid	15.	Rubber "O"-ring
6.	Al_2O_3 tubes	16.	Argon inlet
7.	Al_2O_3 stirring rod	17.	Argon outlet
8.	Al_2O_3 reaction tube	18.	Oxygen sensor
9.	Al_2O_3 guide disk	19.	Fe-Cr alloy
10.	Al_2O_3 cement	20.	Al_2O_3 pedestal

Figure 3.3 - *Reaction tube and crucible assembly*

© University of Pretoria

3.3.1.2 Procedure

Pure chromium (melting point 1875 °C) was used to increase the chromium content of the alloy during the first experimental runs, but the rate at which the chromium dissolved in the melt was too low. To alleviate this problem, an Fe-35%Cr master alloy (melting point 1540 °C) was prepared by melting pure chromium and pure iron in an induction furnace. This master alloy, together with pure iron, was put into the two Cr_2O_3-coated alumina crucibles to yield an 80 g Fe-5%Cr alloy in one crucible and an Fe-25%Cr alloy in the other; 15 g of pure Cr_2O_3 was placed on top of the Fe-Cr alloy in each crucible. After the reaction tube had been sealed with a gas-tight seal, argon gas was fed into the furnace, which was then heated to 1873 K at a rate of 80 °C per hour.

An oxygen sensor was preheated at approximately 350 °C in the upper part of the reaction tube before it was lowered rapidly into the melt to a position approximately 5mm from the bottom of the crucible. The molybdenum wire that served as the electrical contact to the melt was simultaneously lowered to a depth of approximately 2mm below the surface of the melt. Because molybdenum dissolves in an Fe-Cr alloy, the molybdenum content of the alloy was analyzed at regular intervals, but it was always found to be less than 1%. This observation justified the assumption that the influence of the molybdenum on the oxygen activity was negligible, especially because the value of the first-order interaction coefficient of molybdenum on oxygen, e_O^{Mo}, is only -0.035.

After the sensor had been immersed in the Fe-Cr melt, a stable cell potential was obtained after a period of 60 to 90 seconds. However, it is important to ensure that such a plateau is a true representation of the actual EMF generated from the electrochemical cell. That the electrical circuit functions properly was very simply determined by measuring the electrical resistance of the cell (*par. 2.1.2.2*) in the

© University of Pretoria

following manner : A galvanostat was used to apply a direct current of 1 mA to the oxygen concentration cell and the cell potential was registered simultaneously. The resistance of those probes, which generated a constant cell potential, was approximately 15 to 25 ohm. When a probe or the molybdenum contact wire did not make proper electrical contact, the electrical resistance was approximately 2 orders of magnitude higher. Therefore, it was assumed that a relatively low cell resistance was an indication of a reliable measuring circuit which functioned properly.

A silica tube (outside diameter 7mm, inside diameter 5mm, length 1m) was used to sample the alloy for chemical analyses after each oxygen measurement. The oxygen content of the sample was determined with a sample fusion method and a LECO TC 136 analyzer was used for this purpose. All the samples were sound and upon close examination showed no entrapped oxide inclusions. At least three determinations of the oxygen content were made on each sample and the average value was used in further calculations.

The chromium content of the Fe-25%Cr alloy was decreased by the addition of small pieces of pure iron to the melt in one crucible, while the chromium concentration of the Fe-5%Cr alloy in the other crucible was increased by the addition of small pieces of the Fe-35%Cr master alloy. Following this, the melts were stirred mechanically at 300 r/min for 45 minutes, and the procedure was repeated.

3.3.2 Cr_2O_3-crucible (no slag)

Because the ultimate aim in this study was to determine the activities in partially liquid slags, an attempt was made to use the same experimental setup as described in *par. 3.3.1.1* but to replace the solid Cr_2O_3 by a partially liquid (Cr_2O_3-saturated-SiO_2-CaO)-slag. However, the initial experiments indicated clearly that the slag diffused through the porous layer of the Cr_2O_3-coated alumina crucible.

© University of Pretoria

The alumina crucible reacted chemically with the slag and consequently partially dissolved into the slag. This problem necessitated the use of a Cr_2O_3 crucible which prevented the chemical reaction between the crucible and the liquid (Cr_2O_3-saturated-SiO_2-CaO)-slag. Because these Cr_2O_3 crucibles were manufactured in the laboratory, it was imperative that the integrity thereof be proven. For this purpose, oxygen activities were determined in the same Fe-Cr alloys as in the previous experiments (in equilibrium with the Cr_2O_3 crucible) and the results of these two sets of experiments were compared. The oxygen activity of an Fe-Cr alloy determined in a Cr_2O_3-coated Al_2O_3 crucible in equilibrium with solid Cr_2O_3, ought to be the same as that of the same Fe-Cr alloy contained in a pure Cr_2O_3 crucible. This check was designed to qualify the laboratory manufactured Cr_2O_3 crucibles.

Since pure Cr_2O_3 crucibles were not commercially available, suitable crucibles had to be manufactured in the laboratory using an adapted version of a technique developed by Vassiliou[31].

The crucibles were formed in a press at room temperature by the use of a steel mould and rubber die, as schematically illustrated in *Figure 3.4*. The inner and outer diameters of the steel mould were 45mm and 120mm respectively. After the crucible attained a pressure of 125 MPa in a hydrostatic press, it was sintered at 1500 °C for a period of 6 hours. This time and temperature were selected following Toker and Darken[32] who studied the sintering behaviour of Cr_2O_3 at high temperatures and found that a mixture of pure Cr_2O_3 and 2% pure chromium powder sintered at 1500 °C for 6 hours, yielded a product of approximately 5 % porosity.

© University of Pretoria

UNIVERSITEIT VAN PRETORIA
UNIVERSITY OF PRETORIA
YUNIBESITHI YA PRETORIA

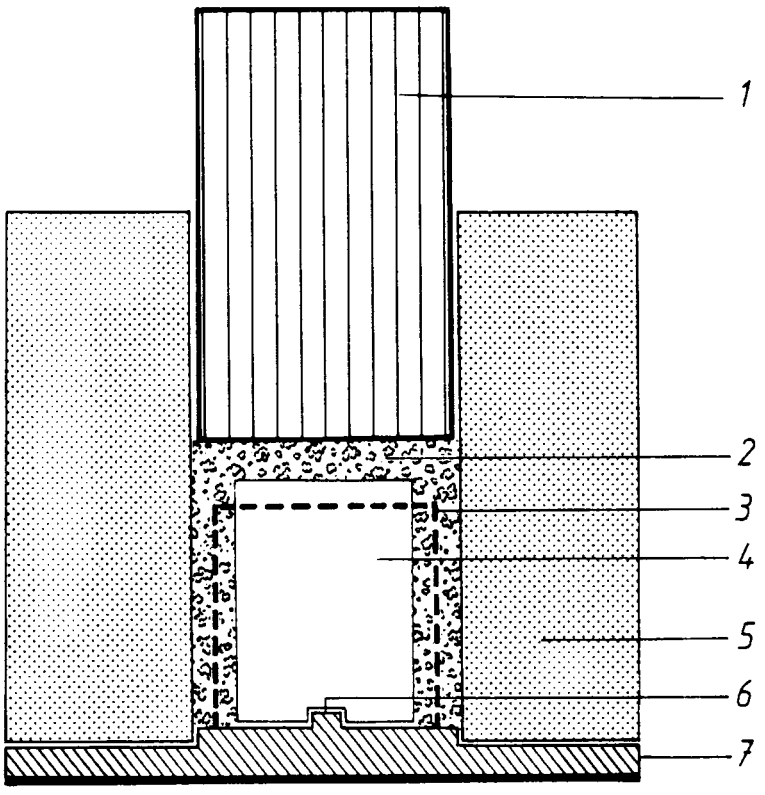

1. Plunger	5. Steel cylinder
2. Powder	6. Center pin
3. Rubber former under pressure	7. Bottom plate
4. Rubber former	

Figure 3.4 - *Steel mould and rubber former*

© University of Pretoria

The experimental procedure was essentially the same as that followed when the Cr_2O_3-coated Al_2O_3 crucibles were used, as described in *par. 3.3.1.2.* However, a single tube lanthanum chromite element furnace equipped with a PID controller, was used. An Fe-35%Cr master alloy together with small pieces of pure iron, were put into the Cr_2O_3 crucible to yield an 80 g Fe-5%Cr alloy. The chromium concentration of the Fe-5%Cr alloy was increased by the addition of small pieces of the Fe-35%Cr master alloy to the melt until the chromium content of the Fe-Cr-alloy reached a level of approximately 25%. The chromium concentration was then decreased by the addition of small pieces of pure iron to the melt and the same procedure of stirring, followed by the measurement of the oxygen potential, was repeated, as described in *par. 3.3.1.2.*

Since these results indicated that the technique could be used successfully for the determination of the oxygen activity in the Fe-Cr-O system when a Cr_2O_3 crucible is used as a container for the Fe-Cr alloy, it was possible to proceed to the next phase of the study.

3.3.3 Cr_2O_3 crucible ($(Cr_2O_3$-saturated-SiO_2-CaO)-slag)

The same experimental technique previously used and described in *par. 3.3.2*, was employed for the determination of the oxygen activity of the Fe-Cr alloy, in which the oxygen potential of the melt was fixed by the equilibrium between a (Cr_2O_3-saturated-SiO_2-CaO)-slag and the chromium dissolved in the iron. Preliminary experiments indicated that the plug type oxygen probes used, were chemically attacked by the slag. After a contact period of approximately two minutes the slag penetrated the alumina tube containing the solid electrolyte and reference electrode, thereby short-circuiting the cell. Hence it was necessary to change the cell design to prevent direct contact between the oxygen sensor and the liquid slag. The crucible assembly designed to achieve this goal is shown schematically in *Figure 3.5*. The

© University of Pretoria

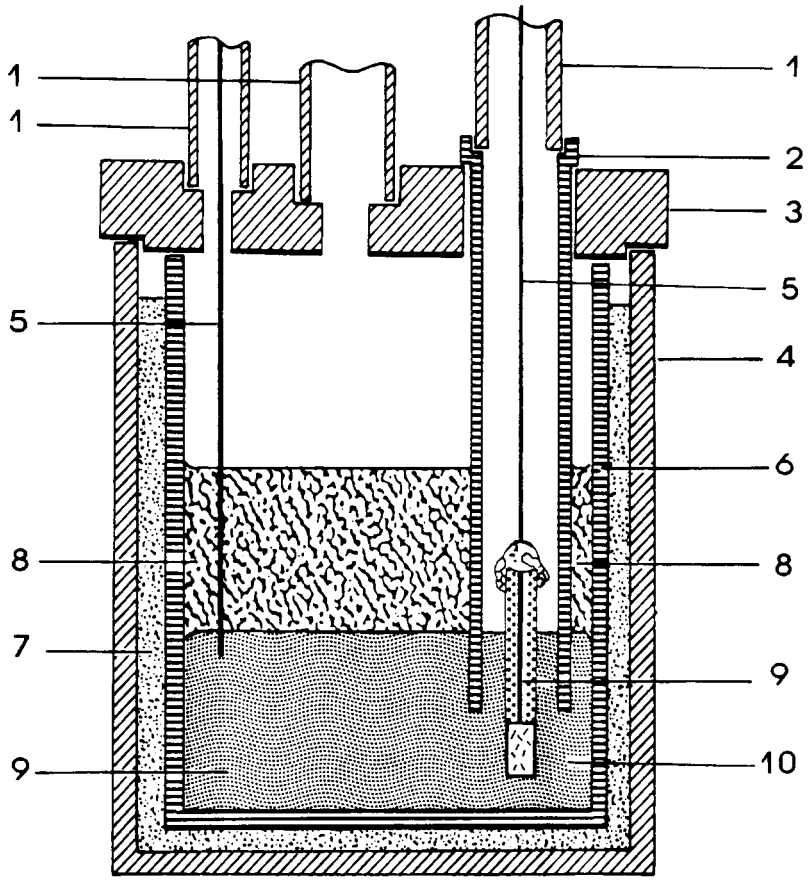

1. Al_2O_3 tubes
2. Cr_2O_3 tube
3. Al_2O_3 guide disk
4. Al_2O_3 crucible
5. Mo wire
6. Cr_2O_3 crucible
7. Cr_2O_3 powder
8. $(Cr_2O_3)_{sat}$ slag
9. Oxygen probe
10. Fe-Cr alloy

Cr_2O_3 crucible dimensions:
Inner diameter 34 mm, Outer diameter 40 mm,
Height 50 mm
Cr_2O_3 tube dimensions:
Inner diameter 12 mm, Outer diameter 20 mm,
Height 40 mm

Figure 3.5 - *Crucible assembly designed to prevent direct contact between the oxygen sensor and $(Cr_2O_{3(sat)}$-SiO_2-$CaO)$-slag*

© University of Pretoria

cylindrical Cr_2O_3 crucible contained the Fe-Cr alloy, while an alumina guide disk supported two alumina tubes as well as a Cr_2O_3 tube. This Cr_2O_3 tube in turn, supported another alumina tube, which served as a guide for the oxygen probes. The Cr_2O_3 tube was positioned in such a way that one end was always below the surface of the Fe-Cr melt.

The slag composition was chosen so that solid Cr_2O_3 and liquid (CrO-SiO_2-CaO)-slag were in equilibrium[33] at 1873 K. A 20 gram mixture containing 16% SiO_2, 16% CaO, and 68% CrO by mass, was prepared by mixing the appropriate quantities of oxide powders under acetone in an agate mortar. The powders were allowed to dry, and were then placed with 90 g of an Fe-Cr alloy containing 5 or 25% Cr in the Cr_2O_3 crucible. Great care was taken to ensure that no slag entered the Cr_2O_3 tube. The oxygen- concentration cells and silica-sampling tubes could now be dipped through the Cr_2O_3 tube directly into the melt, thereby preventing contact with the corrosive liquid slag. Additions of Fe-Cr or Fe were periodically made to change the composition of the alloy as described previously.

3.4 Results and Discussion

Previous researchers[5][26][34] have shown that at 1873 K, stoichiometric Cr_2O_3 is in equilibrium with Fe-Cr alloys which contained between 5 and 25% Cr. Consequently, the oxygen potential of an Fe-Cr alloy in equilibrium with solid Cr_2O_3, is determined by the following metal-oxide equilibrium:

$$2\langle Cr\rangle + \frac{3}{2}[O_2] = \langle Cr_2O_3\rangle, \qquad [3.2]$$

where $\langle\ \rangle$ and [ ] denote the solid and gas phases respectively. The electrochemical cell used in the present study was arranged as follows:

© University of Pretoria

$$(+)\ Mo/(Fe\text{-}Cr)_{alloy}+Cr_2O_3/ZrO_2\text{-}MgO/(Cr+Cr_2O_3)_{ref}\ /\ Mo\ (-), \qquad [3.3]$$

For this cell, equation [2.6] can be rewritten as follows[22][23]:

$$E = \frac{RT}{F}\ln\left[\frac{(P_{O_2})_{alloy}^{\frac{1}{4}} + (P_e)^{\frac{1}{4}}}{(P_{O_2})_{ref}^{\frac{1}{4}} + (P_e)^{\frac{1}{4}}}\right] \qquad [3.4]$$

where E is the electromotive force of cell [3.3],

R is the gas constant,

F is the Faraday constant,

T is the absolute temperature,

$(P_{O2})_{alloy}$ and $(P_{O2})_{ref}$ are the partial pressures of oxygen in the Fe-Cr alloy and the $(Cr+Cr_2O_3)$ reference electrode respectively, and P_e is the partial pressure of oxygen at which the n-type electronic conductivity and the ionic conductivity of the solid electrolyte are equal.

So that the results of the present investigation could be compared to those of previous workers[19][20], the Raoultian chromium activity (a^R_{Cr}) of the Fe-Cr alloy was calculated with reference to pure solid chromium as the standard state. Accordingly, by expanding Equation [3.2] for both electrodes, and by substituting the applicable oxygen potentials in Equation [3.4], the following expression was derived:

$$a^R_{Cr} = \left\{\frac{e^{(\frac{EF}{RT})}[(e^{\frac{\Delta G^\circ}{RT}})^{\frac{1}{6}} + (P_e)^{\frac{1}{4}}] - (P_e)^{\frac{1}{4}}}{(e^{\frac{\Delta G^\circ}{RT}})^{\frac{1}{6}}}\right\}^{-3} \qquad [3.5]$$

ΔG° is the standard free energy change for the reaction depicted by Equation [3.2], and has a value[24] of -6.51704×10^5 J/mol at 1873 K. The P_e-value of the solid electrolyte (ZrO_2 stabilized with 9 mol% MgO) was determined earlier[17], and has

© University of Pretoria

a value of 3.077×10^{-14} atm. The Raoultian chromium activity (a_{Cr}^{R}) and the activity coefficient (γ_{Cr}) of the Fe-Cr alloy contained in Cr_2O_3-coated Al_2O_3 crucibles in equilibrium with pure Cr_2O_3, are summarized in *Table 3.2*.

Table 3.2 - *The Raoultian chromium activities of an Fe-Cr alloy contained in a Cr_2O_3-coated Al_2O_3 crucible, in equilibrium with pure Cr_2O_3 at 1873 K*

Sample no.	Cr %	Cell potential, [mV]	X_{Cr}	a_{Cr}^{R}	$\ln\gamma_{Cr}$
1.1 (D)	22.8	64.3	0.241	0.200	-0.183
1.2 (D)	19.1	73.1	0.202	0.163	-0.214
1.4 (D)	13.7	85.3	0.146	0.123	-0.165
1.5 (D)	10.3	102.0	0.110	0.085	-0.258
1.6 (D)	6.2	124.1	0.066	0.052	-0.237
2.1 (I)	6.1	131.0	0.065	0.045	-0.367
2.2 (I)	9.4	107.0	0.100	0.076	-0.280
2.3 (I)	12.1	95.3	0.129	0.098	-0.268
2.4 (I)	15.8	84.0	0.168	0.127	-0.277
2.5 (I)	21.0	65.5	0.222	0.195	-0.130
2.6 (I)	24.8	56.1	0.261	0.243	-0.072
3.3 (D)	15.8	84.0	0.168	0.127	-0.277
3.4 (D)	10.3	99.8	0.110	0.089	-0.209
3.5 (D)	5.6	138.6	0.060	0.038	-0.444

(D) Measured during a decrease in chromium concentration

(I) Measured during an increase in chromium concentration

© University of Pretoria

The chromium activity and γ_{Cr} determined in the Cr_2O_3 crucibles where the Fe-Cr alloy was in equilibrium with pure solid Cr_2O_3 and with a partially liquid ($Cr_2O_{3(sat)}$-SiO_2-CaO)-slag respectively, are summarized in *Table 3.3*. When the uncertainties in the EMF values, which were in all cases less than $\pm$2 mV, and the uncertainty of $\pm$3 K in the temperature measurement are considered, uncertainties of less than $\pm$4% in the calculated chromium activities are obtained.

Table 3.3 - *The Raoultian chromium activities of an Fe-Cr alloy contained in a Cr_2O_3 crucible, in equilibrium with pure Cr_2O_3 and a ($Cr_2O_{3(sat)}$-SiO_2-CaO)-slag at 1873 K respectively*

Sample no.	Cr %	Cell potential, [mV]	X_{Cr}	a^R_{Cr}	$\ln\gamma_{Cr}$
Cr_2O_3 crucible (no slag)					
4.1 (D)	23.1	69.5	0.243	0.176	-0.315
4.2 (D)	15.8	89.0	0.168	0.112	-0.390
4.3 (D)	9.3	105.7	0.099	0.077	-0.239
4.4 (D)	5.5	141.0	0.059	0.036	-0.490
4.5 (I)	10.3	109.7	0.110	0.071	-0.428
4.6 (I)	16.2	85.7	0.172	0.121	-0.340
4.7 (I)	21.0	72.0	0.222	0.166	-0.282
Cr_2O_3 crucible ($Cr_2O_{3(sat)}$-SiO_2-CaO-slag)					
5.1 (D)	24.5	71.0	0.258	0.171	-0.410
5.2 (D)	15.7	92.2	0.167	0.106	-0.456
5.3 (D)	9.9	115.4	0.105	0.063	-0.512
5.4 (I)	11.9	101.8	0.127	0.085	-0.397
5.5 (I)	18.4	81.8	0.194	0.134	-0.347
5.6 (I)	21.2	77.9	0.224	0.146	-0.427

(D) Measured during a decrease in chromium concentration

(I) Measured during an increase in chromium concentration

© University of Pretoria

UNIVERSITEIT VAN PRETORIA
UNIVERSITY OF PRETORIA
YUNIBESITHI YA PRETORIA

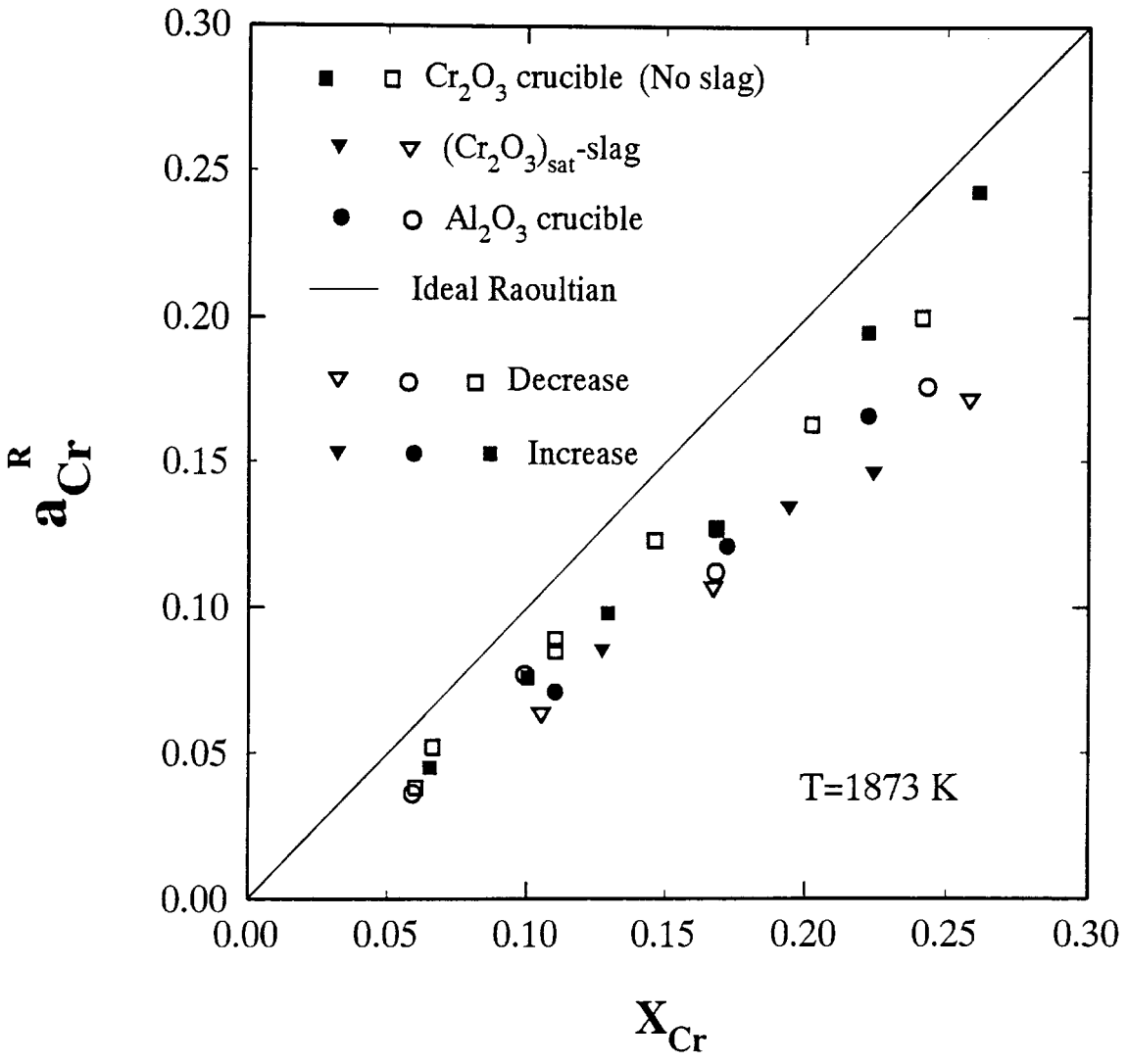

Figure 3.6 - *Relationship between the Raoultian chromium activity at 1873 K and the chromium content of Fe-Cr alloys contained in (a) Al_2O_3 crucibles in equilibrium with pure Cr_2O_3, and (b) Cr_2O_3 crucibles , in equilibrium with pure Cr_2O_3 and a ($Cr_2O_{3(sat)}$-SiO_2-CaO)-slag respectively*

© University of Pretoria

The chromium activities summarized in *Tables 3.2 and 3.3* are shown in *Figure 3.6* as a function of the mole fraction of chromium in the alloy. It is evident that the chromium activity determined during an increase in the chromium concentration of the alloy is in good agreement with that determined during a decrease in chromium content when Cr_2O_3-coated Al_2O_3 crucibles were used to contain the alloy. This is also true for both cases where Cr_2O_3 crucibles contained the alloy, in equilibrium with pure Cr_2O_3 or a partially liquid ($Cr_2O_{3_{sat}}$-SiO_2-CaO)-slag. This observation provides reasonable proof that equilibrium conditions prevailed prior to each activity measurement.

The same graph is shown in *Figure 3.7*, but in this case no distinction is made between measurements made during an increase and decrease in chromium content. It is clear that the values of the Raoultian chromium activities determined in the Fe-Cr alloy contained in Cr_2O_3 crucibles and in equilibrium with pure Cr_2O_3 on the one hand and ($Cr_2O_{3_{sat}}$-SiO_2-CaO)-slag in the other instance are in good agreement. The smaller slag-metal interface in the experiments where the Cr_2O_3 tube was used to prevent direct contact between the oxygen sensor and ($Cr_2O_{3_{sat}}$-SiO_2-CaO)-slag, evidently did not influence the equilibrium conditions because the same activities were obtained in both cases. However, some of the activities measured in the Cr_2O_3-coated alumina crucibles were significantly different from those determined in pure Cr_2O_3 crucibles. This was surprising because in all cases, the activity of Cr_2O_3 in the slag was unity so that the chromium activities in the metal ought to have been the same. If, for instance, it is assumed that the activity of the Cr_2O_3 which is in equilibrium with the alloy when a Cr_2O_3-coated alumina crucible is used, is less than one, the activity of the chromium in the Fe-Cr alloy, increases. Consequently, the difference between the chromium activities measured in the alumina crucible and those measured in the Cr_2O_3 crucibles becomes even greater. The reason for this discrepancy in the activity measurements could not be readily explained and it was necessary to examine various possibilities to establish why erroneous measurements

© University of Pretoria

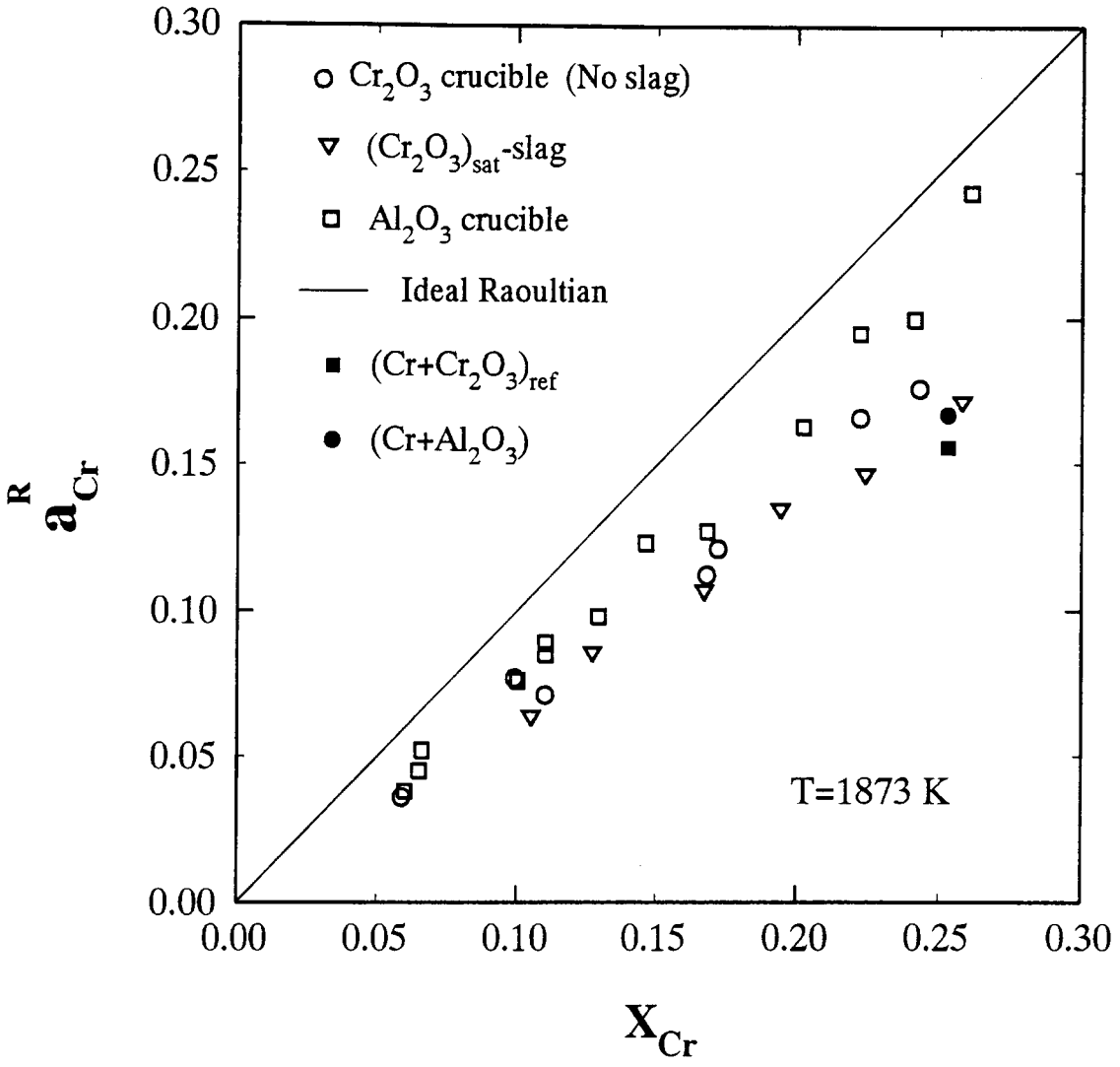

Figure 3.7 - *Relationship between the Raoultian chromium activity and the chromium content of Fe-Cr alloys contained in different crucibles*

© University of Pretoria

UNIVERSITEIT VAN PRETORIA
UNIVERSITY OF PRETORIA
YUNIBESITHI YA PRETORIA

have been made.

The oxygen sensors used for the determination of the oxygen potential in the case where a Cr_2O_3-coated alumina crucible contained the alloy, were slightly different from the probes used for the measurements in the Cr_2O_3 crucibles. These differences are elucidated in *Figure 3.8*. The reference electrode of the probes used for the measurements in the alumina crucibles consisted of a mixture of Cr_2O_3 and Cr powders of which the height was always less than 10mm. The remainder of the alumina tube (length 50mm) was topped up with Al_2O_3 powder (*Figure 3.8 (a)*). A 3mm molybdenum rod of which the one end was slightly sharpened as shown, served as the electrical lead to the Cr_2O_3-reference electrode. Since the alumina tube exhibits a small amount of electronic conduction under the experimental conditions (high temperatures and low oxygen potentials), care has to be taken that the flux of oxygen-ions which migrate from the melt to the reference electrode through the Al_2O_3 tube be negligible with respect to the flux of oxygen-ions migrating from the melt to the reference electrode through the ZrO_2 rod[7]. In this way, polarization at one or both electrodes are minimized. It is therefore important that the ratio of the surface area of the zirconia electrolyte rod to that of the alumina tube in contact with the reference electrode be much greater than one. A calculation, the details of which are summarized in *Appendix 1*, indicates that the height of the reference electrode (Cr_2O_3 and Cr) should indeed be less than 10mm for a 4mm diameter zirconia electrolyte rod, in order to satisfy this condition.

The probes used for the measurement of the oxygen activity in the Cr_2O_3-coated alumina crucibles (*Figure 3.8 (a)*) were dissected and examined by optical and scanning electron microscopy. In some probes a thin layer of alumina powder covered the molybdenum rod and presumably behaved as an isolating layer between the molybdenum rod and the Cr/Cr_2O_3 reference electrode, impeding electrical contact. The possibility that such an insulating layer formes was eradicated by

© University of Pretoria

UNIVERSITEIT VAN PRETORIA
UNIVERSITY OF PRETORIA
YUNIBESITHI YA PRETORIA

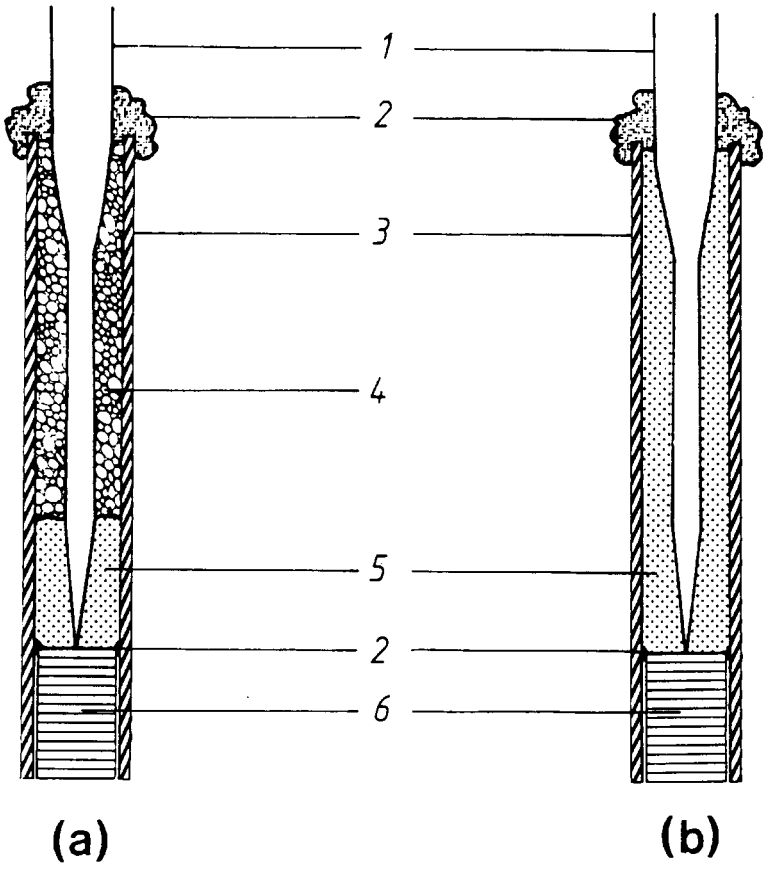

1. Mo rod	4. Al_2O_3 powder
2. Al_2O_3 cement	5. ($Cr + Cr_2O_3$) reference electrode
3. Al_2O_3 tube	6. 9 mol% MgO stabilized ZrO_2 electrolyte

Figure 3.8 - *Schematic illustration of the oxygen probes used during this study, containing different reference electrodes: (a) ($Cr+Cr_2O_3$) and Al_2O_3 (b) ($Cr+Cr_2O_3$) only*

© University of Pretoria

replacing the alumina powder by (Cr_2O_3+Cr) powder as schematically illustrated in *Figure 3.8 (b)*. Although the height of the (Cr+Cr_2O_3) reference electrode was 40mm, the depth of the melt was always less than 15mm, and the probe was dipped into the melt to a position 5mm form the bottom of the crucible. Accordingly, the height of the (Cr+Cr_2O_3) reference electrode indirectly in contact with the melt (via the alumina tube), was still less than 10mm during an electrochemical measurement. Therefore, the conditions required to ensure that the electronic conductivity of the alumina tube does not enhance polarization were still satisfied.

Table 3.4 - *The Raoultian chromium activities of an Fe-24%Cr alloy contained in a Cr_2O_3-coated alumina crucible, determined with two different types of oxygen probes*

Type of probe*	EMF [mV]	Average EMF [mV]	X_{Cr}	a^R_{Cr}
A	73.0			
A	76.1			
A	71.6	74.8	0.253	0.156
A	76.7			
A	76.7			
B	73.7			
B	73.0	72.1	0.253	0.167
B	72.0			
B	69.7			

A: Reference electrode consists of (Cr+Cr_2O_3) only

B: Reference electrode consists of (Cr+Cr_2O_3) and Al_2O_3

© University of Pretoria

The performance of both types of sensors shown in *Figure 3.8* was compared by measuring the Raoultian chromium activity of an Fe-24%Cr alloy contained in a Cr_2O_3-coated alumina crucible. These results are summarized in *Table 3.4* and are also shown in *Figure 3.7*. It is evident that similar chromium activities were determined with the two types of sensors: the average EMF values differed by only 2.7 mV (*Table 3.4*) and the chromium activities are in good agreement with those of the Fe-Cr alloy contained in Cr_2O_3 crucibles, as is evident from *Figure 3.7*. Therefore, the difference in the chromium activities of the Fe-Cr melts when contained in alumina crucibles or Cr_2O_3 crucibles respectively (*Figure 3.7*), can not be ascribed to the use of the different designs of oxygen probes (*Figure 3.8*). More specifically, the thin alumina layer which formed in some probes on the Mo-contact wire, could not have prevented proper electrical contact because almost identical EMF values were obtained when the possibility that such an insulating layer may form, was eliminated.

In a further attempt to clarify the difference in chromium activities measured in the different crucibles (*Figure 3.7*), the original chart recorder outputs (EMF as a function of time), which were obtained during the oxygen measurements were re-examined. This investigation showed that, in the earlier stages of the investigation, the cell resistances of the probes were not always determined. It was later found that it is of the utmost importance that the cell resistance be determined before each measurement, so that the accuracy and reliability of a probe can be verified. The measurements made with unverified probes were consequently discarded in the further analysis. The reassessed, accurate, and reliable values are summarized in *Table 3.5*. It must be emphasized that it was only in the initial stage of the investigation that the cell resistances were not measured. All the measurements made without checking the cell resistance were obtained when the Fe-Cr alloys were contained in Cr_2O_3-coated Al_2O_3 crucibles. Some of these measurements had to be discarded and the reliable measurements are shown in *Table 3.5*. The data pertaining

© University of Pretoria

to measurements in Cr_2O_3 crucibles, shown in *Table 3.3*, all relate to reliable measurements made only after it was established that the probe functioned properly. These accurate and reliable Raoultian chromium activities contained in *Tables 3.3* and *3.5* are shown in *Figure 3.9* as a function of the chromium content.

Table 3.5 - *The reassessed Raoultian chromium activities of an Fe-Cr alloy contained in a Cr_2O_3-coated Al_2O_3 crucible, in equilibrium with pure Cr_2O_3 at 1873 K*

Sample	Cr %	Cell potential, [mV]	X_{Cr}	a^R_{Cr}	$\ln\gamma_{Cr}$
2.1 (I)	6.1	131.0	0.065	0.045	-0.367
2.2 (I)	9.4	107.0	0.100	0.076	-0.280
2.3 (I)	12.1	95.3	0.129	0.098	-0.268
2.4 (I)	15.8	84.0	0.168	0.127	-0.277
3.3 (D)	15.8	84.0	0.168	0.127	-0.277
3.4 (D)	10.3	99.8	0.110	0.089	-0.209
3.5 (D)	5.6	138.6	0.060	0.038	-0.444

(D) Measured during a decrease in chromium concentration

(I) Measured during an increase in chromium concentration

Also shown in *Figure 3.9* are the activities determined in the same system by Fruehan[19] and Heinz[20] respectively. It is evident that the chromium activities determined by Heinz deviate significantly from ideal Raoultian behaviour. There is reason to believe that Heinz may not have attained equilibrium in the course of his experiments. Heinz used essentially the same experimental technique as in the present study, the major difference being the way in which the alloy additions were

© University of Pretoria

UNIVERSITEIT VAN PRETORIA
UNIVERSITY OF PRETORIA
YUNIBESITHI YA PRETORIA

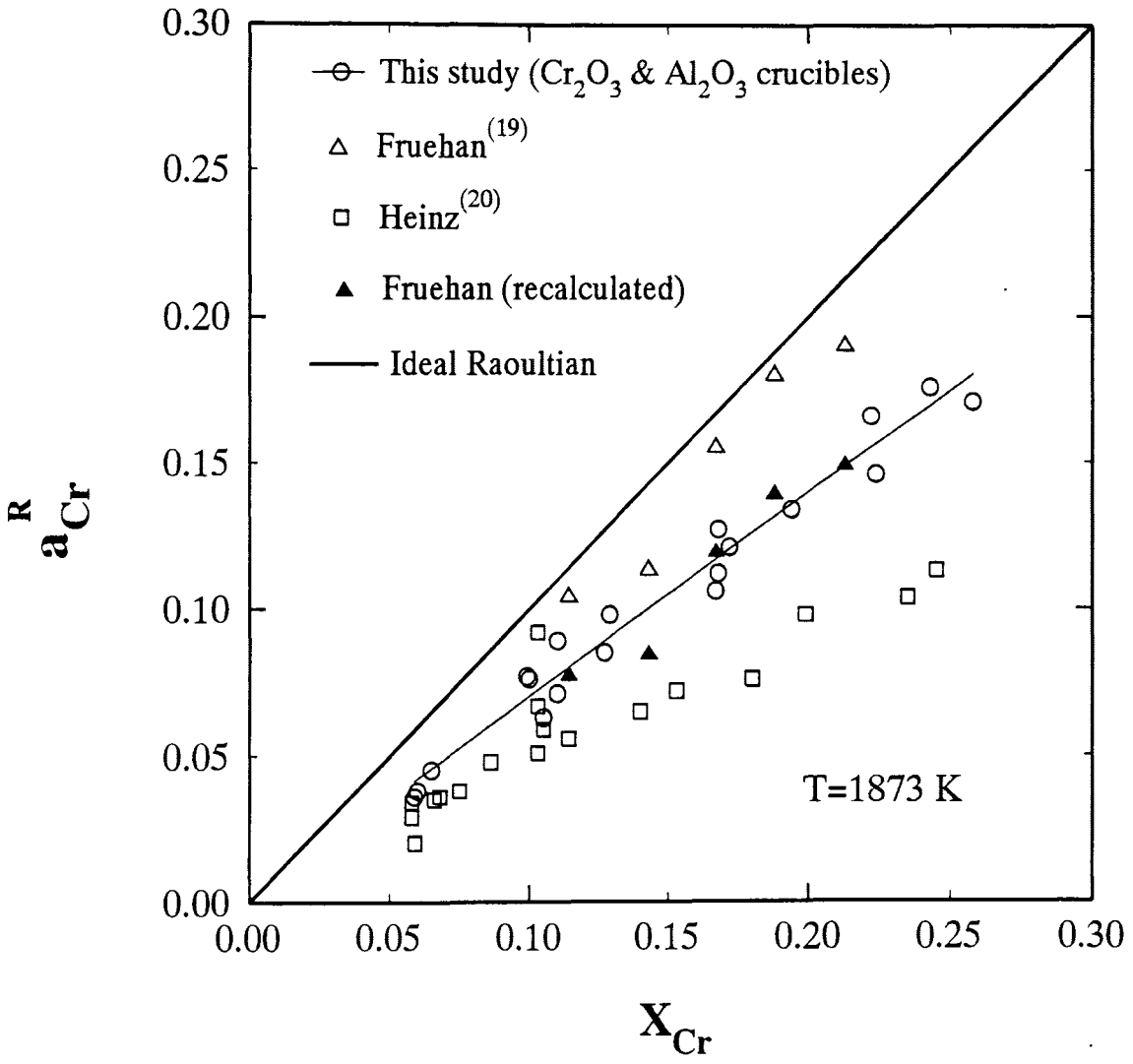

Figure 3.9 - *Comparison of Raoultian chromium activities*

© University of Pretoria

UNIVERSITEIT VAN PRETORIA
UNIVERSITY OF PRETORIA
YUNIBESITHI YA PRETORIA

made. Consideration of the implications of these different alloying techniques may lead to an explanation for the difference in activity values determined in the Fe-Cr-O system. When pure chromium with a melting point of 2148 K is dissolved in a liquid iron alloy at 1873 K, the applicable dissolution rate can be derived from an analysis of heterogeneous reaction kinetics[35]. In such an analysis, a solid impermeable particle is assumed to dissolve by the combined effects of diffusion through a boundary layer and a reaction at the interface between the boundary layer and the solid particle. Conversely, for the dissolution of an Fe-Cr alloy with a melting point of 1813 K, only dissolution kinetics need to be considered, i.e. melting of the Fe-Cr alloy followed by the dissolution of the one liquid into the other. The rate at which the Fe-Cr alloy will dissolve, is evidently much higher than that of a pure chromium particle.

In the present study, the alloying additions consisted of an Fe-Cr alloy with a melting point of 1813 K, and the melt was stirred mechanically for an extended period of 45 minutes. That equilibrium conditions prevailed during the determination of the oxygen activity was confirmed by a comparison of the oxygen activity determined during an increase in chromium content with measurements made when the chromium content was decreased. Heinz, on the other hand, made his measurements only 5 minutes after adding pure chromium. That his measured results are not in full agreement with those of the present study may be related to the fact that he may not have attained equilibrium in the course of his experiments.

There is also a significant difference between the chromium activities determined in the course of the present study, and those of Fruehan[19] and these differences need to be explained. Fruehan used a ZrO_2-4%CaO solid electrolyte in his electrochemical oxygen concentration cell and assumed[36] that this electrolyte was a pure ionic conductor at 1873 K and at oxygen partial pressures greater than 3×10^{-13} atm. Fischer and Pieper[37] subsequently determined a P_e-value of 1.2×10^{-15} atm.

© University of Pretoria

a ZrO_2-6%CaO solid electrolyte at 1873 K. This result indicated that the solid electrolyte used by Fruehan may well have exhibited a noticeable measure of electronic conduction. For instance, if it is assumed that the P_e-value measured by Fischer and Pieper[37] for a ZrO_2-6%CaO electrolyte is applicable to the ZrO_2-4%CaO solid electrolyte used by Fruehan[19], and the chromium activities are re-calculated, good agreement is found with the results obtained in this investigation. These re-calculated activities are also shown in *Figure 3.9*. The importance of taking into consideration the electronic conductivity of a solid electrolyte when it is used in an oxygen concentration cell, has been exemplified in earlier studies[11][13][14][18]. This important point is re-emphasized by the present findings: the apparent discrepancy in the activities measured by Fruehan[19] and in this study, is completely resolved if the electronic conductivity of the solid electrolyte used is duly taken into account.

Also summarized in *Tables 3.3 and 3.5*, are the Raoultian activity coefficients γ_{Cr}, calculated for each experiment from the general relationship:

$$\gamma_{Cr} = \frac{a_{Cr}^{R}}{X_{Cr}} \qquad [3.6]$$

where X_{Cr} and γ_{Cr} are the mol fraction chromium in the alloy and the Raoultian activity coefficient of chromium respectively. The interaction coefficients resulting from the Taylor series expansion of the partial excess Gibbs free energy of mixing of dilute component *i* (in an n-component system) where the solvent, iron, is designated component 1, and by neglecting the third-order terms, can be expressed as[38]:

$$\ln \gamma_i = \ln \gamma_i^0 + \sum_{j=2}^{n} \epsilon_i^j \cdot X_j + \sum_{j=2}^{n} \rho_i^j \cdot X_j^2 + \sum_{j=2}^{n} \sum_{k=2\ (j<k)}^{n} \rho_i^{j,k} \cdot X_j X_k \qquad [3.7]$$

where ϵ_i^j and ρ_i^j are the first and second order Raoultian interaction coefficients of component j on component i and $\rho_i^{j,k}$ is the cross-product second-order term. If it is

© University of Pretoria

UNIVERSITEIT VAN PRETORIA
UNIVERSITY OF PRETORIA
YUNIBESITHI YA PRETORIA

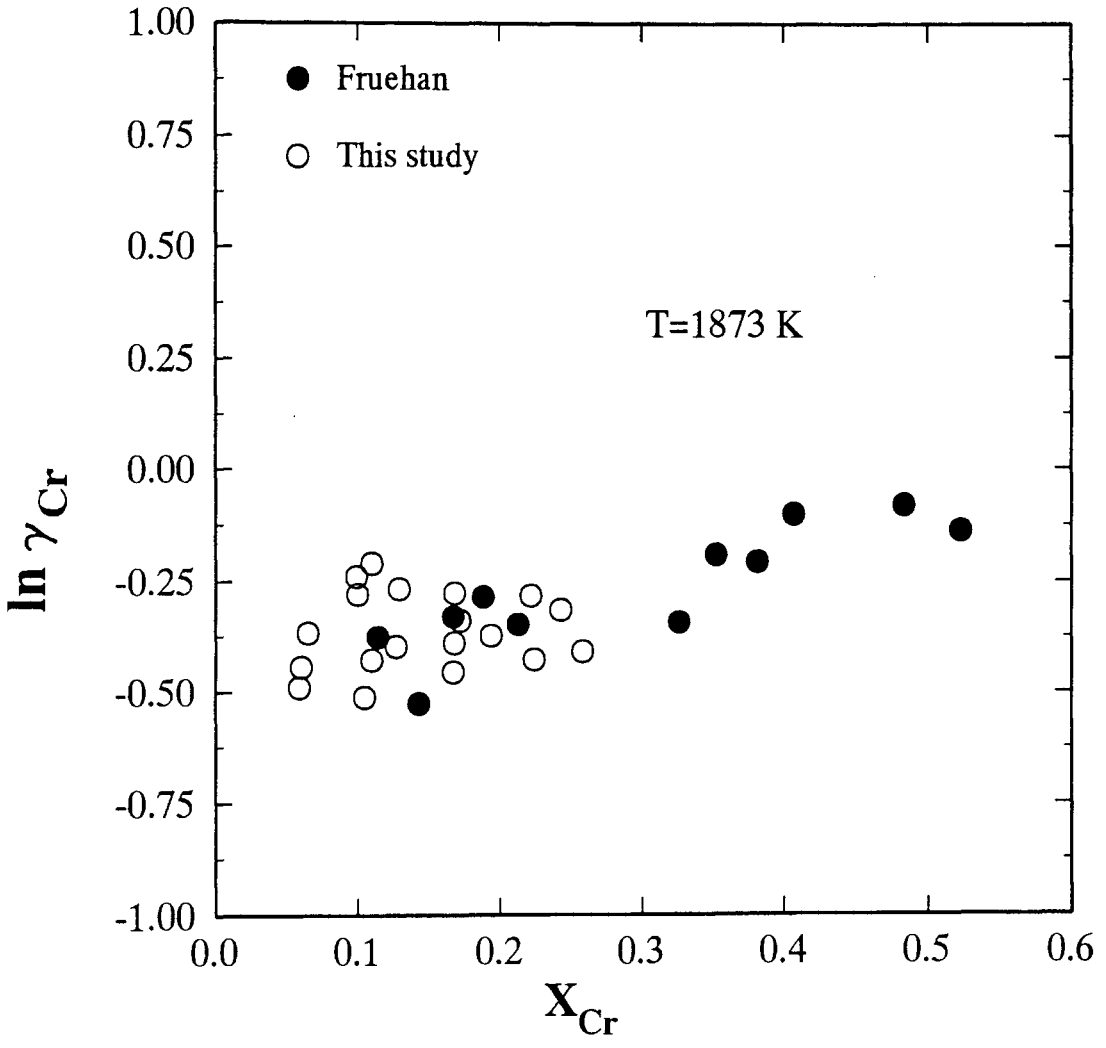

Figure 3.10 - *Relationship between the activity coefficient γ_{Cr} and the chromium content of an Fe-Cr alloy, determined in this study compared to that of Fruehan[19] (recalculated)*

© University of Pretoria

assumed that the mol fraction oxygen is negligible and that the second order interaction coefficient $\rho_{Cr}^{Cr}=0$, equation [3.7] is simplified as follows for the Fe-Cr-O system:

$$\ln \gamma_{Cr} = \ln \gamma_{Cr}^{o} + \epsilon_{Cr}^{Cr} \cdot X_{Cr} \qquad [3.8]$$

The activity coefficient γ_{Cr} determined in this way, is compared to the value suggested by Fruehan[19] in *Figure 3.10*. However, it should be emphasized that the γ_{Cr} values referred to as Fruehan's results, are actually recalculated values, using the original data but incorporating the P_e-value compensation for his EMF measurements. Evidently, the results of this study are in good agreement with that obtained by Fruehan but it should be noted that the chromium content of the alloy studied by Fruehan, varied between 9 and 51 %Cr compared to the range of 5 to 25 %Cr of this study. A least square linear regression method was used to fit a straight line through the data points determined in this study (*Figure 3.10*) and the linear relationship can be expressed as: $\ln\gamma_{Cr} = -0.387 + 0.1965(N_{Cr})$ with a correlation coefficient, r, of 0.18. Although the correlation coefficient is fairly low, this relationship was used to determine γ_{Cr}^{o} as 0.6791 and ϵ_{Cr}^{Cr} as 0.1965 (equation [3.8]).

The relationship between the first order Raoultian (ϵ_i^j) and Henrian (e_i^j) activity coefficients respectively, has been defined by Lupis and Elliott[39] as :

$$\epsilon_i^j = 230 \cdot \frac{M_j}{M_1} \cdot e_i^j + \left[\frac{M_1 - M_j}{M_1}\right] \qquad [3.9]$$

where M_1 and M_j are the molecular weight of the solvent, Fe, and component j respectively. Therefore, by substituting the first order Raoultian interaction coefficient determined in this study ($\epsilon_{Cr}^{Cr} = 0.1965$) into equation [3.9], the first order Henrian activity coefficient e_{Cr}^{Cr}, is calculated as 0.0006.

The standard free energy change (ΔG°) for the reaction

© University of Pretoria

$$\langle Cr \rangle = (\underline{Cr})_{Fe} \qquad [3.10]$$

is related to γ°_{Cr} as follows[38]:

$$\Delta G^{\circ} = RT \ln[\frac{\overset{\circ}{\gamma}_{Cr} \cdot M_{Fe}}{100 \cdot M_{Cr}}] \qquad [3.11]$$

where M_{Fe} and M_{Cr} are the molecular masses of Fe (55.85) and Cr (52) respectively. This yields a ΔG° value at 1873 K of -76.6 kJ/mol.

The Henrian oxygen activity of the Fe-Cr alloy was calculated by consideration of the following equilibrium reaction:

$$(\underline{O})_{Fe} = \tfrac{1}{2}[O_2], \qquad [3.12]$$

where $(\underline{O})_{Fe}$ denotes the oxygen at infinite dilution in liquid iron, and the standard state is 1 % oxygen (by mass) in the iron. Therefore, by substituting the applicable oxygen potentials for the reference electrode (equation [3.2]) and the alloy (equation [3.12]) into equation [3.4], the following expression was derived:

$$a_O^H = \left\{ \frac{e^{(\frac{EF}{RT})}[(P_{O_2})_{ref}^{\frac{1}{4}} + (P_e)^{\frac{1}{4}}] - (P_e)^{\frac{1}{4}}}{(e^{\frac{-\Delta G^{\circ}}{RT}})^{\frac{1}{2}}} \right\}^2 \qquad [3.13]$$

ΔG° is the standard free energy change for the reaction depicted by equation [3.12] and has a value of 1.22529×10^5 J/mol at 1873 K[7]. The activity coefficient of oxygen f_O, was calculated by the following general relationship:

$$f_O = \frac{a_O^H}{(\%\underline{O})_{Fe}} \qquad [3.14]$$

where a_O^H is the Henrian activity of oxygen and $(\%\underline{O})_{Fe}$ is the dissolved oxygen content of the Fe (per cent by mass), determined by chemical analysis.

© University of Pretoria

The Henrian oxygen activities (a_O^H), the oxygen content (%O) and the Henrian activity coefficient, f_O, are summarized in *Table 3.6*. The oxygen contents of the alloys (%O) are compared to those of previous workers in *Figure 3.11*. It is evident that the oxygen concentration of the Fe-Cr alloy is the lowest in the range 5 to 10% Cr (370 ppm) and these results are in good agreement with those of Chen and Chipman[34]. The oxygen content determined by Fruehan[19] is slightly lower.

The following reaction occurs under equilibrium conditions:

$$2(\underline{Cr})_{Fe} + 3(\underline{O})_{Fe} = <Cr_2O_3> \qquad [3.15]$$

If it is assumed that $f_{Cr}=1$, the following equation is obtained:

$$\log a_O^H = -\frac{2}{3}\log (\%\underline{Cr}) + \frac{1}{3}\log a_{<Cr_2O_3>} + \frac{1}{3}\log K \qquad [3.16]$$

The Henrian oxygen activities determined from the experimental results are shown as a function of the mass percentage chromium in the alloy, in *Figure 3.12* and these results may be compared to the expected relationship in equation [3.16]. The slope of the curve is approximately -2/3 indicating that $a_{<Cr2O3>} = 1$ and this result confirms that the slag was indeed saturated with Cr_2O_3.

The Henrian interaction coefficients resulting from the Taylor series expansion of the partial excess Gibbs free energy of mixing of dilute component *i* (in an n-component system) where the solvent, iron, is designated component 1, (neglecting the third-order terms) can be expressed as[38]:

$$\log f_i = \sum_{j=2}^{n} e_i^j . (\%j) + \sum_{j=2}^{n} r_i^j . (\%j)^2 + \sum_{j=2}^{n} \sum_{k=2\ (j<k)}^{n} r_i^{j,k} . (\%j)(\%k) \qquad [3.17]$$

where e_i^j and r_i^j are the first and second order Henrian interaction coefficients of component j on component i, and $r_i^{j,k}$ is the cross-product second-order term. The terms *%j* and *%k* indicate the concentration of components *j* and *k* in mass %.

© University of Pretoria

UNIVERSITEIT VAN PRETORIA
UNIVERSITY OF PRETORIA
YUNIBESITHI YA PRETORIA

Table 3.6 - *The Henrian oxygen activities and oxygen activity coefficients of an Fe-Cr alloy at 1873 K*

Sample no.	Cr %	EMF [mV]	a_O^H	[O] [ppm]	log f_O	log f_O^{Cr}	f_{Cr}	log K_{Cr-O}
2.1 (I)	6.1	131.0	0.018	369	-0.310	-0.304	0.992	3.6693
2.2 (I)	9.4	107.0	0.013	455	-0.553	-0.545	0.993	3.7418
2.3 (I)	12.1	95.3	0.011	430	-0.604	-0.596	0.998	3.7466
2.4 (I)	15.8	84.0	0.009	n.d	-	-	-	-
3.3 (D)	15.8	84.0	0.009	n.d.	-	-	-	-
3.4 (D)	10.3	99.8	0.011	n.d.	-	-	-	-
3.5 (D)	5.6	138.6	0.020	n.d.	-	-	-	-
4.1 (D)	23.1	69.5	0.007	n.d.	-	-	-	-
4.2 (D)	15.8	89.0	0.010	n.d.	-	-	-	-
4.3 (D)	9.3	105.7	0.013	n.d.	-	-	-	-
4.4 (D)	5.5	141.0	0.021	373	-0.253	-0.246	0.991	3.5632
4.5 (I)	10.3	109.7	0.013	401	-0.480	-0.474	0.997	3.6094
4.6 (I)	16.2	85.7	0.009	452	-0.688	-0.680	1.002	3.6773
4.7 (I)	21.0	72.0	0.008	551	-0.865	-0.856	1.005	3.7230
5.1 (D)	24.5	71.0	0.007	679	-0.962	-0.951	1.004	3.6100
5.2 (D)	15.7	92.2	0.010	501	-0.690	-0.682	1.000	3.5792
5.3 (D)	9.9	115.4	0.014	424	-0.468	-0.461	0.995	3.5381
5.4 (I)	11.9	101.8	0.012	427	-0.558	-0.551	0.998	3.6350
5.5 (I)	18.4	81.8	0.009	526	-0.780	-0.771	1.002	3.6465
5.6 (I)	21.2	77.9	0.008	573	-0.843	-0.833	1.004	3.5971

(D) Measured during a decrease in chromium concentration

(I) Measured during an increase in chromium concentration

© University of Pretoria

UNIVERSITEIT VAN PRETORIA
UNIVERSITY OF PRETORIA
YUNIBESITHI YA PRETORIA

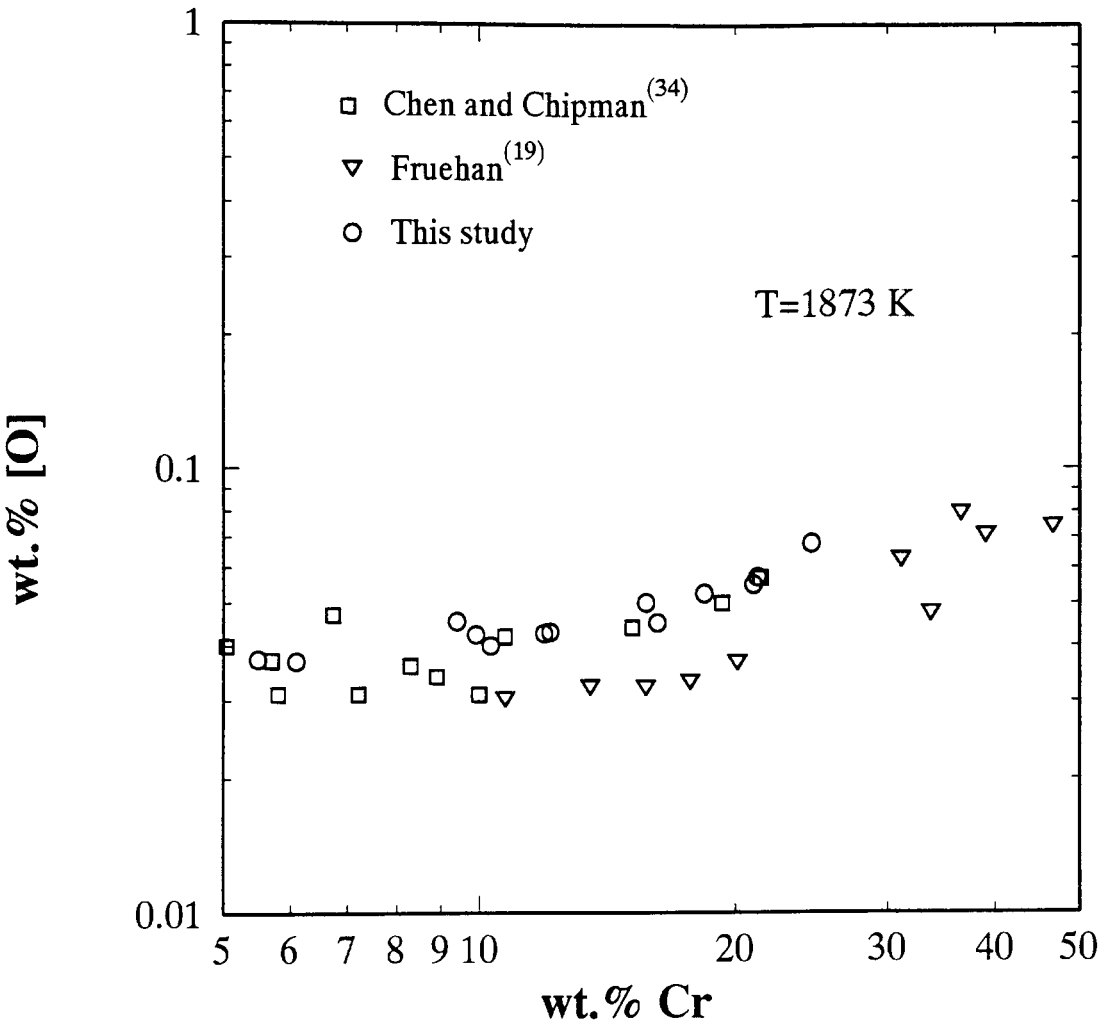

Figure 3.11 - *Relationship between the chromium concentration and the oxygen content of Fe-Cr alloys.*

© University of Pretoria

Equation [3.17] simplifies as follows for the Fe-Cr-O system: ($r_i^{j,k}$ is omitted because it is not known with sufficient accuracy) :

$$\log f_O = e_O^{Cr} \cdot (\%\underline{Cr}) + r_O^{Cr} \cdot (\%\underline{Cr})^2 + e_O^{O} \cdot (\%\underline{O}) + r_O^{O} \cdot (\%\underline{O})^2 \quad [3.18]$$

If the interaction parameters f_O^{Cr} and f_O^{O} are defined as:

$$\log f_O^{Cr} = e_O^{Cr} \cdot (\%\underline{Cr}) + r_O^{Cr} \cdot (\%\underline{Cr})^2 \quad [3.19]$$

and

$$\log f_O^{O} = e_O^{O} \cdot (\%\underline{O}) + r_O^{O} \cdot (\%\underline{O})^2 \quad [3.20]$$

respectively, equation [3.18] can be rewritten as follows:

$$\log f_O = \log f_O^{Cr} + \log f_O^{O} \quad [3.21]$$

The interaction parameter f_O^{Cr} calculated by equation [3.19] with $e_O^{O}=-0.2$[40], is shown in *Figure 3.13* as a function of the mass percentage chromium. An algorithm that fits these data points is $\log f_O^{Cr} = -0.056(\%\underline{Cr}) + 0.0007(\%\underline{Cr})^2$, meaning that $e_O^{Cr} = -0.056$ and $r_O^{Cr} = 0.0007$.

Wagner[38] derived an useful relationship between first order Raoultian interaction coefficients, ϵ, as follows:

$$\epsilon_i^j = \epsilon_j^i \quad [3.22]$$

and Lupis and Elliott[41] derived the relationship between the second order Raoultian interaction coefficient and the Henrian interaction coefficients as:

$$\rho_i^j = \frac{230}{M_{Fe}} [100M_j^2.r_i^j + M_j(M_{Fe} - M_j)e_i^j] + \frac{1}{2}(M_{Fe} - \frac{M_j}{M_{Fe}})^2 \quad [3.23]$$

where M_{Fe} and M_j are the molecular mass of the solvent Fe and component *j* respectively. If the interaction coefficients $e_O^{Cr} = -0.056$ and $r_O^{Cr} = 0.0007$ are

© University of Pretoria

UNIVERSITEIT VAN PRETORIA
UNIVERSITY OF PRETORIA
YUNIBESITHI YA PRETORIA

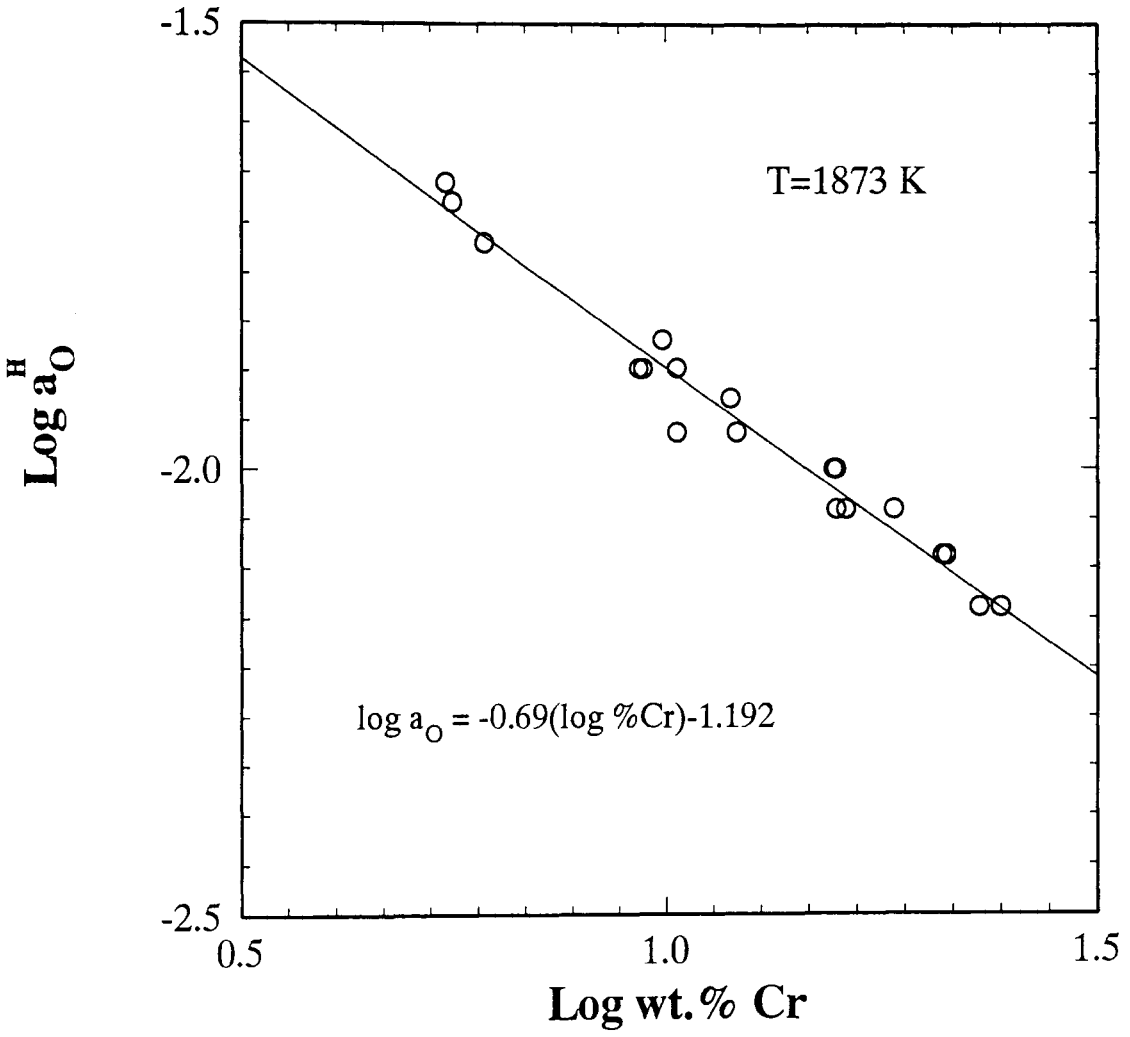

Figure 3.12 - *Relationship between the chromium content of Fe-Cr alloys and the Henrian oxygen activity at 1873 K.*

© University of Pretoria

UNIVERSITEIT VAN PRETORIA
UNIVERSITY OF PRETORIA
YUNIBESITHI YA PRETORIA

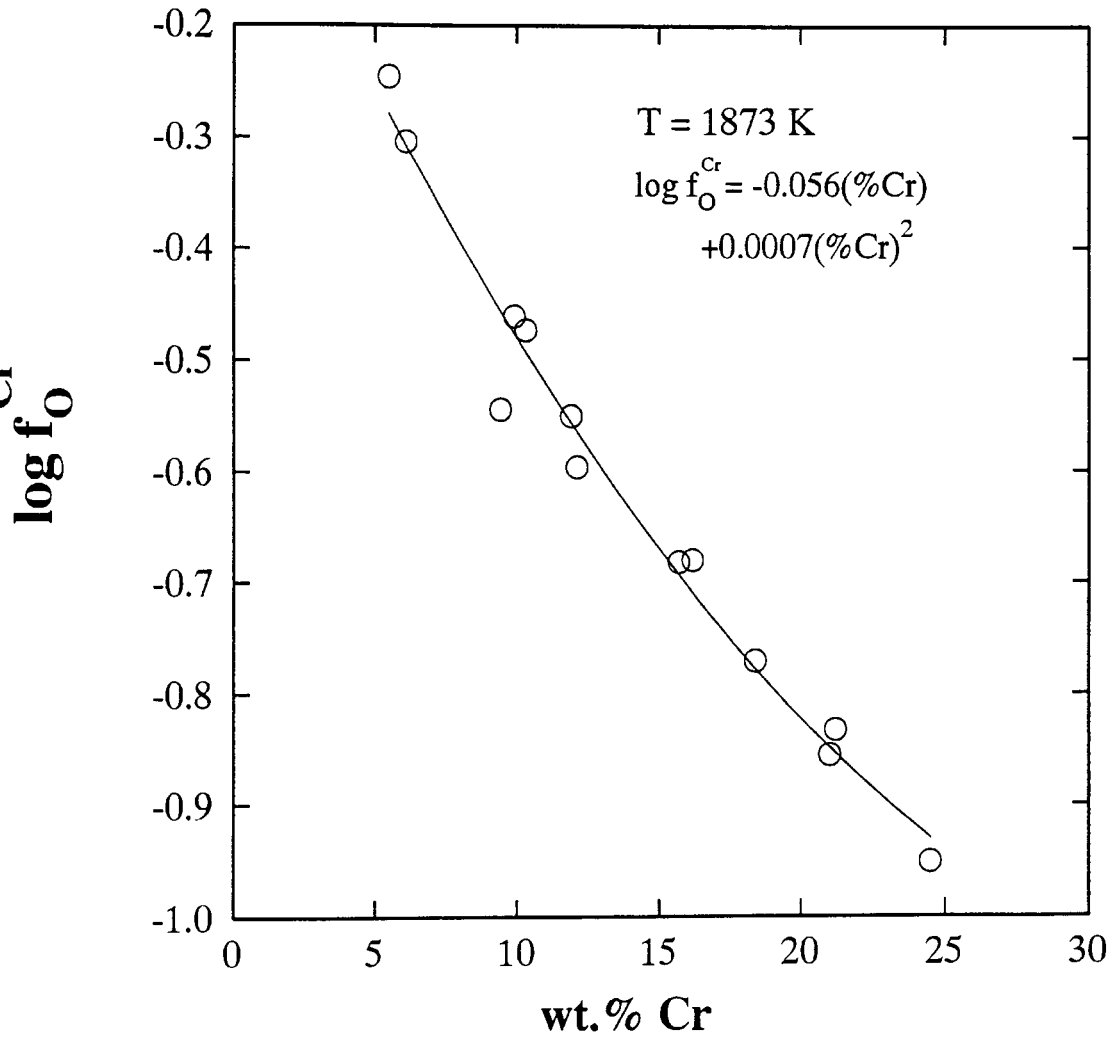

Figure 3.13 *Relationship between the oxygen interaction parameter f_O^{Cr}, and the chromium content of an Fe-Cr alloy at 1873 K*

© University of Pretoria

UNIVERSITEIT VAN PRETORIA
UNIVERSITY OF PRETORIA
YUNIBESITHI YA PRETORIA

substituted in equation [3.9], ϵ_O^{Cr}= -11.923 and according to equation [3.22], ϵ_{Cr}^{O}=-11.923. Similarly, e_{Cr}^{O}=-0.1918 and ρ_O^{Cr} = 13.13 (equation [3.23]). The interaction coefficients determined in this study, are summarized in *Table 3.7.*

Table 3.7 - *The interaction coefficients determined in this study compared to those of Sigworth and Elliott*[40]

Coefficient	This study	Sigworth and Elliott
γ_{Cr}^{o}	0.6793	1.0
ϵ_{Cr}^{Cr}	0.1965	0.0047*
e_{Cr}^{Cr}	0.0006	-0.0003
e_{O}^{Cr}	-0.0560	-0.04
r_{O}^{Cr}	0.0007	0.0
ϵ_{O}^{Cr}	-11.9230	-8.50*
ϵ_{Cr}^{O}	-11.9230	-8.50*
e_{Cr}^{O}	-0.1918	-0.14
ρ_{O}^{Cr}	13.1300	-0.59*

* Calculated from e_i^j values

The main reason for the substantial difference in ρ_O^{Cr} (*Table 3.7*) is directly related to the coefficient r_O^{Cr}, determined as 0.0007 in this study compared to 0.0 of Sigworth and Elliott (equation [3.23]).

As previously indicated, the activity of Cr_2O_3 is unity and the constant $K_{Cr\text{-}O}$ for the reaction depicted by equation [3.15], is related to a_O^H and a_{Cr}^H as follows:

$$K_{Cr-O} = \frac{1}{a_{(Cr)}^2 \cdot a_{(O)}^3} \qquad [3.24]$$

© University of Pretoria

The activity coefficient of chromium (f_{Cr}) was calculated by using the interaction coefficients determined in this study (e_{Cr}^{O}=-0.1918, e_{Cr}^{Cr}=0.0006) and these values are summarized in *Table 3.6*. The constant $K_{Cr\text{-}O}$ (equation [3.24]), summarized in *Table 3.6* is fairly constant over the range of chromium concentration of the alloy. Log $K_{Cr\text{-}O}$ = 3.6413$\pm$0.12 and the standard free energy change of the reaction depicted by equation [3.15] at 1873 K is -1.3056x10^5 J/mol. This is in good agreement with a value of 3.567 for log $K_{Cr\text{-}O}$ and -1.2822x10^5 J/mol for ΔG° obtained from the results presented in *Figure 3.12*, where it was assumed that f_{Cr}=1.

By combining the standard free energy changes for the reactions depicted by equations [3.10], [3.12] and [3.15], ΔG° for the reaction

$$2\langle Cr\rangle + \frac{3}{2}O_2 = \langle Cr_2O_3\rangle \qquad [3.25]$$

determined in this study is -651.35 kJ/mol. This value is compared to those of previous workers in *Table 3.8*.

Table 3.8 - *ΔG° for the reaction $2\langle Cr\rangle + 3/2O_2 = \langle Cr_2O_3\rangle$ as determined in this study, compared to those of previous workers*

Previous studies	**ΔG° [kJ/mol]**
Barin and Knacke[42]	643.17
Toker, Darken and Muan[43]	646.78
This study	651.35
Elliott and Gleiser[24]	651.70

The results summarized in *Table 3.8* clearly indicates that the standard free energy change for the reaction depicted by equation [3.24] determined in this study, is in

© University of Pretoria

good agreement with those of previous workers. These results prove that the oxygen activity measurements made in the Fe-Cr-O system, are accurate and reliable.

This study has furthermore shown that the experimental cell-design in which a Cr_2O_3-tube is used to prevent direct contact between an oxygen probe and a corrosive Cr_2O_3-containing, partially liquid slag, can be used successfully to determine the chromium activity in an Fe-Cr alloy at 1873 K, of which the oxygen activity is low. Therefore, the same type of crucible assembly was used in the development of the electrochemical technique for the determination of the oxygen activity in the Mn/MnO system at 1873 K, of which the oxygen potential is lower than that of the Cr/CrO system. The details of this investigation are discussed in the next chapter.

© University of Pretoria

UNIVERSITEIT VAN PRETORIA
UNIVERSITY OF PRETORIA
YUNIBESITHI YA PRETORIA

CHAPTER 4

ACTIVITY MEASUREMENTS IN (MnO-SiO_2-MgO)-SLAGS IN EQUILIBRIUM WITH (MnO-MgO) SOLID SOLUTIONS AND Mn METAL AT 1873 K

4.1 Introduction

A literature survey indicated that successful electrochemical measurements have not been made previously in any slag in the liquid state at 1873 K. However, it was shown in this study (*Chapter 3*), that it was possible to make accurate and reliable measurements in the Fe-Cr-O system, where an Fe-Cr alloy was in equilibrium with a Cr_2O_3-saturated liquid slag at 1873 K. There is therefore reasonable evidence that it should be possible to make successful electrochemical measurements in the Mn/MnO system at 1873 K, provided that the crucible assembly prevents direct contact between the oxygen probe and the liquid slag and polarization effects at one or both electrodes of the sensor can be minimized. However, the oxygen potential in the Mn/MnO system is lower than that of the Cr/Cr_2O_3 system, indicating that a different reference electrode might have to be used.

In order to determine the MnO-activity of a (MnO-SiO_2-MgO)-slag by the electrochemical technique, the oxygen potential of the slag has to be determined and a representative slag sample has to be taken simultaneously. However, because the liquid slag is in equilibrium with a (MnO-MgO) solid solution[44], the slag sample has to be quenched to separate the solid solution and the liquid slag phases so that the MnO content of the liquid slag phase can be determined uniquely. It was therefore necessary to develop a slag sampling technique which would ensure that the slag samples were quenched effectively.

© University of Pretoria

4.2 Thermodynamic Relations

The relationship between the activity of MnO in (MnO-SiO_2-MgO)-slags and the composition of such slags can be determined by equilibrating the slag with melts of known manganese activity. The activity of MnO in the (MnO-SiO_2-MgO)-slag can then be determined from the following relationships:

$$(Mn) + \frac{1}{2}[O_2] \rightleftharpoons <MnO>_{slag} \qquad [4.1]$$

where < >, [ ], and ( ) denote the solid, gas and liquid phases respectively. The activity of MnO with reference to pure solid MnO can be expressed as:

$$a_{<MnO>} = (P_{O_2})^{\frac{1}{2}} . a_{Mn} . \exp \frac{-\Delta G^\circ}{RT} \qquad [4.2]$$

Since the standard free energy change for the reaction depicted by equation [4.1] is known ($\Delta G^\circ = -2.41795 \times 10^5$ J/mol)[42] and the activity of Mn is unity when pure molten Mn metal is equilibrated with the slag, the activity of MnO can be obtained if the partial pressure of oxygen (P_{O2}) is known. This value of P_{O2} in the slag can be determined by electrochemical means. Using the Schmalzried equation[23][24] as discussed in *Chapter 2*, the EMF of an appropriate electrochemical cell can be expressed as:

$$E = \frac{RT}{F} \ln\left[\frac{(P_{O_2})_{slag}^{\frac{1}{4}} + (P_e)^{\frac{1}{4}}}{(P_{O_2})_{ref}^{\frac{1}{4}} + (P_e)^{\frac{1}{4}}}\right] \qquad [4.3]$$

The activity coefficient γ_{MnO}, is related to the activity of MnO as follows:

$$a_{MnO} = \gamma_{MnO} . N_{MnO} \qquad [4.4]$$

N_{MnO} is the mol fraction MnO of the slag.

© University of Pretoria

Furthermore, the relationship between the activity of MnO in the slag and the activity of MnO in the (MnO-MgO) solid solution phase with reference to pure solid MnO respectively, can be expressed as:

$$a_{<MnO>slag} = a_{<MnO>solid\ solution} \qquad [4.5]$$

4.3 Experimental Aspects

In the course of the initial experimental runs using a similar crucible assembly to that depicted in *Figure 3.5*, it was found that slag samples could not effectively be taken with a steel rod, a technique commonly used for this purpose in the study of slag/metal systems in the temperature range below 1450 °C. Therefore a means had to be devised to establish the prevailing slag phase composition. The details of this technique are discussed below.

4.3.1 Analysis of the Phase Composition of the Slag

The same slag/metal composition used in the electrochemical cell-arrangement were equilibrated separately. However, the actual thermal cycle to which the electrochemical cell-arrangement was subjected, was simulated closely in these experiments. These experiments were performed in view of establishing the phase relationships in the slag at a given temperature and it was assumed that the phase composition of the slag in the simulation experiments was the same as that prevailing during the actual electrochemical measurements. The effective quenching of the slag is of the utmost importance if the phase relationships prevailing at 1873 K are to be determined by metallographic means at room temperature. This was achieved by quenching the whole crucible containing both the slag and the metal. One gram each of the oxide mixtures and manganese metal powder were thoroughly mixed before equilibration and contained in a MgO crucible (outside diameter 16mm, inside diameter 10mm and height 20mm), manufactured by the same technique as the large

© University of Pretoria

MgO crucibles described in *par.4.3.2*. The slags used in these experiments were taken from the same bulk mixtures used to prepare the slag pellets for the electrochemical measurements (*par.4.3.2*).

The slag and the metal were equilibrated within these magnesia crucibles in a vertical molybdenum wound resistance furnace, containing an alumina reaction tube and equipped with a PID temperature controller. High purity argon gas was flushed through the alumina reaction tube and the MgO crucible, containing the metal and the slag, was suspended in a molybdenum wire basket as shown schematically in *Figure 4.1*. The molybdenum basket was suspended by a thin molybdenum wire (0.3mm diameter) which, in turn, was fixed at the ends of two molybdenum wires of 0.9mm diameter as shown in the figure. These extension wires were protected by an alumina sheath and the whole assembly was slowly lowered into the hot zone of the furnace at 1873 K. The temperature was regulated within ± 3 °C. In order to quench the crucible, an electrical current was pulsed by means of a galvanostat through the molybdenum wire circuit, causing the thin molybdenum wire to melt at the position where it was attached to the basket. The crucible fell under gravitational force into a water bath at room temperature, contained in a glass container and positioned at the bottom of the reaction tube.

The quenched crucible with its contents was cut in half using a diamond saw and prepared for optical microscopy and microprobe analysis. The chemical compositions of the individual phases were determined using a JEOL 733 electron microprobe at an accelerating potential of 25 kilovolts and a beam current of 2.5 nano-amperes. The counting time varied between 60 and 100 seconds and oxide and silicate standards were used to quantify the analyses of MnO, MgO and SiO_2. On average, three different grains of each phase were analyzed in detail.

© University of Pretoria

UNIVERSITEIT VAN PRETORIA
UNIVERSITY OF PRETORIA
YUNIBESITHI YA PRETORIA

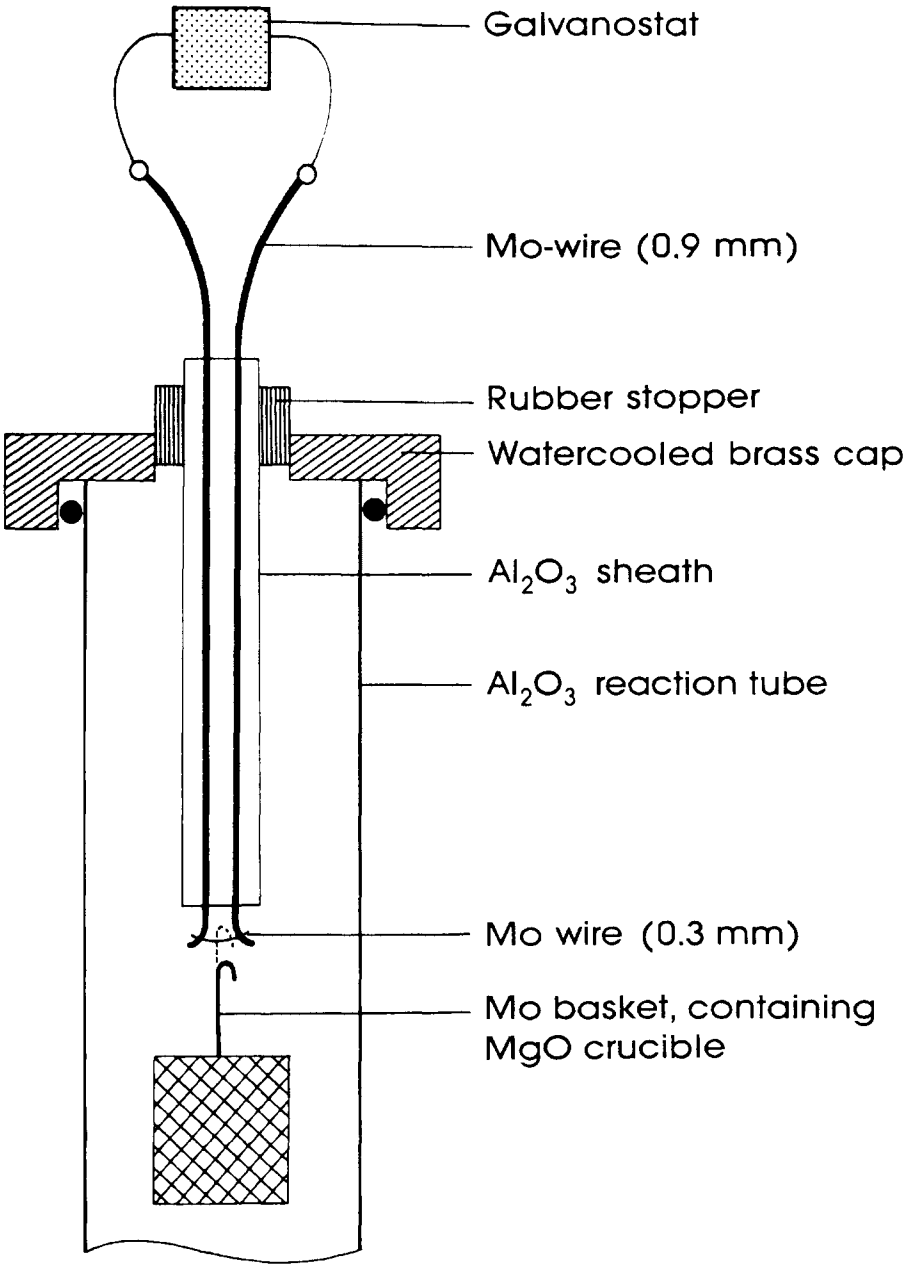

Figure 4.1 - *Schematic illustration of the crucible assembly for the quenching experiments*

© University of Pretoria

4.3.2 Oxygen Activity Measurements

Since the activity of MnO in (MnO-SiO_2-MgO)-slags was to be measured, MgO crucibles were used to contain the slag and the metallic Fe-Mn alloy or pure Mn. The porosity of commercially available MgO crucibles is approximately 25% and preliminary tests have shown that these crucibles were penetrated by the slag and the metal and did not function satisfactorily. It was therefore necessary to manufacture MgO crucibles in the laboratory. This was done in the following manner:

"Seawater" MgO which contained approximately 3% Al_2O_3 was supplied by Vereeniging Refractories (Pty.) Ltd. as ball mill fines and were ground to a particle size of less than 100μm. A slip, containing 0.2 ml ethanol per gram MgO, was then slipcast into a plaster mould. The wall thickness of the eventual MgO crucible casting was determined by the contact time of the slip with the mould before decantation. This contact period varied between 1 and 5 seconds to yield a wall thickness of approximately 1 to 2mm. The plaster mould, which consisted of 2 symmetrical parts, was then carefully removed from the crucible casting. The casting was allowed to dry for 24 hours at room temperature before it was heated at a rate of 100 °C per hour to 1973 K, sintered for two hours and then cooled slowly. The porosity of the crucibles manufactured in this way was approximately 15% and evaluation tests indicated that the crucible contained the slag and metal satisfactorily and that little interaction between the slag/metal and the crucible occurred at 1873 K. A MgO tube, similar to the Cr_2O_3 tube used during the chromium activity measurements (*Chapter 3*), was also prepared with this slip casting technique and subjected to the same sintering cycle as the MgO crucibles.

A crucible assembly similar to the arrangement described in *Chapter 3*, was used in this part of the study and is shown in *Figure 4.2*.

© University of Pretoria

UNIVERSITEIT VAN PRETORIA
UNIVERSITY OF PRETORIA
YUNIBESITHI YA PRETORIA

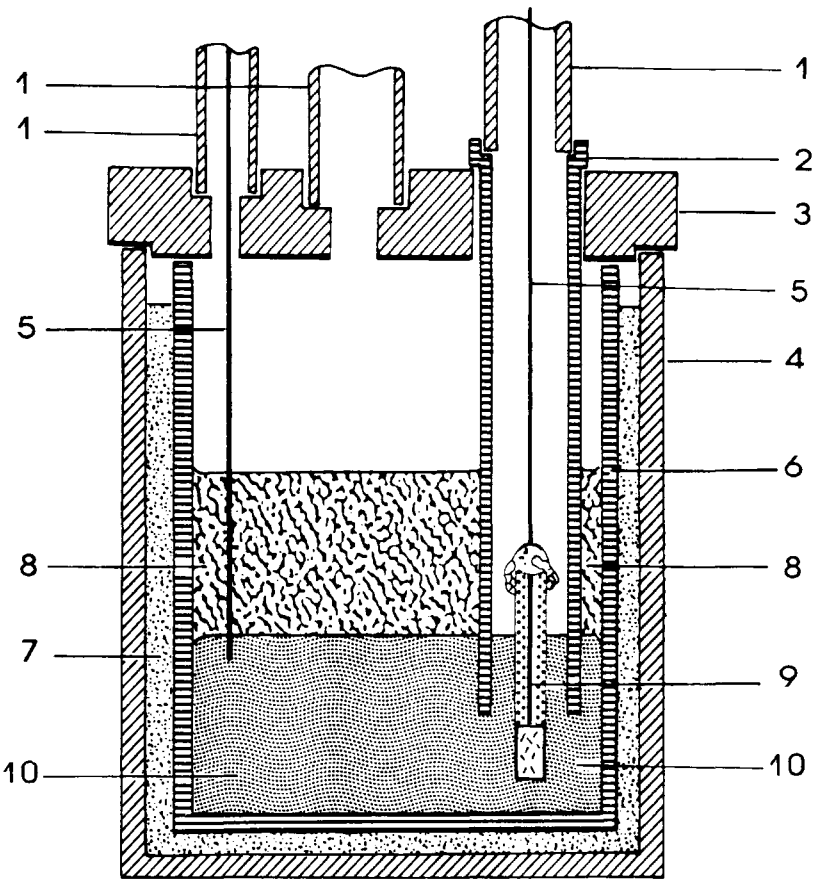

1. Al_2O_3 tubes
2. MgO tube
3. Al_2O_3 guide disk
4. Al_2O_3 crucible
5. Mo wire
6. MgO crucible
7. MgO powder
8. (MgO_{sat}-SiO_2-MnO)-slag
9. Oxygen probe
10. Mn melt

Figure 4.2 - *Crucible assembly for oxygen activity measurements in (MnO-SiO_2-MgO)-slags at 1873 K*

© University of Pretoria

A MgO crucible (outside diameter 36mm, inside diameter 34mm, height 50mm) located in an alumina protection crucible, contained the Mn melt while an alumina guide disk supported two alumina tubes as well as a MgO tube. The MgO tube in turn, supported another alumina tube, which served as a guide for the oxygen probes. The MgO tube was positioned in such a way that one end was always below the surface of the Mn melt. The cell assembly was placed on an alumina pedestal in the constant-temperature heat zone of the furnace, the temperature of the furnace being controlled by a Pt-6%Rh/Pt-30%Rh thermocouple, located next to one of the elements. The temperature of the crucible assembly was measured with a Pt/Pt-10%Rh thermocouple placed adjacent to the cell arrangement. The temperature-measuring circuit was calibrated against the melting point of palladium, and the overall error in the temperature measurements was found to be less than 3 °C. A molybdenum wire (0.9mm diameter) served as the electrical contact to the melt.

The experimental procedure followed in the course of an experimental run, differed quite substantially from that described in *Chapter 3*:

130 Grams of electrolytic manganese (99.9% pure) supplied by the Manganese Metal Co. (Pty) Ltd, was crushed, ground and placed in the MgO crucible. After the reaction tube had been sealed with a gas tight seal, argon was fed into the reaction tube and the furnace was heated at a rate of 80 °C per hour up to 1873 K. When the melt reached the desired temperature of 1873 K, 15 grams of slag pellets were added to the manganese melt through one of the alumina tubes. The pellets used for this purpose, were prepared as follows:

Reagent grade oxides supplied by Merck (Pty) Ltd and Sarchem (Pty) Ltd, were used as starting materials to prepare the various slag compositions. Fifty gram mixtures of the desired composition were prepared by carefully weighing the exact amount of each reagent. The mixtures were then ground under acetone to a particle size of less than

© University of Pretoria

UNIVERSITEIT VAN PRETORIA
UNIVERSITY OF PRETORIA
YUNIBESITHI YA PRETORIA

300 μm in an agate mortar. 40 Grams of each slag mixture were then mixed with 1.6 gram Mn powder, and pellets of 6mm diameter were made. These pellets were sintered for 2 hours at 1473 K under an argon atmosphere. After this treatment the pellets had sufficient mechanical strength to be added to the melt successfully.

After equilibrium between slag and metal was attained, an EMF measurement was made. The oxygen sensors, containing zirconia rods of 20mm length, tended to crack when lowered rapidly into the melt, and these probes were therefore lowered over a period of approximately 8 minutes to a position just above the melt, and finally to a position within the melt, approximately 5mm from the bottom of the crucible. This procedure prevented crack formation in the probes. A molybdenum wire of 0.9mm diameter which served as the electrical contact lead to the melt, was simultaneously lowered to a depth of approximately 2mm below the surface of the melt. The cell potential was recorded as a function of time. As a control measure the electrical resistance of the cell was also determined by the application of a 1 mA current to the cell, as described in *Chapter 3*. A silica tube was used to obtain a sample of the metal phase for the purpose of chemical analyses, after the final oxygen activity measurement of an experimental run was made.

4.4 Results and Discussion

4.4.1 Analysis of the Slag Phase Compositions and the Determination of the MnO Activity in the Liquid Slag

The vapour pressure of Fe is approximately 0.1 kPa and that of Mn 3 kPa at 1873 K[45]. It is therefore to be expected that considerable vaporization of Mn will occur if pure Mn is used as the metal phase in the experimental arrangement described. In an attempt to minimize Mn vaporization, a diluted Fe-Mn alloy, containing 5%

© University of Pretoria

Mn, was equilibrated with the (MnO-SiO_2-MgO)-slag during the initial experiments. However, it appeared that some of the Fe in the Fe-Mn alloy was oxidized to FeO in the course of an experiment and microprobe analysis indicated that the slag contained up to 10% FeO after equilibration. Moreover, the Mn content of the Fe-Mn alloy also decreased with time as a result of the vaporization of the manganese metal thereby causing the activity of Mn to decrease as a function of time. To alleviate these problems, pure Mn was used instead of an Fe-Mn alloy in the further experiments with the result that the Mn activity of the melt was maintained at unity throughout an experimental run.

The ternary phase diagram for the ternary system MnO-MgO-SiO_2 as determined by Glasser and Osborn[44] was used as the starting point in establishing the applicable phase relationships. Before the equilibrium phase relationships could be obtained, it was necessary to determine the reaction time required to establish equilibrium between the (MnO-SiO_2-MgO)-slag, the (MnO-MgO) solid solution and the manganese metal. To achieve this, two different slag compositions containing at least 50% MnO, were equilibrated with manganese metal for different periods, *viz* 15, 30, 60 and 120 minutes and quenched as previously described. Metallographically prepared sections of the quenched slag samples were then analyzed on a microprobe. The composition of various liquid slag grains in each sample was determined and was found to be the same in all samples equilibrated for 30 minutes or longer. The chemical composition of various grains of the solid solution in each sample was also determined and likewise it was found that the composition of all the solid solution grains was essentially the same. Accordingly, there is good reason to believe that a period of 30 minutes is sufficient to attain equilibrium between the slag, the solid solution and the metal. Furthermore, the homogeneity of the (MnO-MgO) solid solution phase equilibrated for 30 minutes, was checked by executing a number of sequential analyses with an electron microprobe beam along straight lines in several directions across the exposed surface of several grains of the solid solution. No

© University of Pretoria

UNIVERSITEIT VAN PRETORIA
UNIVERSITY OF PRETORIA
YUNIBESITHI YA PRETORIA

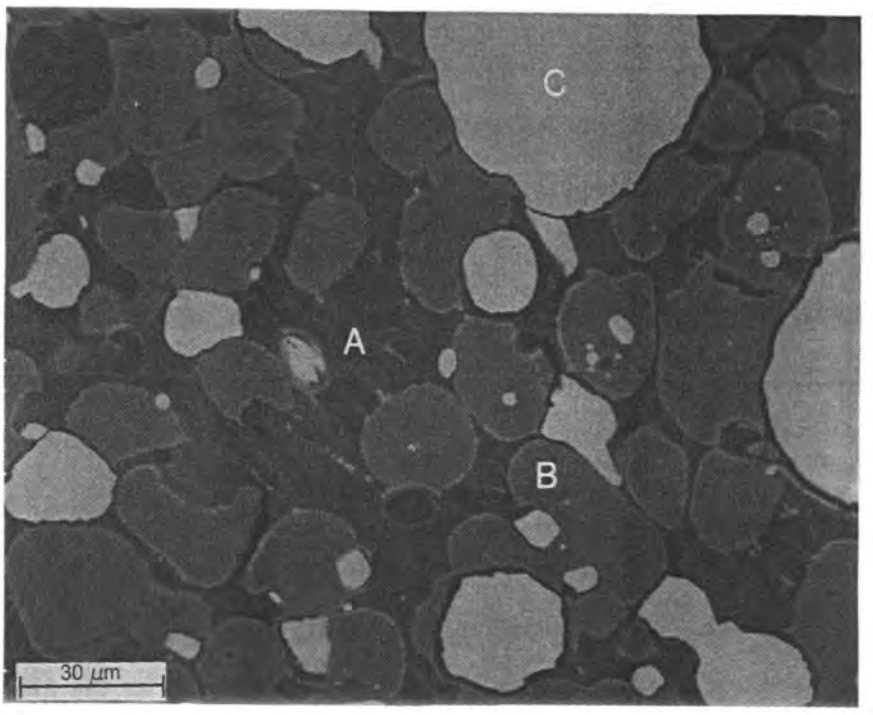

Figure 4.3 - *Back scattered electron image of a quenched slag sample (600x), showing the phases in equilibrium at 1873 K:*

A = Liquid slag

B = (MnO-MgO) solid solution

C = Manganese metal

© University of Pretoria

significant deviations in the composition of the solid solutions were observed, confirming that equilibrium between the slag and the metal is attained within 30 minutes. However, a reaction time of 60 minutes was used in all subsequent experiments to ensure that equilibrium was attained.

An example of a back-scattered electron image of a quenched sample, is shown in *Figure 4.3*. Three different phases are clearly discernable. The white phase consists of Mn metal droplets while the darker grey, spherical phase, represents the (MnO-MgO) solid solution. The solid solution and the manganese metal are embedded in the slag, the colour of which is slightly darker than that of the solid solution. If a proper interpretation is to be given to the metallographic features in these samples, it is essential that assurance is given that the structure observed at room temperature, is indeed representative of the phase equilibria which existed at 1873 K. This prerequisite deserves some comment with regard to the experimental procedure followed in this study. It is of the utmost importance that the mass and volume of the crucible, and its contents, be minimized to ensure that the quenching is so effective that the phases which are in equilibrium at 1873 K, are retained upon quenching to room temperature. Should the samples not be quenched rapidly enough from 1873 K, the liquid slag will crystallize partially and the composition of the slag phase will not be homogeneous. However, extreme care was taken in this study to ensure a rapid enough quench rate and the homogeneity of the phases achieved upon quenching, as determined by the microprobe analyses indicated that the quench rate was rapid enough to fulfil this requirement.

The chemical compositions of the different oxide mixtures used as feed material, are summarized in *Table 4.1* and superimposed in *Figure 4.4* on an isothermal section, at 1873 K, of the MnO-MgO-SiO_2 system proposed by Glasser and Osborn[44]. The mixtures 3M1, 3M2, and 3M3 were selected to fall within the phase field where the (MnO-MgO) solid solution and liquid are stable and in equilibrium at 1873 K, while

© University of Pretoria

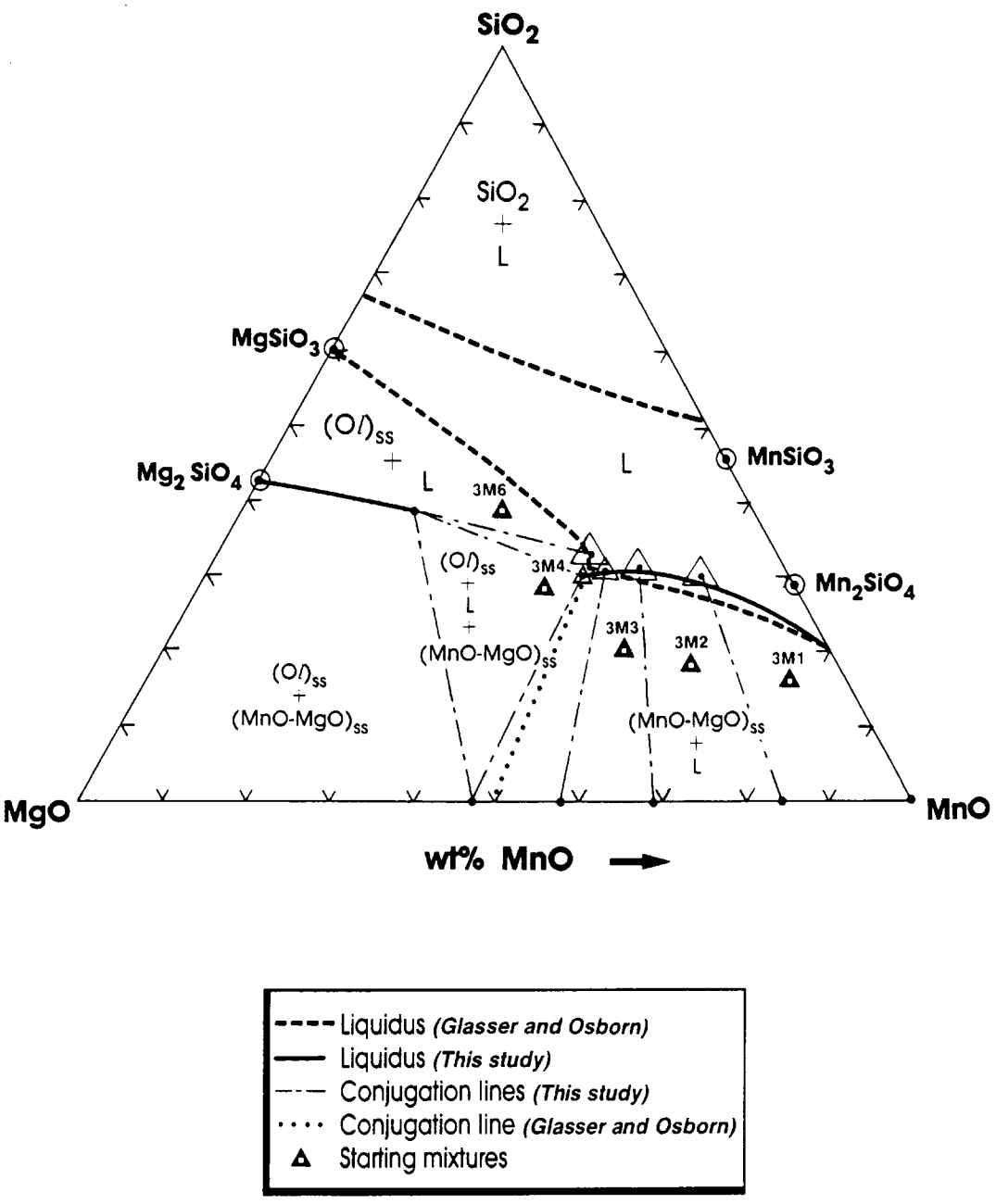

Figure 4.4 - *Equilibrium phase compositions in the system MnO-SiO_2-MgO in contact with metallic manganese at 1873 K determined in this study compared to that obtained by Glasser and Osborn*[44]

© University of Pretoria

UNIVERSITEIT VAN PRETORIA
UNIVERSITY OF PRETORIA
YUNIBESITHI YA PRETORIA

mixture 3M4 was selected to fall within the phase field where olivine, the (MnO-MgO) solid solution and liquid are stable. Mixture 3M6 was chosen to contain olivine and liquid at equilibrium.

Table 4.1 - *Chemical compositions of starting oxide mixtures and expected phase assemblages at 1873 K*

	3M1	3M2	3M3	3M4	3M6
%MgO	7	18	25	30	30
%MnO	77	64	55	42	32
%SiO_2	16	18	20	28	38
% metal added	50	50	50	50	50
Expected phases in equilibrium at 1873 K	$(MnO\text{-}MgO)_{ss}$ + liq.	$(MnO\text{-}MgO)_{ss}$ + liq.	$(MnO\text{-}MgO)_{ss}$ +liq.	$(MnO\text{-}MgO)_{ss}$ + olivine + liq.	Olivine +liq.

The compositions of the liquid, the olivine and the solid solutions of the different quenched samples are summarized in *Table 4.2* and are also shown in *Figure 4.4*. Al_2O_3 levels of up to 5% by mass were detected in some of the liquid slags**, and the compositions of these slag phases are indicated by triangles in *Figure 4.4*. The slag compositions indicated by the solid circles within the centre of the triangles, were used to construct a liquidus curve. The liquidus curves determined by Glasser and Osborn[44] are also shown in *Figure 4.4* and there is reasonably good

** The alumina present in the liquid slag probably originated from the MgO crucible, because the MgO powder used for the manufacturing of the crucibles contained approximately 4 per cent alumina by mass.

© University of Pretoria

agreement with the results of this study, indicating that the limited presence of Al_2O_3 in the slags of this study does not cause a serious discrepancy. Conjugation lines determined in this study, which link the equilibrium slag and solid solution compositions at 1873 K, are also shown. It is evident that the compositions of both the final slag and the solid solution phases of mixtures 3M1, 3M2 and 3M3, were enriched in MgO compared to the starting mixtures. This does not apply to mixtures 3M4 and 3M6, which were chosen to contain olivine at equilibrium. The higher MgO content in the final slag and solid solution phases of mixtures 3M1, 3M2 and 3M3 was probably due to an initial reaction of the MgO crucible with the liquid slag, although a protective layer of (MnO-MgO) solid solution precipitated on the crucible wall as the reaction proceeded until equilibrium was attained. A conjugation line between the solid solution and liquid obtained by extrapolating the data of Glasser and Osborn[44] to 1873 K, is also shown in *Figure 4.4* and this conjugation line is likewise in good agreement with the results of this study.

The activity of MnO in solid solutions of MnO and MgO at 1873 K, has been determined by Tsai[6] and his results are presented in *Figure 4.5*. These data were used to determine the activity of MnO in the slag by equation [4.5] and these activities are summarized in *Table 4.3*. The activity of MnO in the slag is shown in *Figure 4.6* as a function of the mol fraction MnO. The activity of MnO in slags in the MnO-MgO-SiO_2 system at 1873 K, has not been determined previously and for the sake of comparison, the results obtained by Mehta and Richardson[4] at 1923 K, are also shown in *Figure 4.6*. The activities determined in this study are in good agreement with those determined by Mehta and Richardson for slags with similar chemical compositions. The liquid composition in the MnO-SiO_2 binary system where MnO saturation at 1873 K is obtained, as determined by Glasser[46], is also shown in *Figure 4.6*. This is also in good agreement with the extrapolated values determined in this study.

© University of Pretoria

UNIVERSITEIT VAN PRETORIA
UNIVERSITY OF PRETORIA
YUNIBESITHI YA PRETORIA

Table 4.2 - *Compositions of the equilibrium phases of the different samples that were in equilibrium with manganese metal at 1873 K*

	3M1		3M2		3M3	
	Liquid	**Solid sol.**	**Liquid**	**Solid sol.**	**Liquid**	**Solid sol.**
%MgO	9.3	15.2	16.1	31.1	20.9	42.5
	(0.2)*	(0.3)	(0.1)	(0.7)	(1.2)	(1.5)
%MnO	58.0	84.8	50.3	68.9	46.8	57.5
	(0.3)	(0.3)	(0.9)	(0.7)	(2.1)	(1.5)
%SiO_2	28.5	---	29.9	---	30.0	---
	(0.9)		(1.4)		(1.1)	
%Al_2O_3	4.2	---	3.7	---	2.3	---
	(0.8)		(1.0)		(0.9)	

	3M4			3M6	
	Liquid	**Solid sol.**	**Olivine**	**Liquid**	**Olivine**
%MgO	24.4	53.0	41.1	20.6	42.0
	(1.2)	(0.2)	(0.1)	(0.8)	(0.6)
%MnO	44.6	47.0	20.1	43.1	19.1
	(1.2)	(0.2)	(0.2)	(2.3)	(0.7)
%SiO_2	29.2	---	38.8	31.1	38.9
	(0.6)		(0.1)	(2.1)	(0.0)
%Al_2O_3	1.8	---	---	5.2	---
	(0.8)			(0.3)	

*( ) Standard deviation

© University of Pretoria

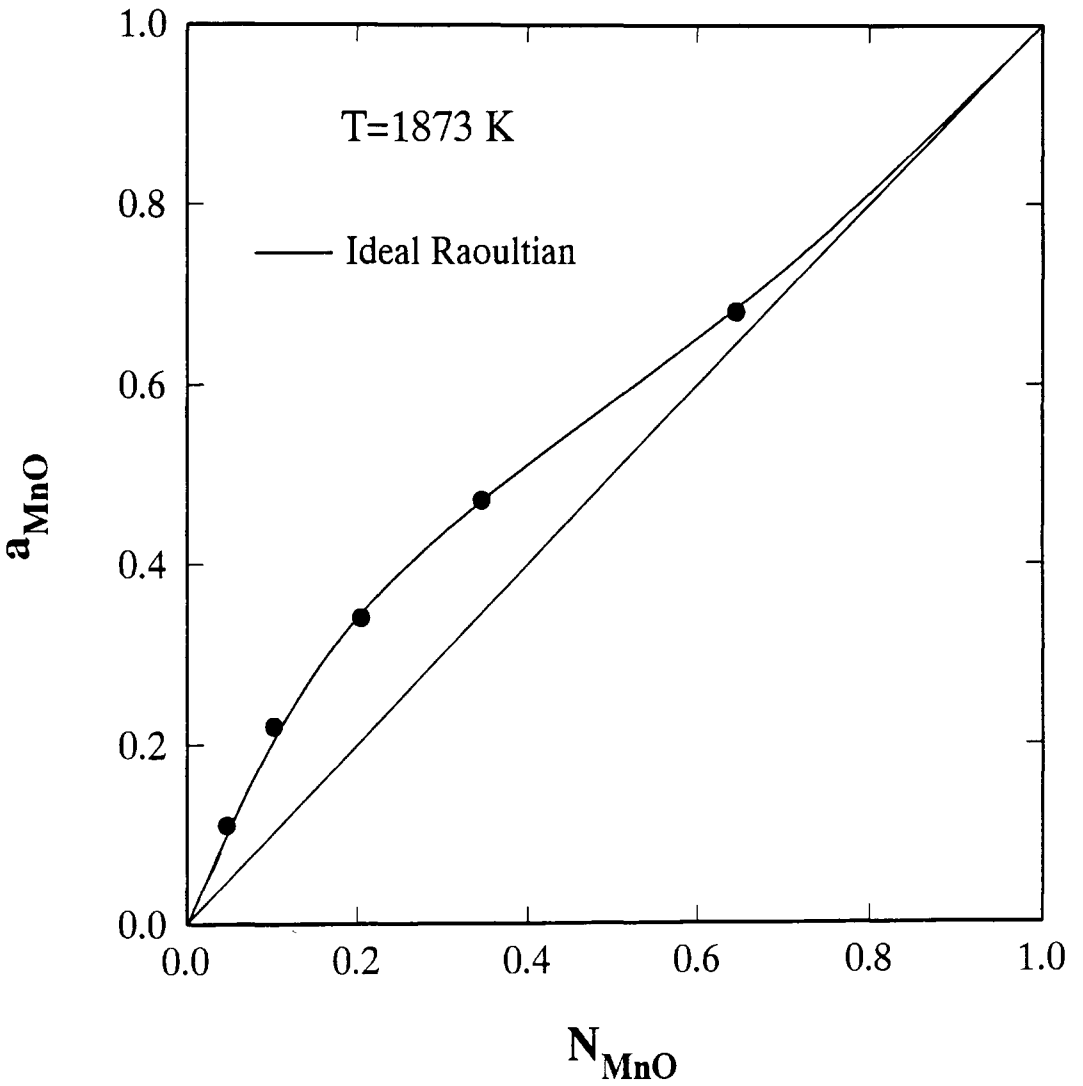

Figure 4.5 - *Activity-composition relations of MnO in (MnO-MgO) solid solutions at 1873 K (After Tsai[6])*

© University of Pretoria

UNIVERSITEIT VAN PRETORIA
UNIVERSITY OF PRETORIA
YUNIBESITHI YA PRETORIA

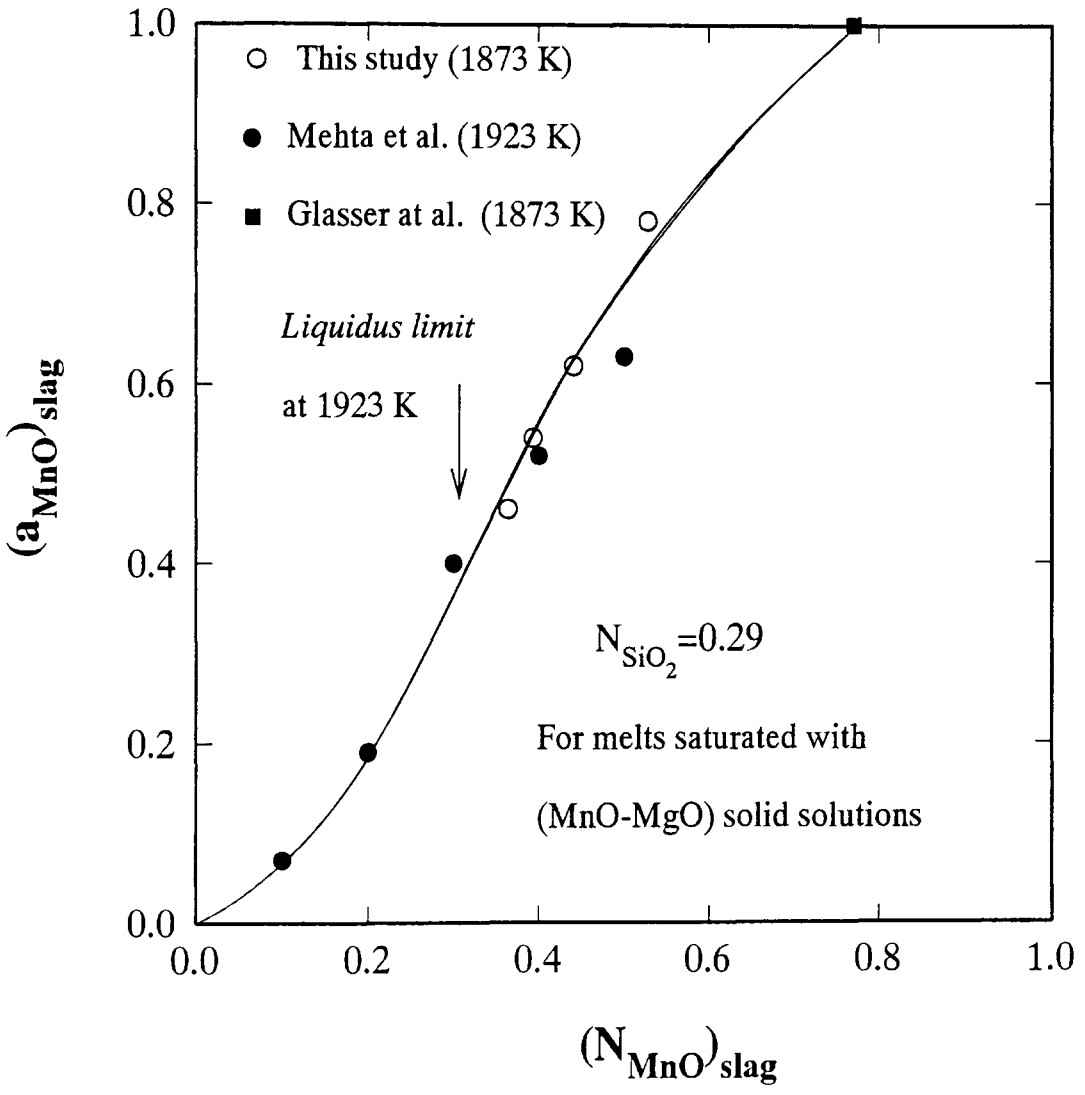

Figure 4.6 - *Relationship between the activity of MnO and the MnO content of (MnO-SiO_2-MgO)-slags saturated with (MnO-MgO) solid solutions at 1873 K*

© University of Pretoria

Table 4.3 - *Normalized composition of the liquid phase in equilibrium with the solid solution and manganese metal at 1873 K (mole fractions), and the MnO activity of the liquid slag*

Mixture no.	N_{MnO}	N_{SiO2}	N_{MgO}	a_{MnO}
3M1	0.528	0.300	0.172	0.78
3M2	0.427	0.307	0.266	0.62
3M3	0.388	0.295	0.317	0.54
3M4	0.361	0.285	0.354	0.46

The activity of MnO as a function of the mol fraction MnO in the binary MnO-SiO_2 system determined at 1923 K by Abraham *et al*[3]., is shown in *Figure 4.7*. The effect of CaO additions to the MnO-SiO_2 system on the activity of MnO is highlighted and shows that CaO increases the activity of MnO. The results of the present study are also shown in this figure and indicate that additions of MgO also increase the activity of MnO.

The saturation limit of MnO in the liquid component of some (MnO-MgO-SiO_2)-slags determined in the present study, is shown in *Figure 4.8* as a function of the MgO:MnO ratio at a constant SiO_2 content of approximately 29% by mass. The solubility of MnO in the slag decreases, as expected, with an increase in the MgO:MnO ratio. The solubility of MnO will have to be limited in slags which are to be used in the production of steels with a high manganese content. The results of this study, shown in this figure, are consequently experimental confirmation that this can be achieved by increasing the MgO:MnO ratio in the slag.

© University of Pretoria

UNIVERSITEIT VAN PRETORIA
UNIVERSITY OF PRETORIA
YUNIBESITHI YA PRETORIA

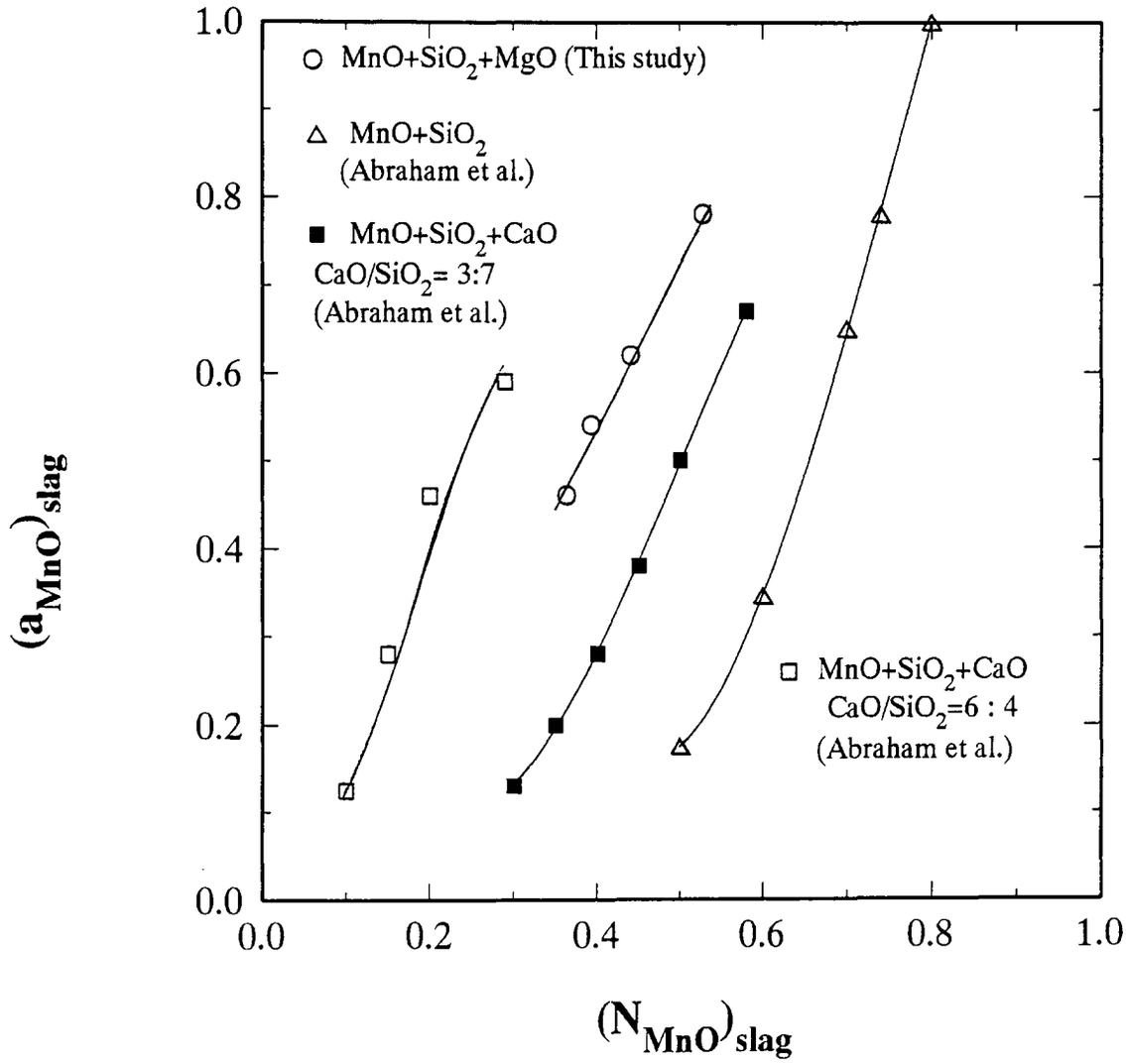

Figure 4.7 - *Relationship between the activity of MnO and the MnO content of different MnO-containing slags at 1873 K*

© University of Pretoria

UNIVERSITEIT VAN PRETORIA
UNIVERSITY OF PRETORIA
YUNIBESITHI YA PRETORIA

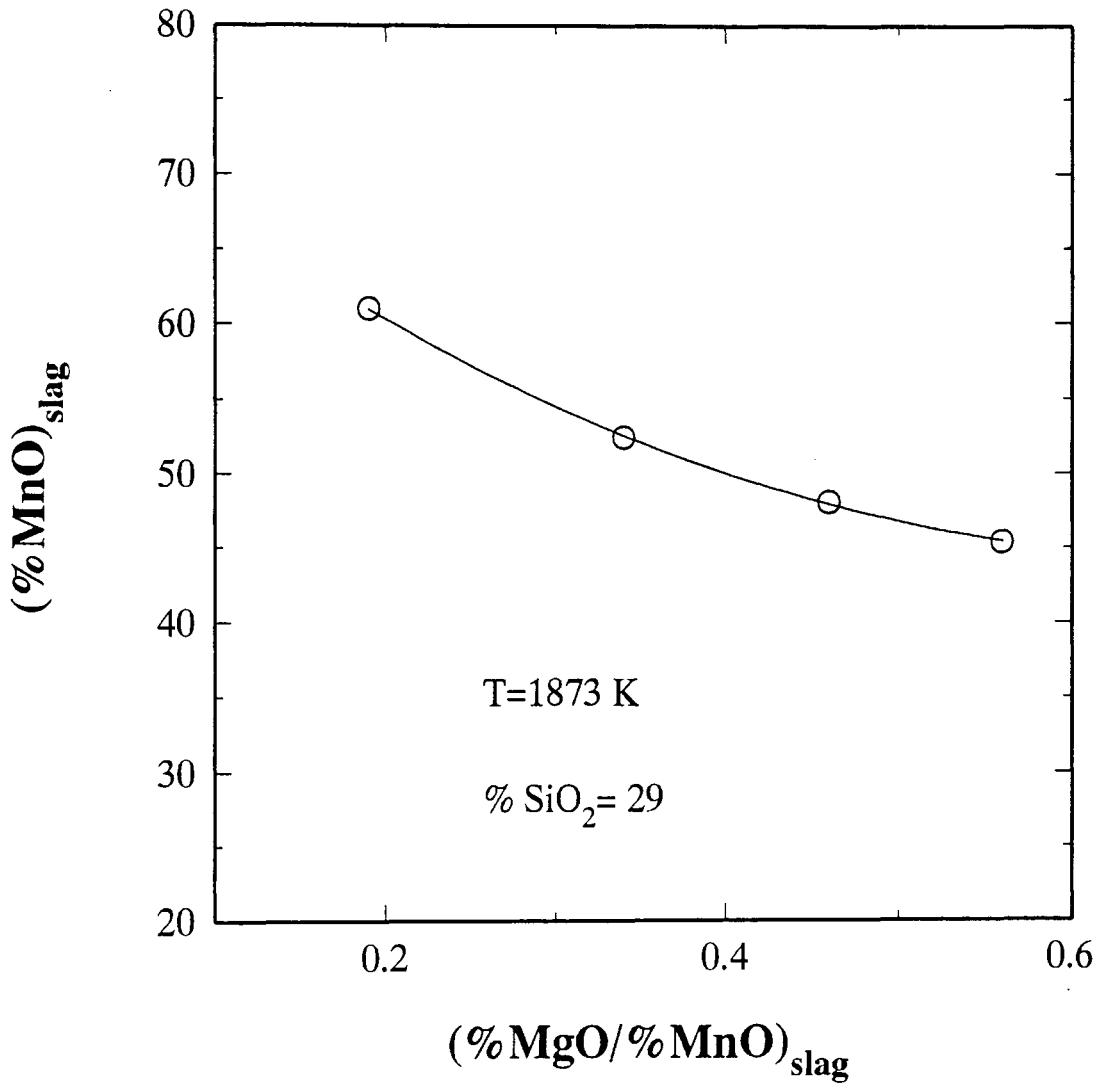

Figure 4.8 - *Relationship between the MnO content and the MgO:MnO ratio of the liquid phase in the MnO-SiO_2-MgO system at 1873 K determined in this study*

© University of Pretoria

These results indicate that the activity of MnO in (MnO-MgO-SiO_2)-slags which are saturated with (MnO-MgO) solid solutions and in contact with pure molten manganese metal, can be determined reliably by determining the chemical compositions of the constituent phases in equilibrium at high temperature. This conclusion can be made because the findings of this study are in good agreement with the results of previous workers who employed different experimental techniques to determine the activity of MnO in slags. Accordingly, this technique can also be used with confidence to determine the composition of the different equilibrium phases when the electrochemical technique is used to determine the oxygen potential of the slag/metal system. Furthermore, the electrochemical measurements can be verified by comparing the partial pressure of oxygen determined using electrochemical oxygen probes, to that calculated from the results obtained with this method, since the melts are in equilibrium with Mn and the activity of MnO in the melts is known.

4.4.2 Oxygen Activity Measurements

Slag no. 3M2 (*Table 4.1*), was equilibrated with manganese metal in the first experimental run. The first oxygen probe was lowered into the melt 60 minutes after the slag pellets were added. However, the manganese vapour attacked the alumina cement which attached the molybdenum wire to the alumina tube of the sensor, causing separation between the electrical lead and the sensor. Analyses of the cement by scanning electron microscopy (SEM), indicated that sodium oxide which originated from the waterglass used as binder in the cement, reacted with manganese vapour. Manganese metal vapour most probably replaced the sodium oxide in the binding phase to form a manganese-silicate phase. The melting point of this manganese silicate is well below 1873 K, yielding a liquid at 1873 K which caused the separation of the Mo-wire and the alumina tube in which the solid electrolyte is contained. To alleviate this problem, mono aluminium phosphate was used as binder

© University of Pretoria

UNIVERSITEIT VAN PRETORIA
UNIVERSITY OF PRETORIA
YUNIBESITHI YA PRETORIA

instead. This cement performed satisfactorily and it was used to attach the molybdenum wire to the probe in subsequent experiments. Because the partial pressure of oxygen in the Mn/MnO system is lower than that in the Cr/Cr_2O_3 system, it is not desirable to use the Cr/Cr_2O_3 reference electrode in the measurement of the oxygen potential of the Mn/MnO system. It was consequently necessary to evaluate the performance of other reference electrodes as well, firstly from a theoretical point of view, and secondly under the experimental conditions pertaining to these experiments.

4.4.2.1 $(Cr+Cr_2O_3)$

As a first step in this analysis, the same type of reference electrode $(Cr+Cr_2O_3)$ which had been used in the measurement of the chromium activities in the Fe-Cr-O system (*Chapter 3*), was used for the oxygen activity measurements in the Mn/MnO system. Because the oxygen partial pressure of the $(Cr+Cr_2O_3)$ reference electrode is higher than that of the $(MnO-SiO_2-MgO)$-slag at 1873 K, oxygen ions would tend to migrate from the reference electrode to the melt. In an attempt to curtail the polarization resulting from oxygen ion transfer, and also to study the effect thereof, different mass ratios of $Cr:Cr_2O_3$ *viz* 1:1, 3:1, 20:1 and 50:1 were evaluated. Probes containing zirconia solid electrolyte rods of 10mm length were used.

It was not possible to obtain stable EMF plateaus during the initial runs and it became evident that polarization at one or both electrodes occurred to such an extent that these measurements could not be used to determine the oxygen potential of the system. The most elegant way to overcome the problem of polarization is to either use a reference electrode of which the partial pressure of oxygen is similar to that of the slag, or to use a solid electrolyte with a very low electronic conductivity. Thoria solid electrolytes are known to display very little electronic conductivity, but because of the difficulties in obtaining this type of electrolyte and also the problems

© University of Pretoria

UNIVERSITEIT VAN PRETORIA
UNIVERSITY OF PRETORIA
YUNIBESITHI YA PRETORIA

encountered in the handling of radio-active materials, the alternative approach, to use a suitable reference electrode, was investigated.

4.4.2.2 $(Ta+Ta_2O_5)$

Janke[25] used a $(Ta+Ta_2O_5)$ reference electrode in a tubular MgO stabilized zirconia solid electrolyte sensor to determine the oxygen partial pressure of an aluminium deoxidised iron melt at 1873 K. Stable plateaus were recorded within 20 seconds. Because the P_{O2} of the $(Ta+Ta_2O_5)$ reference electrode is of the same order as that of the Mn/MnO system (1.07×10^{-14} atm.)[24], it offered an interesting alternative to the Cr/Cr_2O_3 reference electrode. However, this reference electrode has not been used previously in the present study and it was therefore necessary to evaluate the performance and reliability of this reference electrode in a system of known oxygen potential. For this purpose P_{O2}-measurements were made in the Fe-Cr-O system.

The same experimental procedure as described in *par. 3.3.2* was followed during these experiments, the only difference being that an Fe-Cr alloy with a fixed Cr content (20% Cr) was used. As a control measure, oxygen sensors containing the same reference electrode $(Cr+Cr_2O_3)$ previously used (*Chapter 3*), were used to establish the oxygen potential in the melt. Stable plateaus were recorded and the chromium activities were also in the same order than those measured earlier. Evidently, equilibrium conditions prevailed and the $(Ta+Ta_2O_5)$ reference electrode could be evaluated.

It was not possible to record stable plateaus with oxygen sensors in which $(Ta+Ta_2O_5)$ reference electrodes were used and in which the zirconia solid electrolyte rods were 10mm in length, even though different mass ratios of $Ta:Ta_2O_5$ were used. Because oxygen transfer through the solid electrolyte is reduced as the

© University of Pretoria

UNIVERSITEIT VAN PRETORIA
UNIVERSITY OF PRETORIA
YUNIBESITHI YA PRETORIA

oxygen gradient across the solid electrolyte is lowered, polarization can be curtailed, to some extent at least, by increasing the length of the solid electrolyte. Consequently, zirconia solid electrolyte rods, 20mm in length, were also evaluated. Stable plateaus were recorded and the results are summarized in *Table 4.4*.

Table 4.4 - *Oxygen potentials and Raoultian chromium activities of an Fe-20%Cr alloy measured with oxygen probes containing 20mm zirconia solid electrolyte rods and employing ($Ta+Ta_2O_5$) as the reference electrode at 1873 K.*

Probe no.	EMF [mV]	$(P_{O2})_{alloy}$ [atm]	a^R_{Cr}
1	133.1	2.636×10^{-12}	0.39
2	157.2	5.726×10^{-12}	0.22
3	138.4	3.136×10^{-12}	0.35
4	149.4	4.472×10^{-12}	0.27
5	135.2	2.825×10^{-12}	0.37

The standard free energy change ($\Delta G°$) for the reaction:

$$2\langle Ta\rangle + \frac{5}{2}[O_2] = \langle Ta_2O_5\rangle \qquad [4.6]$$

is -1.2515×10^6 J/mol[24] and this value was used to determine the oxygen partial pressure of the alloy by equation [4.3]. The corresponding Raoultian chromium activities (see *Chapter 3)* are also presented in *Table 4.4*. The EMF values varied between 133 and 157 mV and this variation may be compared to a maximum variation of ± 2 mV when ($Cr+Cr_2O_3$) reference electrodes were used (*Chapter 3*). As shown in *Figure 3.9*, the Raoultian chromium activity of an Fe-20%Cr alloy is 0.14. This activity can now be compared to the activities measured with the

© University of Pretoria

UNIVERSITEIT VAN PRETORIA
UNIVERSITY OF PRETORIA
YUNIBESITHI YA PRETORIA

($Ta+Ta_2O_5$) reference electrodes in the same alloy. These values, as shown in *Table 4.4*, varied between 0.22 and 0.39. The EMF signals generated in the electrochemical cell employing a Ta/Ta_2O_5 reference electrode are clearly erroneous and it is necessary to explain this serious discrepancy.

The phase diagram of the Ta-O system[47] shown in *Figure 4.9*, illustrates clearly that the stable phases in the temperature range 1550 °C to 1880 °C, are α and L_{II}. When a mixture of Ta and Ta_2O_5 powders reach a temperature of 1600 °C, an α solid solution, containing approximately 5 atomic per cent oxygen, and an L_{II} liquid phase, with a composition different from Ta_2O_5, will form. It is consequently not Ta and Ta_2O_5 which are in equilibrium, and the $\Delta G°$ value of the $<Ta>/<Ta_2O_5>$ reaction can not be used to calculate the prevailing P_{O2} (equation [4.6]). Moreover, the α-solid solution will change in composition with time, up to an oxygen content of approximately 5%, and the liquid L_{II} will also form as a function of time. The oxygen potential in the Ta/Ta_2O_5 mixture will consequently change as a function of time and the prevailing oxygen potential in this system can not be determined with any degree of accuracy. Clearly, the oxygen potential will not reach a constant value until the equilibrium phases are formed and even then there is great uncertainty because of the dearth of knowledge about the interaction of liquid Ta_xO_y with the zirconia solid electrolyte. To study the change in composition of the Ta and Ta_2O_5 powders, an oxygen probe was heated to 1480 °C (below the liquidus) and kept at this temperature for 8 minutes before it was rapidly cooled to room temperature. This probe, and some of the probes which were used for EMF measurements at 1600 °C, were dissected and the powders contained in each probe were mounted in epoxy and prepared for microscopic analysis. *Figure 4.10 (a)* represents the microstructure of the ($Ta+Ta_2O_5$) reference mixture which was kept at 1480 °C for 8 minutes (400x magnification), while *Figure 4.10 (b)* illustrates the microstructure (at the same magnification) of the ($Ta+Ta_2O_5$) mixture after it had been in the melt at 1600 °C for a period of 7 minutes.

© University of Pretoria

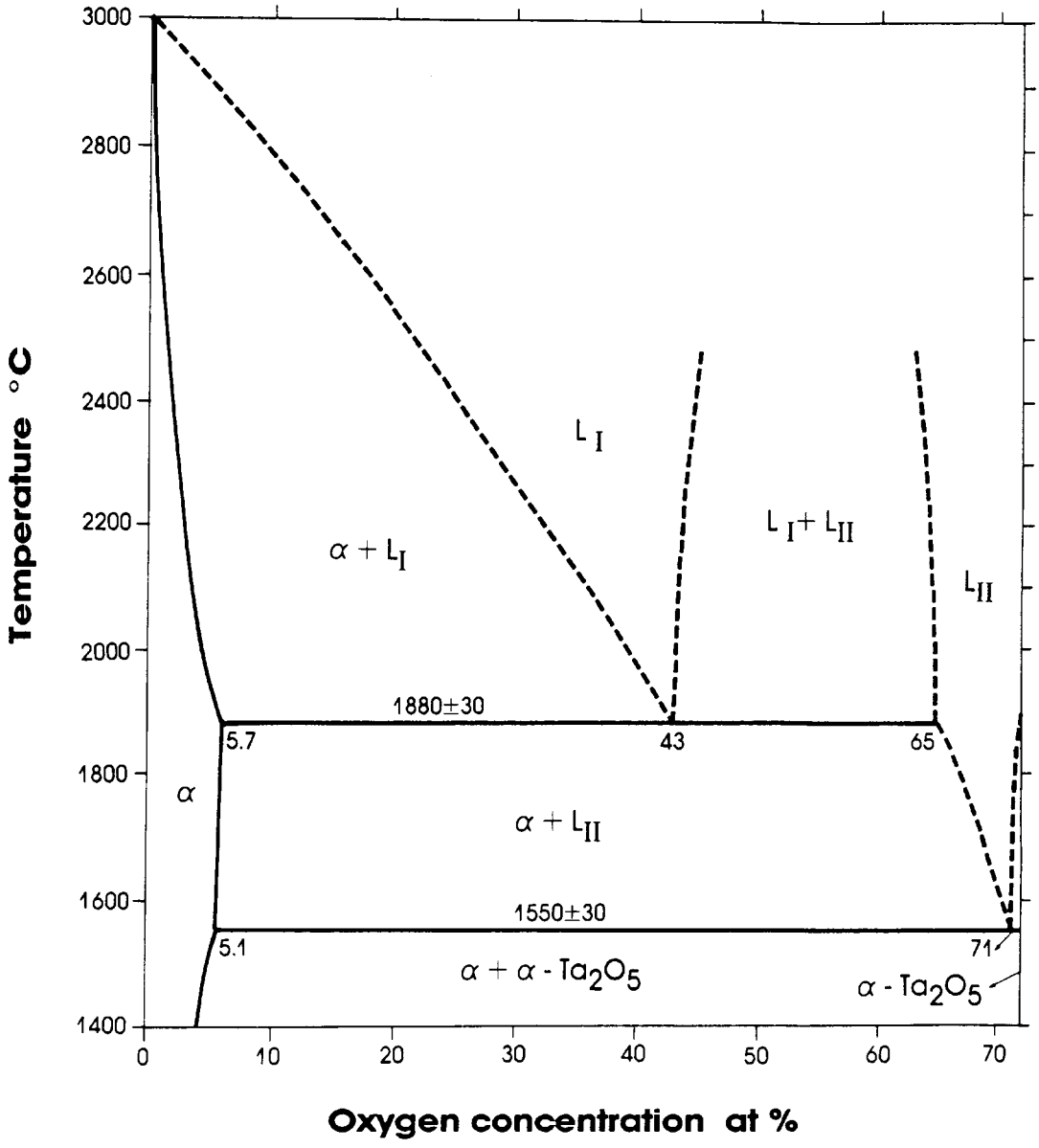

Figure 4.9 - *Phase diagram of the Ta-O system*[47]

© University of Pretoria

UNIVERSITEIT VAN PRETORIA
UNIVERSITY OF PRETORIA
YUNIBESITHI YA PRETORIA

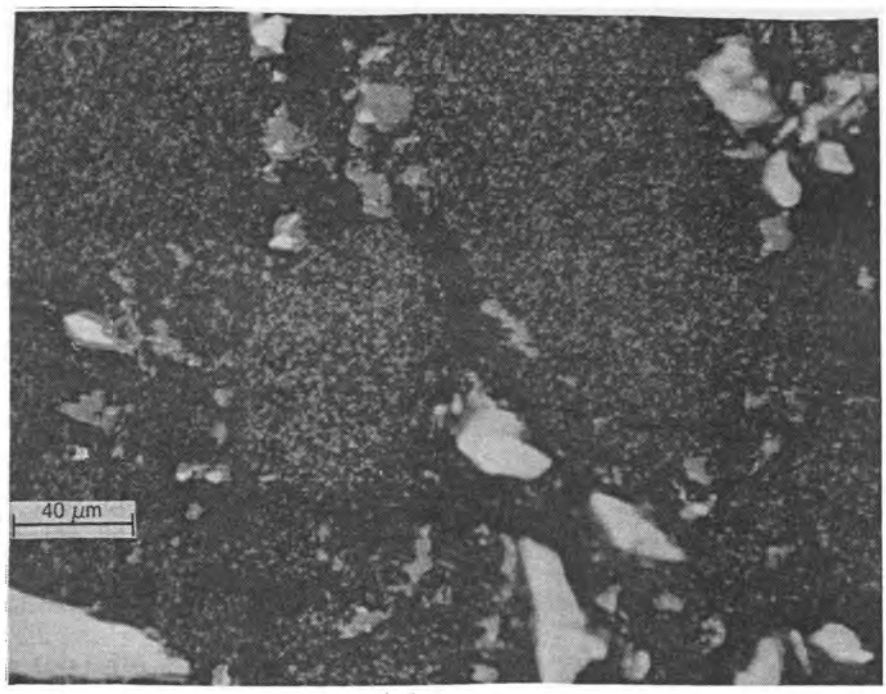

(a)

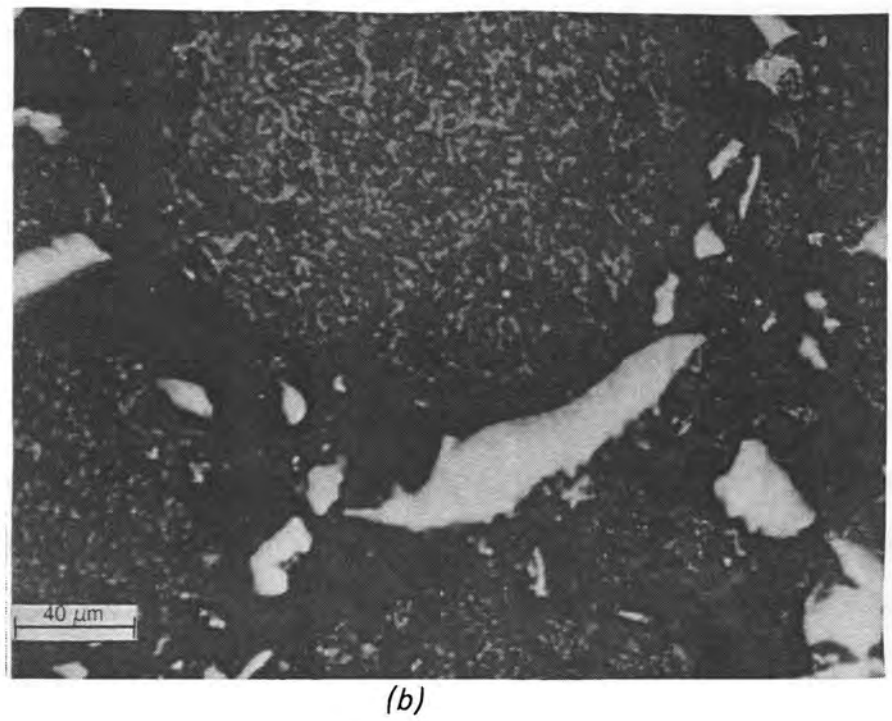

(b)

Figure 4.10 - *Microstructure of the ($Ta+Ta_2O_5$) reference electrodes (400x)*
(a) Heated to and kept at 1480 °C for 8 minutes
(b) After use in an oxygen probe kept for 7 minutes in an Fe-Cr melt at 1600 °C

© University of Pretoria

The big white phase represent Ta particles while the Ta_2O_5 particles are represented by grey areas, consisting of light grey and darker grey phases respectively. A comparison of the oxide phases reveals that the light grey phase in the particle of *Figure 4.10 (b)* is larger than that in *Figure 4.10 (a)*. The reason for this difference in microstructure is most probably related to the formation of a liquid phase at 1600 °C. Evidently, Ta and Ta_2O_5 are not the only phases present in the reference electrode. The formation of a liquid phase as a function of time at 1600 °C and the changing composition of the α-phase result in a change in the prevailing oxygen potential thereby yielding the Ta/Ta_2O_5 reference electrode unsuitable for use in an plug type oxygen sensor. This conclusion is in sharp contrast to reported success with the use of a tubular probe employing the Ta/Ta_2O_5 reference electrode[25]. In his experiments, Janke[25] determined the oxygen potential of an Fe-C-Al alloy. According to him, accurate measurements were made when the P_{O2} of the alloy was approximately the same as that of the Ta/Ta_2O_5 reference electrode (10^{-14} atm.). This reported success with the use of Ta/Ta_2O_5 as reference electrode deserves further comment.

Janke used a thin-walled zirconia solid electrolyte tube so that the total immersion time was only 20 seconds. Temperature equilibrium was evidently attained within 20 seconds so that a significant change in the composition of the α-solid solution could hardly have occurred. Also, very little liquid formation is expected in the few seconds the probe was at a temperature of 1600 °C so that a quasi-equilibrium between Ta and Ta_2O_5 may be assumed in Janke's experiments.

In the present investigation a solid electrolyte rod, 20mm in length, was used as solid electrolyte with the result that temperature equilibrium was only achieved after approximately 7 minutes. The reference electrode was consequently 20 times longer at temperature and a liquid phase may well have formed. The significantly different performance of the Ta/Ta_2O_5 reference electrode in the present investigation

© University of Pretoria

UNIVERSITEIT VAN PRETORIA
UNIVERSITY OF PRETORIA
YUNIBESITHI YA PRETORIA

compared to Janke's experience can therefore be explained, at least in a qualitative fashion.

4.4.2.3 (Nb+NbO)

Janke[25] also successfully used (Nb+NbO) reference electrodes in tubular MgO stabilized zirconia solid electrolyte sensors, for measurements in aluminium deoxidised iron at 1600 °C. The phase diagram of Nb-O[48], presented in *Figure 4.11*, shows that Nb(s) and NbO(s) are the stable phases at 1600 °C. Since NbO is not generally commercially available, an attempt was made to produce NbO from Nb_2O_5 powder. Nb_2O_5 powder was mixed with pure Nb powder, heated to 1600 °C under an argon protection gas, kept at temperature for at least 1 hour and cooled to room temperature. Since NbO is the stable oxide phase at 1600 °C, it was expected that the Nb_2O_5 would be reduced to NbO during this heating cycle. However, X-ray diffraction analysis of the sample indicated that the only oxide phases present were NbO_2 and NbO_6. Evidently, NbO has to be used as starting material for a (Nb+NbO) reference electrode.

Janke[49] confirmed that pure NbO powder should be used in these type of reference electrodes. Following his suggestion, pure NbO powder was obtained from CERAC Co. Ltd. and the (Nb+NbO) reference electrode was evaluated. This was done by measuring the oxygen potential of an Fe-Cr alloy of known activity (*Figure 3.9*), containing 20% Cr and in equilibrium with pure Cr_2O_3 at 1600 °C. Oxygen sensors containing 20mm solid electrolyte plugs were used and Nb:NbO mass ratios of 1:3, 6:1, and 12:1 were experimented with but no stable plateaus could be obtained with these probes. X-ray analysis were performed on the (Nb+NbO) reference mixtures of probes used and it was found that Nb and NbO were the only phases present. The poor performance of these probes was consequently attributed to polarization effects at one of the electrodes.

© University of Pretoria

UNIVERSITEIT VAN PRETORIA
UNIVERSITY OF PRETORIA
YUNIBESITHI YA PRETORIA

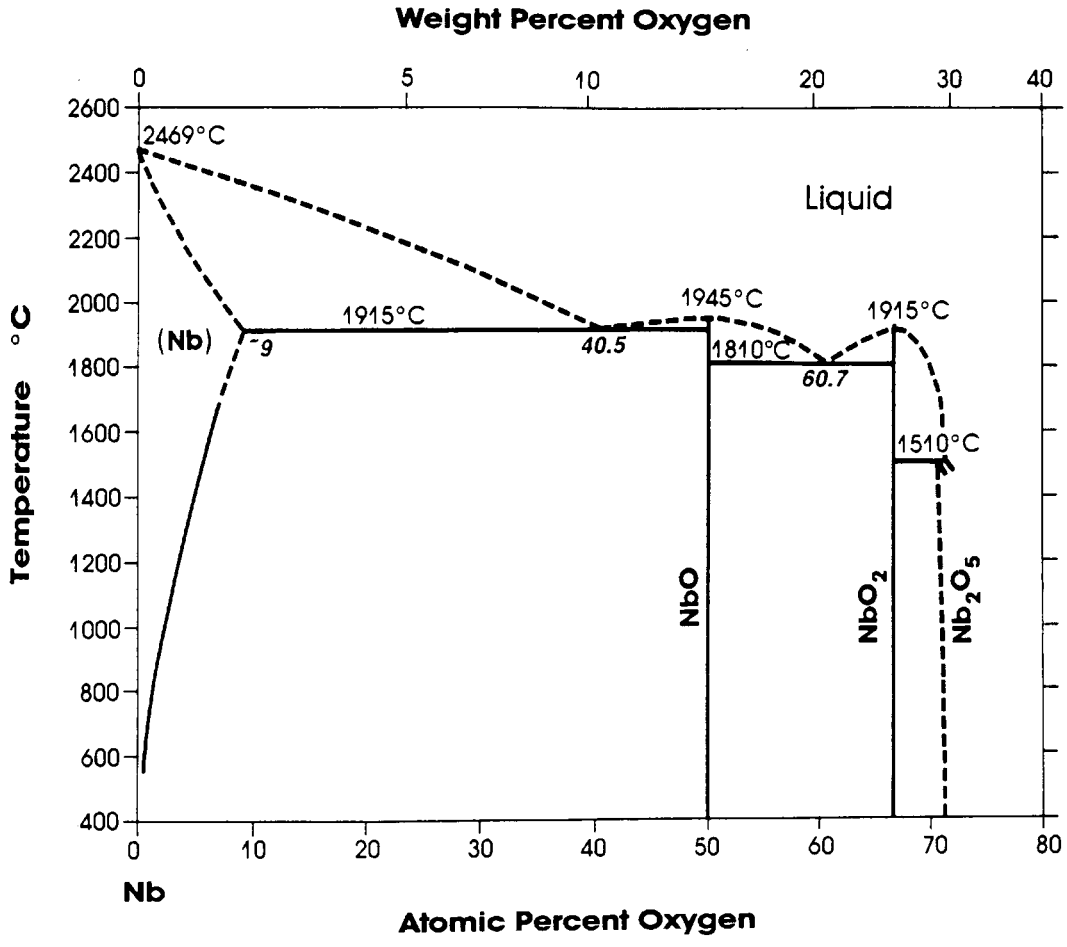

Figure 4.11 - *Phase diagram of the Nb-O system*[48]

© University of Pretoria

The standard free energy change ($\Delta G°$) for the reaction:

$$<Nb> + \frac{1}{2}[O_2] = <NbO> \qquad [4.7]$$

is -2.516×10^5 J/mol[42] and the oxygen potential of the Nb/NbO reference electrode at 1600 °C is compared to those of the other reference electrodes and an Fe-20%Cr alloy in *Table 4.5*. The oxygen partial pressures of pure Mn in equilibrium with MnO of which the activities are 0.1 and 1 respectively (equation [4.1]), are also presented in *Table 4.5*. These same partial pressures of oxygen are schematically shown in *Figure 4.12*.

Table 4.5 - *The partial pressure of oxygen of the different reference electrodes used in the plug-type oxygen sensors of this study, an Fe-20%Cr alloy and Mn in equilibrium with MnO at 1873 K*

System	P_{O2} [atm]
Fe-20%Cr alloy	1.051×10^{-11}
Cr/Cr_2O_3	7.638×10^{-12}
Mn/MnO ($a_{MnO}=1$)	3.259×10^{-14}
Mn/MnO ($a_{MnO}=0.1$)	3.259×10^{-16}
Ta/Ta_2O_5	1.065×10^{-14}
Nb/NbO	9.250×10^{-15}

The oxygen gradient across the solid electrolyte of an oxygen sensor which contains a Nb/NbO reference electrode and which is used for measurements in an Fe-20%Cr alloy, is much higher than that of a probe containing a Cr/Cr_2O_3 electrode. Consequently, the driving force for oxygen ions to migrate from the melt to the Nb/NbO reference electrode is much greater.

© University of Pretoria

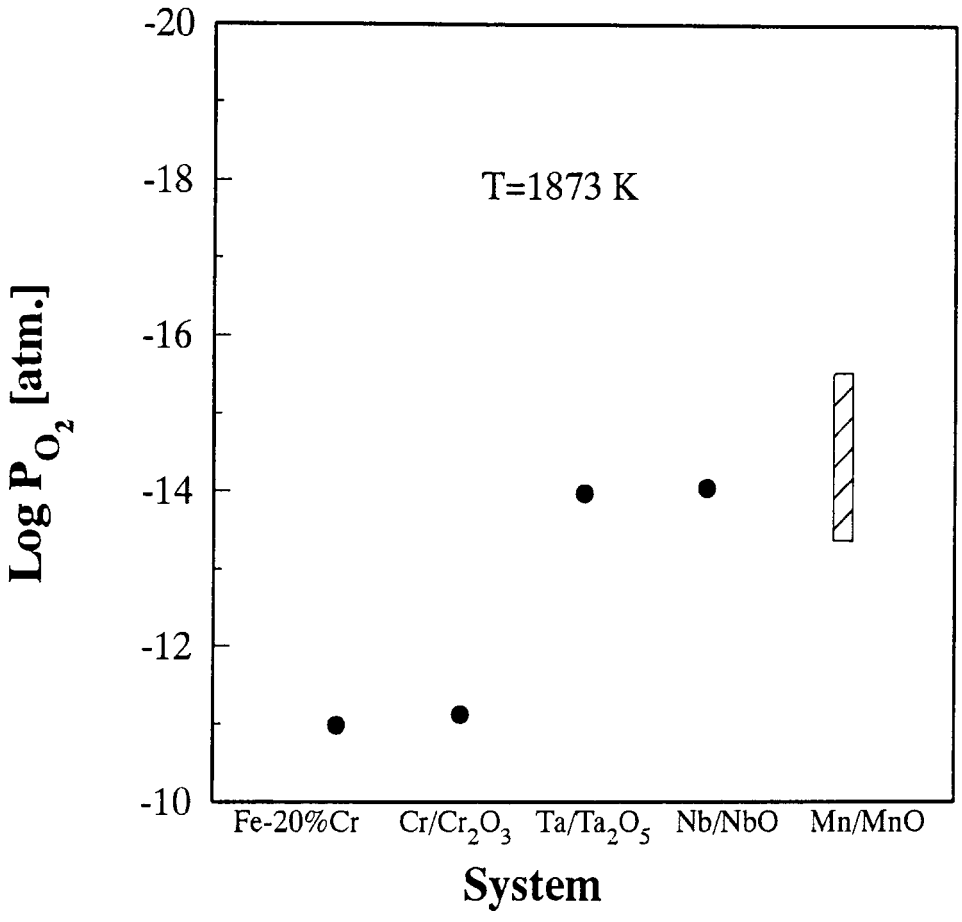

Figure 4.12 - *Schematic representation of the partial pressure of oxygen of the different metal-oxide systems, summarized in Table 4.3*

© University of Pretoria

There is consequently good reason to believe that the major difference in oxygen potential between the Nb/NbO reference electrode and the Fe-20%Cr alloy, caused polarization and this is the reason why stable EMF plateaus were not recorded. However, it is also evident from *Figure 4.12*, that the oxygen partial pressure of the Nb/NbO electrode is similar to that of the Mn/MnO system and for this reason the Nb/NbO reference electrode was used in the determination of the oxygen activity in liquid (MnO-SiO_2-MgO)-slags.

The experimental procedure described in *par. 4.3.2*, was followed during the evaluation of the (Nb+NbO) reference electrode in (MnO-SiO_2-MgO)-slags. The composition of the starting slag mixture (3M2) is summarized in *Table 4.2*. Oxygen probes containing solid electrolyte rods of 20mm length and different ratios of Nb:NbO, were used. Surprisingly, EMF plateaus were recorded after approximately 4 minutes in the melt. Although it was shown that Cr/Cr_2O_3 reference electrodes polarized when used in oxygen probes containing solid electrolytes of 10mm length (*par. 4.4.2.1*), polarization could be minimized, to a certain extent at least, by increasing the plug length to 20mm. Therefore, oxygen probes containing electrolyte rods of 20mm length and Cr/Cr_2O_3 reference electrodes, were also evaluated and plateaus were recorded after approximately 2 minutes in the melt. These results are summarized in *Table 4.6*.

From the results presented in *Table 4.6*, it is evident that the EMF values obtained with different sensors containing (Nb+NbO) and ($Cr+Cr_2O_3$) reference electrodes respectively, were fairly constant (variation of ± 3 mV). However, these EMF values were much higher than expected. Therefore, this difference in the expected EMF values and that obtained experimentally, had to be explained and was further investigated.

© University of Pretoria

UNIVERSITEIT VAN PRETORIA
UNIVERSITY OF PRETORIA
YUNIBESITHI YA PRETORIA

Table 4.6 - *Results of measurements in (MnO-SiO_2-MgO)-slags with oxygen probes containing 20mm zirconia solid electrolyte rods and ($Nb+NbO$) and ($Cr+Cr_2O_3$) reference electrodes respectively*

Probe no.	Reference electrode	EMF [mV]	P_{O2} [atm.] ($P_e=3x10^{-17}$atm.)	a_{MnO}
1	Nb:NbO = 1:3	139.8	$5.866x10^{-17}$	0.04
2	Nb:NbO = 1:3	140.0	$5.812x10^{-17}$	0.04
3	Nb:NbO = 6:1	134.1	$7.585x10^{-17}$	0.05
4	Nb:NbO = 3:1	140.0	$5.812x10^{-17}$	0.04
5	$Cr:Cr_2O_3$ = 1:20	206.5	$1.822x10^{-15}$	0.24
6	$Cr:Cr_2O_3$ = 1:20	212.0	$1.512x10^{-15}$	0.22
7	$Cr:Cr_2O_3$ = 1:20	207.5	$1.761x10^{-15}$	0.23

Figure 4.13 illustrates the influence of variations in the P_e-value of a solid electrolyte on the cell potential (EMF) when the activity of MnO (a_{MnO}) in the liquid slag, varies between 0 and 1. From *Figure 4.13*, it is evident that cell potentials smaller than 95 mV are expected to be measured when the activity of MnO varies between 0 and 1, and ZrO_2 solid electrolyte sensors (P_e = $3.077x10^{-14}$ atm., this study) are used with Nb/NbO reference electrodes. If the P_e-value of the solid electrolyte however, is $3x10^{-17}$ atm., cell potentials varying between -25 and +220 mV are expected (*Figure 4.13*). Therefore, as a starting point, it was assumed that the P_e-value of the solid electrolytes was $3x10^{-17}$ atm., in order to explain the relatively high EMF values obtained with sensors containing Nb/NbO reference electrodes. The oxygen potentials and MnO activities determined accordingly are also summarized in *Table 4.6*. From these results, it is evident that the MnO activities of the liquid slag

© University of Pretoria

obtained with sensors containing Nb/NbO reference electrodes, varied between 0.04 and 0.05

Similarly, EMF values smaller than approximately 190 mV are expected to be measured when oxygen sensors containing Cr/Cr_2O_3 reference electrodes and zirconia solid electrolytes with a P_e-value of $3.077x10^{-14}$ atm., are used. However, *Figure 4.13* clearly shows that for a P_e-value of $3x10^{-17}$ atm., EMF values which vary between 120 and 400 mV, are to be expected. Since the measured EMF values were in the order of 210 mV, it was assumed that the P_e-value of these electrolytes was $3x10^{-17}$ atm. Accordingly, the MnO activities determined varied between 0.22 and 0.24 as is evident from the results presented in *Table 4.6*.

The MnO content of the (MnO-MgO) solid solution in equilibrium with the slag used in these experiments (3M2-*Table 4.2*) is 68.9% (N_{MnO}=0.56). According to Tsai[6] (*Figure 4.5*), the MnO activity of this (MnO-MgO) solid solution at 1873 K is 0.62. Therefore, the MnO activity of the ($MnO-SiO_2$-MgO)-slag (3M2) is expected to be 0.62 (equation [4.5]). Hence, serious contradictions exist: Firstly, it seems that the P_e-value of the electrolyte decreased. Secondly, the MnO activities obtained with Nb/NbO and Cr/Cr_2O_3 reference electrodes differ (0.05 and 0.24) and thirdly, the activity of MnO determined with both reference electrodes significantly differs from the MnO activity determined by Tsai[6]. These discrepancies had to be further investigated.

In the course of the experimental determination of the oxygen activity in the ($MnO-SiO_2$-MgO)-slags, the cell resistances of the probes containing ($Cr+Cr_2O_3$) reference electrodes were 90 ohm or higher. These values are much higher than those used for oxygen activity measurements in the Fe-Cr-O system at 1873 K (*Chapter 3*), containing 10mm plugs and ($Cr+Cr_2O_3$) reference electrodes (15 to 25 ohm). This increase in cell resistance was an indication that the microstructure of the solid

© University of Pretoria

UNIVERSITEIT VAN PRETORIA
UNIVERSITY OF PRETORIA
YUNIBESITHI YA PRETORIA

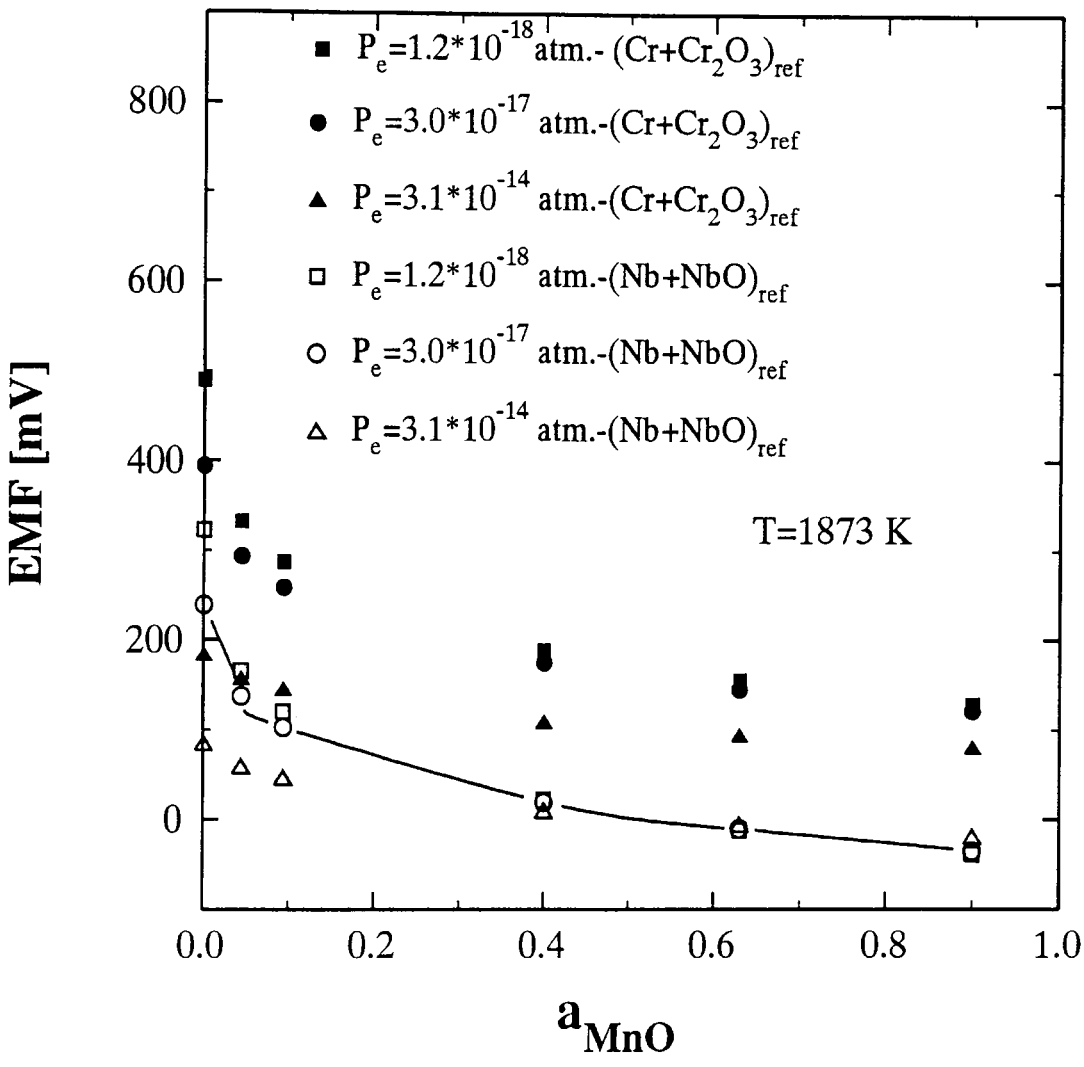

Figure 4.13 - *Activity of MnO as a function of the cell potential of oxygen sensors containing Nb/NbO and Cr/Cr_2O_3 reference electrodes and electrolytes with different P_e-values*

© University of Pretoria

UNIVERSITEIT VAN PRETORIA
UNIVERSITY OF PRETORIA
YUNIBESITHI YA PRETORIA

electrolytes used for measurements in the (MnO-SiO_2-MgO)-slag might possibly have changed. Therefore, these electrolyte rods were subjected to microprobe analysis.

Figure 4.14 present an example of the microstructure close to the one end of a solid electrolyte rod which was kept for 5 minutes directly above the (MnO-SiO_2-MgO)-slag in the constant heat zone of the furnace. The microstructure of a layer of approximately 50 μm evidently differs quite substantially from the remaining microstructure. The chemical composition of this layer and that of the remainder of the electrolyte, are summarised in *Table 4.7*

Table 4.7 - *The chemical composition determined on the microprobe of a solid electrolyte held directly above the Mn melt at 1873 K.*

Location	**%MnO**	**%MgO**	**%ZrO_2**
One end, closest to melt (50 μm)	7.3	4.1	88.6
Remainder of electrolyte	0	4.0	96.0

The Mn content (expressed as MnO) of the grains in a layer of 50 μm thickness, at the one end of the electrolyte which was in contact with the Mn vapour, is approximately 7%. The solid electrolyte had therefore already reacted with the Mn metal vapour before the probe was even dipped into the melt. The microstructure of a sensor which had been dipped into the melt, was also analyzed. The chemical composition of the electrolyte along a longitudinal section, was determined at points of 50 μm apart. These results are summarised in *Table 4.8*

© University of Pretoria

UNIVERSITEIT VAN PRETORIA
UNIVERSITY OF PRETORIA
YUNIBESITHI YA PRETORIA

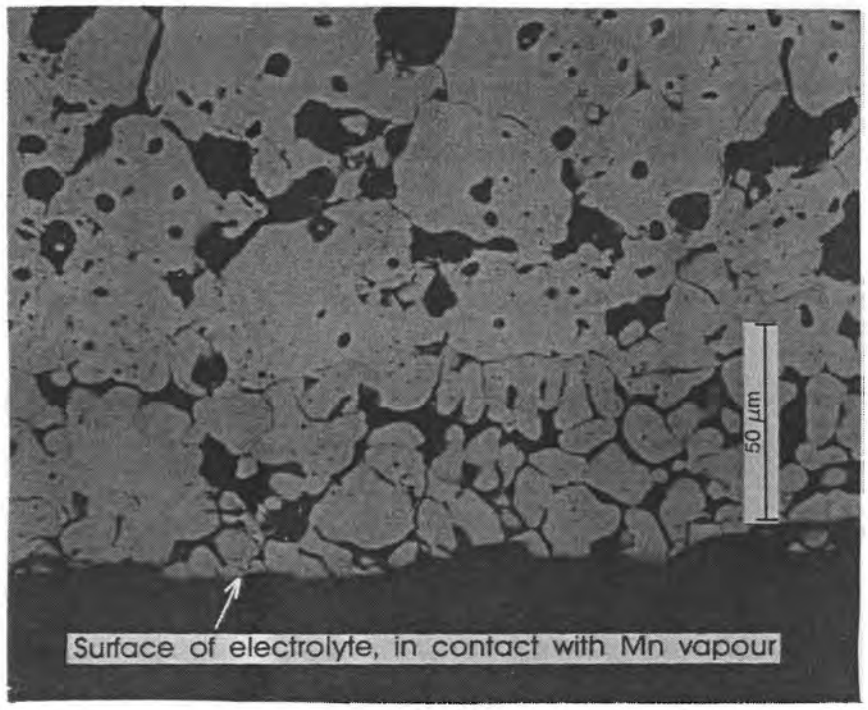

Figure 4.14 - *Microstructure of a zirconia solid electrolyte rod, held for 5 minutes above a Mn melt at 1873 K. (600x)*

© University of Pretoria

UNIVERSITEIT VAN PRETORIA
UNIVERSITY OF PRETORIA
YUNIBESITHI YA PRETORIA

Table 4.8 - *Chemical composition of a solid electrolyte rod along a longitudinal section, which was in contact with the Mn melt at 1873 K*

Distance from one end, closest to melt	**%MnO**	**%MgO**	**%ZrO_2**
30 μm	0.5	4.5	95.0
80 μm	3.7	4.6	91.7
130 μm	3.5	4.6	91.9
180 μm	2.9	4.5	92.6
230 μm	1.4	4.6	93.0
280 μm	1.8	4.6	93.6
330 μm	0.0	4.7	95.3
380 μm	0.0	4.5	95.5
990 μm	0.0	4.6	95.6

The results presented in *Table 4.8* clearly indicate that Mn (expressed as MnO) was present in the zirconia electrolyte. However, it was detected in a layer of approximately 300 μm thickness only. The remainder of the electrolyte rod did not contain any Mn. To demonstrate the distribution of Mn in the zirconia grains of an electrolyte used for measurements in the (MnO-SiO_2-MgO)-slag, point analyses were made at distances 5 μm apart. These spots are shown in *Figure 4.15*, and the chemical compositions are summarized in *Table 4.9*. These results show that the Mn was dispersed fairly homogeneously throughout the ZrO_2 grains.

© University of Pretoria

UNIVERSITEIT VAN PRETORIA
UNIVERSITY OF PRETORIA
YUNIBESITHI YA PRETORIA

Table 4.9 - *Chemical composition of spots 5 μm apart, of a zirconia grain after use in a Mn melt at 1873 K*

Distance from grain boundary	%MnO	%MgO	%ZrO_2
5 μm	3.4	4.7	91.9
10 μm	2.6	5.1	92.3
15 μm	2.8	5.2	92.0
20 μm	4.0	5.0	91.0
25 μm	4.2	5.0	90.8
30 μm	4.6	5.0	90.4
35 μm	4.4	5.0	90.6

Another cause of the poor performance of these probes in the (MnO-SiO_2-MgO)-slags, could be that the alumina cement which attaches the zirconia solid electrolyte rod to the thin walled alumina tube, influenced the electrical characteristics of the sensor. However, there was not a continuous electrical conduction path for electrons or oxygen ions to migrate from the one electrode to the other, because the cement only attached the upper and lower ends of the solid electrolyte rod to the alumina tube, as schematically shown in *Figure 4.16*. Furthermore, Mn was not detected in the cement located nearest to the reference electrode. Hence, the extremely low partial pressures of oxygen measured in the (MnO-SiO_2-MgO)-slags could not be attributed to the behaviour of the alumina cement.

© University of Pretoria

UNIVERSITEIT VAN PRETORIA
UNIVERSITY OF PRETORIA
YUNIBESITHI YA PRETORIA

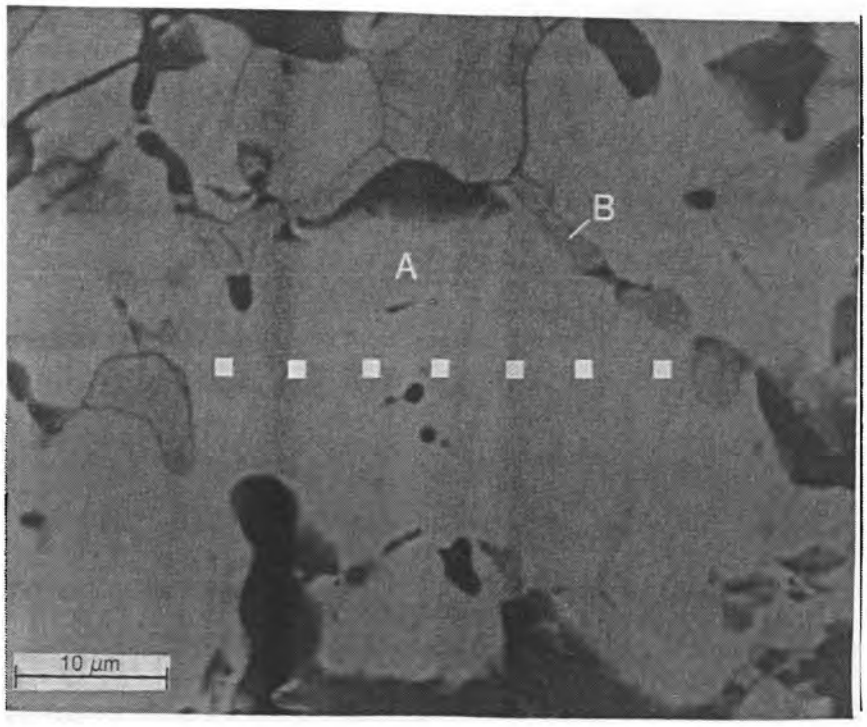

Figure 4.15 - *ZrO_2 grain subjected to microprobe analysis (2000x). The squares indicate analyzed areas.*

A = ZrO_2 grain

B = Mn metal

© University of Pretoria

UNIVERSITEIT VAN PRETORIA
UNIVERSITY OF PRETORIA
YUNIBESITHI YA PRETORIA

Although it is not fully proven, there is good reason to believe that the discrepancies related to activity measurements in the (MnO-SiO_2-MgO)-slag, can be ascribed to the MnO that was detected in the zirconia matrix. The following explanation can be given: The MnO content of the zirconia layer which was in direct contact with the melt, is approximately 3.5% (N_{MnO}=0.045) as shown in *Table 4.8*. Mn metal (vapour and/or liquid) evidently diffused into the zirconia matrix along the grain boundaries, as is evident from *Figure 4.15*. The Mn diffused over a distance of at least 50 μm when the electrolyte was in contact with the Mn vapour for a period of approximately 7 minutes (*Table 4.8*). The Mn further diffused into the zirconia electrolyte when it was dipped into the Mn metal, during a period of approximately 5 minutes to form a manganese containing layer of 300 μm thickness. The rate of Mn diffusion and the reaction with ZrO_2 is enhanced, because liquid Mn reacts with solid ZrO_2 at 1873 K. Similar reaction rates occurred when the slag of composition 3M2 was equilibrated with Mn metal at 1873 K. The (MnO-MgO) solid solution was formed within 15 minutes, although full equilibrium between the slag and solid solution phases was only attained after the elapse of 30 minutes.

The Mn reacted with the magnesia stabilized zirconia to form a layer of MnO-MgO-ZrO_2 solid solution. If $\gamma_{MnO} = 1$, according to equation [4.4], $a_{MnO} = N_{MnO}$. Therefore, the activity of MnO in the solid solution is approximately 0.045 if a P_e-value of $3x10^{-17}$ is applicable. It is possible that the oxygen potential of the melt at the electrolyte/melt interface, was determined by the MnO activity in the MnO-MgO-ZrO_2 solid solution layer rather than by the MnO activity of the (MnO-SiO_2-MgO)-slag (equation [4.1]). A similar meganism is used in the silicon sensor developed by Iwase[50]. This electrochemical silicon sensor consists, like an oxygen probe, of a zirconia solid electrolyte tube. The only difference between the design of the oxygen and silicon probes, is that a mixture of ZrO_2 and $ZrSiO_4$ is painted onto the magnesia stabilized zirconia electrolyte tube of the silicon sensor. When this sensor is dipped into an Fe-C-Si melt, the oxygen potential of the melt in the vicinity of the tubular

© University of Pretoria

UNIVERSITEIT VAN PRETORIA
UNIVERSITY OF PRETORIA
YUNIBESITHI YA PRETORIA

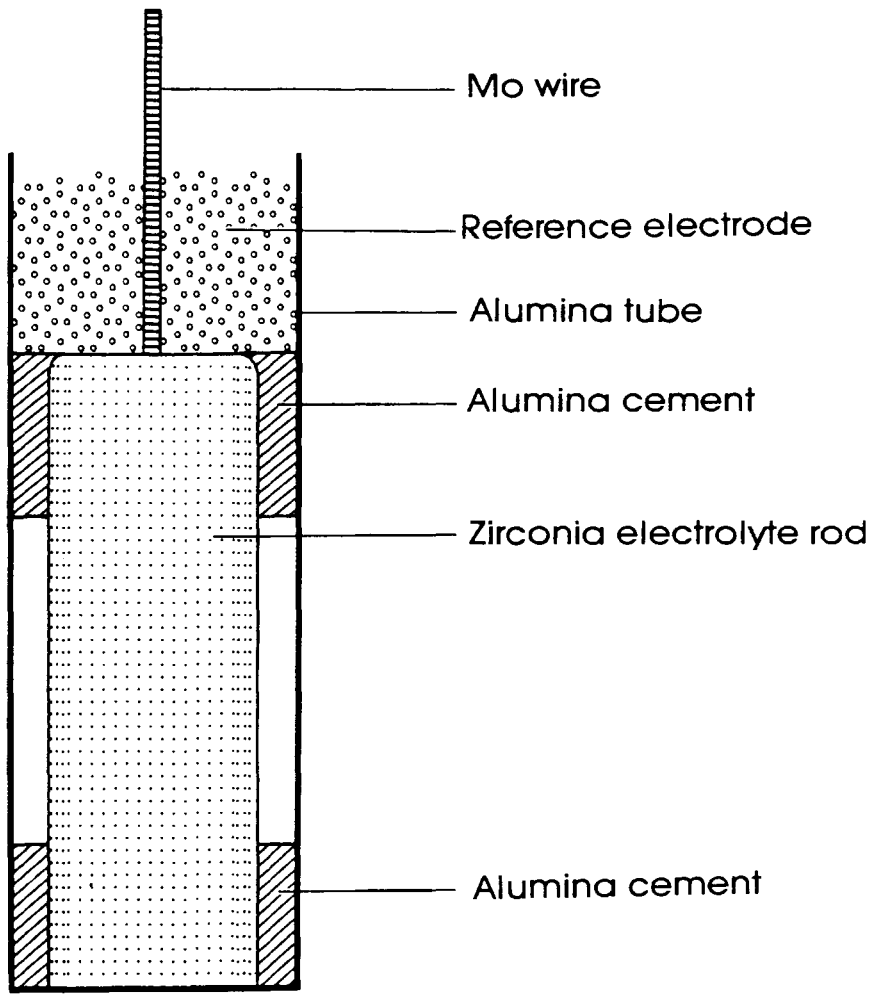

Figure 4.16 - *Schematic illustration of the alumina tube, containing the solid electrolyte rod and reference electrode.*

© University of Pretoria

UNIVERSITEIT VAN PRETORIA
UNIVERSITY OF PRETORIA
YUNIBESITHI YA PRETORIA

probe is fixed by the reaction between the SiO_2 in the $ZrSiO_4$ (painted onto the zirconia tube) and the silicon dissolved in the metal. Therefore, the measured EMF value is used to determine the oxygen potential. Consequently, the silicon content of the melt can be determined since the activity of SiO_2 in the $ZrSiO_4$ is known.

In this study, the MnO activities summarized in *Table 4.6*, were determined with the assumption that the P_e-value of the electrolyte is $3.0x10^{-17}$. This means that the P_e-value of the electrolyte decreased from $3.077x10^{-14}$ atm. to $3.0x10^{-17}$ atm. in the course of an oxygen measurement. It can be assumed that, if the n-type electronic conductivity of the zirconia layer of 300 μm thickness which contained MnO was lower than the remainder of the solid electrolyte, the n-type electronic conductivity of the electrolyte as a whole, would be determined by that of the 300 μm layer. It has been shown previously that, as the fraction cubic zirconia contained in a magnesia stabilized zirconia solid electrolyte increases at a specific temperature, the P_e-value of the electrolyte decreases accordingly[17]. Therefore, if it can be shown that the fraction cubic zirconia contained in the layer of the MnO containing solid electrolyte is higher than that of the remainder of the electrolyte, the conjecture that the P_e-value of the electrolyte decreased in the course of an oxygen measurement, would be valid.

In an effort to substantiate this premise experimentally, an attempt was made to determine the volume fraction of cubic zirconia present in an electrolyte which contained Mn and also in one which did not contain Mn. Because the zirconia layer which contained Mn was only 300 μm thick, it was not possible to estimate the fraction cubic zirconia in this layer. Therefore, experiments which simulated the conditions under which the Mn metal vapour reacted with the solid electrolytes, were performed. Two zirconia solid electrolyte rods of 20mm length, were ground to a particle size less than 100 μm. In the first experiment, the zirconia powder and Mn metal powder were put into an alumina crucible in the manner schematically shown

© University of Pretoria

UNIVERSITEIT VAN PRETORIA
UNIVERSITY OF PRETORIA
YUNIBESITHI YA PRETORIA

in *Figure 4.17 (a)*. The crucible was lowered into the heat zone of the furnace at 1873 K under an argon atmosphere, kept there for 20 minutes and rapidly raised to the upper part of the reaction tube where the temperature was approximately 373 K. The crucible and its contents cooled from 1873 K to a temperature of 673 K over a period of approximately 4 minutes, before it was removed from the reaction tube. In the following experiment, the same procedure was followed but no Mn metal was present, as shown schematically in *Figure 4.17 (b)*. The ZrO_2 powder of both experiments were subjected to X-Ray powder diffractometry to determine the volume fraction cubic zirconia contained in these samples[51][52][53]. The relative amount of cubic phase present was determined by the ratio of the diffraction intensities of cubic and monoclinic zirconia, as expressed in equation [4.8]:

$$X = \frac{I_c(111)}{I_c(111) + I_m(11\bar{1})} \qquad [4.8]$$

where $I_c(111)$ and $I_m(11\bar{1})$ denote the peak heights of the diffraction patterns of the (111) plane of cubic zirconia and the $(11\bar{1})$ plane of monoclinic zirconia respectively. The intensity ratio so obtained was converted to the volume fraction of cubic zirconia by the use of a calibration curve proposed by Nakamura and Moryia[52]. These results are summarized in *Table 4.10.*

Table 4.10 - *Phase composition of the zirconia solid electrolytes containing MnO, compared to that where MnO is absent*

ZrO_2 Electrolyte	**Cubic zirconia [%] (by volume)**
MnO present	83
MnO absent	51

© University of Pretoria

UNIVERSITEIT VAN PRETORIA
UNIVERSITY OF PRETORIA
YUNIBESITHI YA PRETORIA

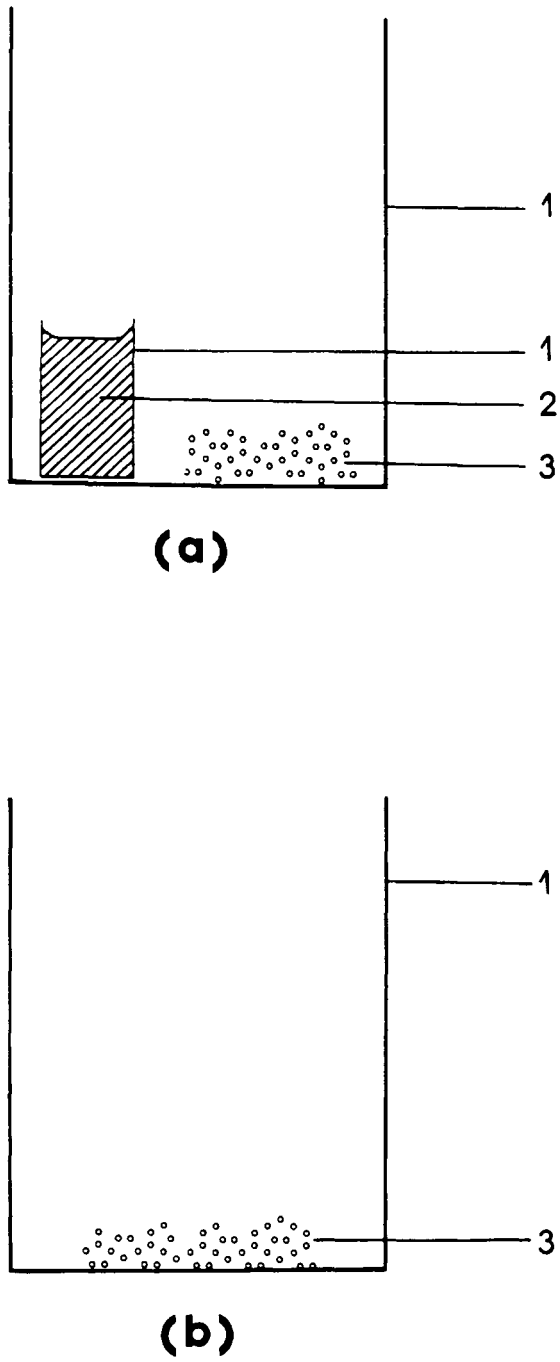

1. Al_2O_3 crucible
2. Mn metal
3. ZrO_2 powder

Figure 4.17 - *Schematic representation of the crucible assembly, used to establish the influence of MnO on the degree of stabilization of zirconia solid electrolytes*

© University of Pretoria

UNIVERSITEIT VAN PRETORIA
UNIVERSITY OF PRETORIA
YUNIBESITHI YA PRETORIA

From the results presented in *Table 4.10*, it is evident that the fraction cubic zirconia of the MnO containing solid electrolyte, is 83% compared to 51% of the electrolyte where MnO is absent. Therefore, it seems that the MnO stabilizes the cubic phase in these electrolytes. Consequently, the P_e-value of the solid electrolyte might have decreased indeed due to the fraction cubic zirconia which increased in the course of an oxygen measurement. However, it should be noted that the reduction and oxidation of Mn according to the reactions $Mn^{3+} + e^- = Mn^{2+}$ and $Mn^{2+} + h^{\cdot} = Mn^{3+}$, could also effect the ionic conductivity of the solid electrolyte. The possibility of this mechanism is not discussed because experimental evidence of the oxidation state of Mn in the ZrO_2 matrix is inadequate to confirm such an explanation.

Examples of the EMF recordings of sensors containing (Nb+NbO) and ($Cr+Cr_2O_3$) reference electrodes, are shown in *Figure 4.18 (a) and (b)* respectively. Four minutes elapsed after immersion into the melt, before a plateau was recorded with the (Nb+NbO) reference electrode. Because the sensor was kept for a minimum period of 3 minutes directly above the melt, temperature equilibrium should have been attained before immersion into the melt and therefore, a stable plateau should be recorded within 30 seconds after immersion into the melt. However, since the MnO content of the zirconia solid electrolyte increased as a function of time, the fraction cubic zirconia increased accordingly and therefore, the P_e-value decreased continuously during the 4 minute period before a stable plateau was recorded (*Figure 4.18 (a)*). The critical thickness of this ZrO_2 layer was probably in the range of 300 μm and consequently, any further increase in thickness would not affect the P_e-value. After a period of approximately 5 minutes however, the Nb/NbO reference electrode possibly started to polarize and therefore the cell potential decreased accordingly.

It should be noted that the cell potential of sensors containing ($Cr+Cr_2O_3$) reference electrodes reached a maximum approximately 2 minutes after immersion into the melt (*Figure 4.18 (b)*). This maximum cell potential probably did not represent a stable plateau, because the Cr/Cr_2O_3 reference electrode most probably polarized from the moment that the probe was immersed into the melt, since the difference between the oxygen partial pressure of the reference electrode and that of the melt was extremely large (*Figure 4.12*). Therefore, the cell potential recorded was the

© University of Pretoria

UNIVERSITEIT VAN PRETORIA
UNIVERSITY OF PRETORIA
YUNIBESITHI YA PRETORIA

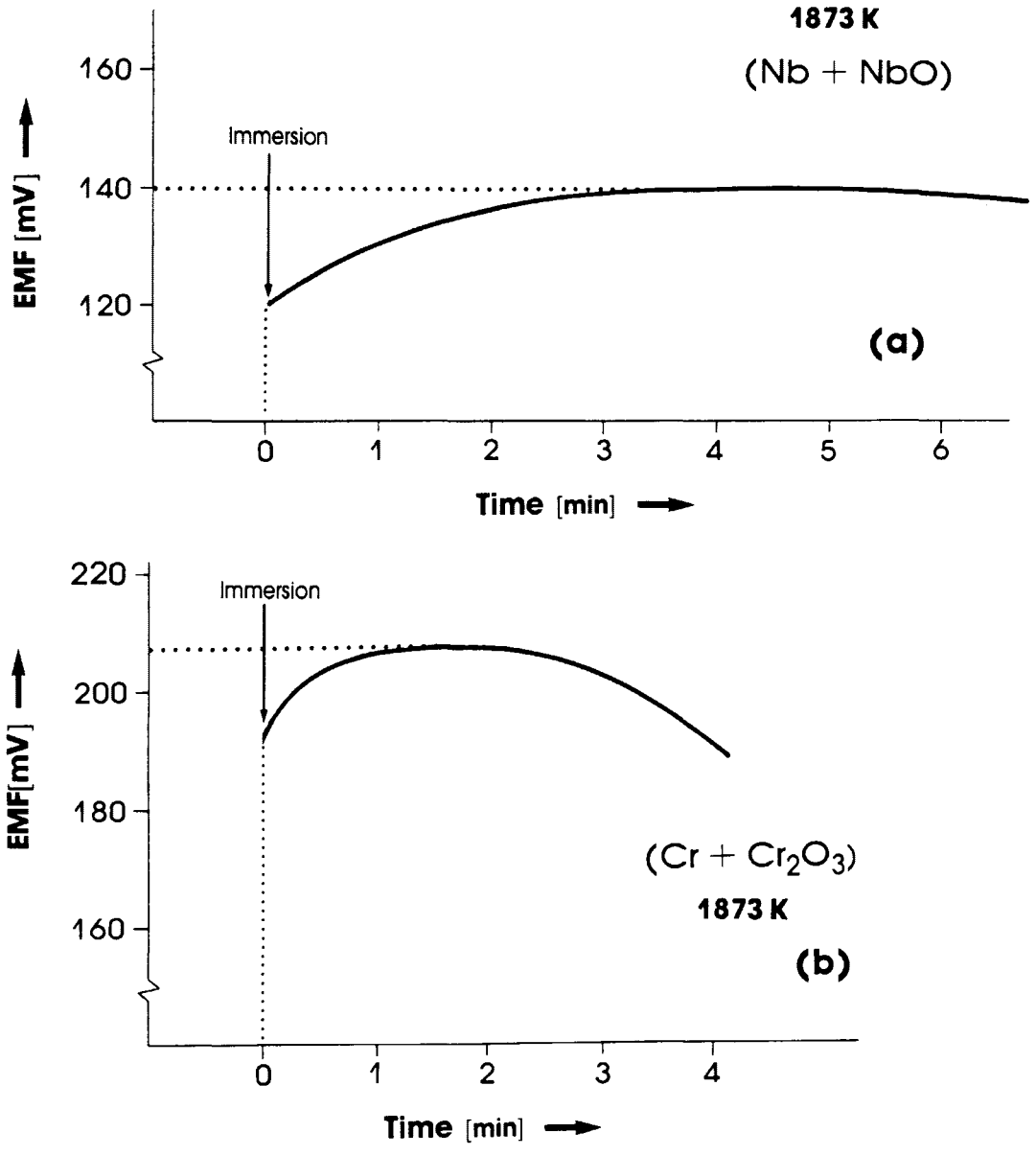

Figure 4.18 - *EMF recordings of oxygen probes containing (a) (Nb+NbO) and (b) ($Cr+Cr_2O_3$) reference electrodes, used for measurements in a ($MnO-SiO_2-MgO$)-slag at 1873 K.*

© University of Pretoria

result of a combination of the P_e-value which decreased and the Cr/Cr_2O_3 reference electrode which polarized. This assumption also explains the MnO activity of 0.22 determined with this probe (*Table 4.6*), because the EMF 'plateau' was probably much lower than the actual EMF (when polarization was absent).

This study has shown that magnesia stabilized zirconia electrolytes can not be used to determine the oxygen potential of manganese metal at 1873 K accurately and reliably, and therefore alternative solid electrolytes should be used. Schwerdfeger[54] used tubular yttria stabilised thoria solid electrolytes to measure oxygen activities in Mn melts which were in equilibrium with pure solid MnO at temperatures up to 1550 °C. These sensors were positioned directly above the crucible at room temperature and heated together with the melt at a rate of approximately 100 °C per hour to 1550 °C before immersion of the probe into the melt. Stable plateaus were recorded and therefore, clear evidence exists that the Mn metal does not react with yttria stabilised thoria solid electrolytes at temperatures up to 1550 °C. Consequently, it should be possible to use thoria solid electrolyte rods successfully in the plug-type oxygen probe which had been developed in this study. The crucible assembly, combined with the slag sampling quenching technique developed in this study, should therefore be used to measure the MnO activities at different compositions in $(MnO\text{-}SiO_2\text{-}MgO)$-slags. These measurements could be extended to determine the influence of different oxides such as CaO, Al_2O_3, Na_2O and CaF_2 on the thermodynamic behaviour of MnO in these slags at 1873 K.

© University of Pretoria

UNIVERSITEIT VAN PRETORIA
UNIVERSITY OF PRETORIA
YUNIBESITHI YA PRETORIA

CHAPTER 5

SUMMARY AND CONCLUSIONS

A plug type oxygen probe containing a magnesia stabilized zirconia rod, has been developed. The purpose of this cell design was to minimize polarization when employed at high temperatures in slag/metal systems of low oxygen potential. The accuracy and reliability of this probe was evaluated by determining the Cr activity in Fe-Cr alloys in equilibrium with pure Cr_2O_3 at 1873 K. The Fe-Cr alloy was stirred for at least 45 minutes before an EMF measurement was made in order to ensure that equilibrium between the Fe-Cr alloy and Cr_2O_3 was fully attained. The chromium activities deviate negatively from ideal Raoultian behaviour in the range 5 to 25 %Cr. It was possible to resolve the apparent differences in the chromium activities determined in this study and those found by previous investigators. A detail analysis of the experimental procedure followed by one of the previous researchers, indicated that an equilibration period of 5 minutes was insufficient if pure chromium is added to the alloy. The chromium activities obtained by another author by electrochemical means were recalculated by using the applicable P_e-value for the solid electrolyte which he used. These recalculated activities were in good agreement with those determined in the present study and the results re-emphasized he importance of the fact that the P_e-value of the solid electrolytes employed in oxygen probes should be known accurately if reliable oxygen activity measurements are to be made.

A crucible assembly, containing a Cr_2O_3 crucible and a Cr_2O_3 tube was designed to prevent direct contact between a (Cr_2O_{3sat})-slag and the oxygen probe. Both the Cr_2O_3 crucible and tube were manufactured in the laboratory using a cold pressing and sintering technique. The integrity of this cell design was evaluated by determining the chromium activity of an Fe-Cr alloy which was in equilibrium with a liquid

© University of Pretoria

UNIVERSITEIT VAN PRETORIA
UNIVERSITY OF PRETORIA
YUNIBESITHI YA PRETORIA

(CrO-SiO_2-CaO)-slag saturated with pure Cr_2O_3 at 1873 K. A visual examination of the crucible assembly and the oxygen probe, indicated that contact between the oxygen probe and liquid slag did not occur. Furthermore, the period required for equilibrium to be established between the slag and the metal was not affected adversely, although the slag-metal interface was smaller in this experimental set-up compared to the crucible assembly previously used (without a Cr_2O_3 tube).

The same type of crucible assembly was used for the determination of the activity of MnO in (MnO-SiO_2-MgO)-slags saturated with (MnO-MgO) solid solutions and in equilibrium with Mn at 1873 K. Magnesia crucibles and MgO tubes manufactured in the laboratory, satisfactorily contained the slag and metal at 1873 K. However, representative slag samples could not be taken in the course of an EMF measurement, and slag samples were obtained by using an alternative technique. In this technique, small MgO crucibles containing the slag and the metal, were equilibrated for a period of 60 minutes before the whole crucible with its contents was quenched to room temperature. The composition of the slag and the solid solution phases were determined with a microprobe, and the MnO activity of the slag was determined from the known activity-composition relations of the solid solution which was in equilibrium with the slag. These findings were in good agreement with the results of previous workers who employed different experimental techniques, indicating that this experimental technique to determine the activity of MnO is reliable and accurate. Furthermore, these results could also be used to determine the oxygen potential of the slag/metal system under investigation. Accordingly, the techniques used to determine the composition of the slag and solid solution phases pertaining at equilibrium, can be very elegantly utilized to evaluate the accuracy of the electrochemical technique to measure the oxygen activity in liquid slags of similar composition. The partial pressure of oxygen determined with the aid of electrochemical oxygen probes, can be compared to the values determined with this quenching and analyzing methods, since the molten slag is in equilibrium

© University of Pretoria

UNIVERSITEIT VAN PRETORIA
UNIVERSITY OF PRETORIA
YUNIBESITHI YA PRETORIA

with liquid Mn metal and the activity of the MnO in the melts have been established.

In the course of the electrochemical sensing of the oxygen potential of the (MnO-SiO_2-MgO)-slags which were in equilibrium with Mn metal and saturated with (MnO-MgO) solid solutions, the Mn vapour attacked the alumina cement which attached the oxygen probe to a molybdenum extension wire. The waterglass which served as binder for the Al_2O_3 powder, was replaced with mono aluminium phosphate and this cement performed satisfactorily. It was evident from the EMF recordings obtained in the (MnO-SiO_2-MgO)-slags with oxygen probes containing (Cr+Cr_2O_3) reference electrodes, that extensive polarization occurred. Therefore, a (Ta+Ta_2O_5) reference electrode, of which the oxygen potential is similar to that of the Mn/MnO system, was evaluated. However, it was shown that the formation of a liquid phase within this electrode at 1873 K, causes uncertainties in the oxygen potential of this electrode in the course of an electrochemical measurement.

(Nb+NbO) reference electrodes were also evaluated. Stable EMF plateaus were recorded in the (MnO-SiO_2-MgO)-slags, but these values were incorrect. SEM analysis of the solid electrolyte rods after use in the Mn melts, revealed that a layer of 0.3mm thickness of the solid electrolyte rod which was in contact with the melt, chemically reacted with the Mn. It is believed that the oxygen partial pressure at the electrolyte/melt interface was fixed by the reaction between the MnO present in the ZrO_2 grains and the Mn metal rather than by the slag/metal equilibrium. Furthermore, the MnO which penetrated the ZrO_2 grains, stabilized the cubic phase in the solid electrolyte. This increased the ionic conductivity of the electrolyte and explains the fairly high EMF values measured. Evidently, zirconia solid electrolytes can not be used for measurements in systems where Mn metal is present at 1873 K. However, previous workers have shown that thoria solid electrolyte tubes are impervious to Mn metal at temperatures as high as 1823 K. Therefore, thoria solid electrolyte tubes could be used to measure MnO activities in (MnO-SiO_2-MgO)-slags

© University of Pretoria

by using the same experimental set-up developed in this study, where direct contact between the sensor and the slag is prevented.

In conclusion: Reliable and accurate oxygen activities have been determined in the Fe-Cr-O system at 1873 K and therefore, this study has shown that the experimental difficulties inherent to the electrochemical technique, when used at 1873 K for the determination of the oxygen potential of different slag/metal systems, can be conquered. However, the kinetic and thermodynamic behaviour of the slag/metal system should be analyzed carefully in order to develop an optimum experimental design, which can be used to obtain accurate and reliable results.

© University of Pretoria

UNIVERSITEIT VAN PRETORIA
UNIVERSITY OF PRETORIA
YUNIBESITHI YA PRETORIA

APPENDIX 1

Example of a calculation to determine the height of a Cr-Cr_2O_3 pellet, used as reference electrode in a plug-type oxygen probe

In the ceramic combination of a cylindrical ZrO_2 electrolyte plug, fitted into the open end of an insulating Al_2O_3-tube together with a Cr-Cr_2O_3 pellet, oxygen may occur due to the condition

$$j_{O_2} = j_{O^{2-}(ZrO2)} = -2j_{e(Al2O3)} \qquad [A]$$

Therefore with respect to cell design it has to be ensured that

$$\frac{K_{(Al_2O_3)} \cdot t_{e(Al_2O_3)}}{l_{Al_2O_3}} \cdot 2l_{ref} < \frac{K_{(ZrO_2)} \cdot t_{e(ZrO_2)}}{l_{ZrO_2}} \cdot d_{ZrO_2} \qquad [B]$$

where $k_{(Al2O3)}$ = conductivity of pure Al_2O_3 [$ohm^{-1}.cm^{-1}$]

$l_{(Al2O3)}$ = thickness of Al_2O_3-tube [cm]

l_{ref} = height of the Cr-Cr_2O_3 reference electrode [cm]

$t_{e(Al2O3)}$ = the electronic transport number of the Al_2O_3 tube

$k_{(ZrO2)}$ = conductivity of ZrO_2 electrolyte [$ohm^{-1}.cm^{-1}$]

$t_{e(ZrO2)}$ = the electronic transport number of the ZrO_2 electrolyte

$l_{(ZrO2)}$ = length of the ZrO_2 electrolyte rod [cm]

$d_{(ZrO2)}$ = diameter of the ZrO_2 electrolyte rod [cm]

t_e of the solid electrolyte is related to the P_{O2} and P_e-value of the electrolyte in the following manner[23]:

© University of Pretoria

UNIVERSITEIT VAN PRETORIA
UNIVERSITY OF PRETORIA
YUNIBESITHI YA PRETORIA

$$t_e = 1 - \frac{1}{1 + \left(\frac{P_{O_2}}{P_e}\right)^{-\frac{1}{4}}} \qquad [C]$$

The partial pressure of oxygen of the Cr/Cr_2O_3 reference electrode is $7.6x10^{-12}$ atm. at 1873 K[24] and therefore, the values of the different constants depicted by equation [B] under these conditions, are summarized as follows:

According to Pappis et al.[55], pure polycristalline Al_2O_3 is predominantly electronic conductive: $t_{e(Al2O3)} = 1$ and $k_{(Al2O3)} = 5x10^{-5}$.

The P_e-value of the 9 mol% MgO stabilized ZrO_2 electrolyte used in this study is $3.077x10^{-14}$ atm at 1873 K[17] and therefore,

$$t_e(ZrO_2) = 0.201 \quad \text{(equation [C])}.$$

The conductivity $K_{(ZrO2)}$ of a 6 mol% MgO stabilized ZrO_2 zirconia solid electrolyte determined by Janke et al.[56] is assumed to be applicable to the 9 mol% MgO stabilized ZrO_2 electrolyte used in this study. Therefore, $K_{(ZrO2)} = 0.13$.

When a ZrO_2 solid electrolyte rod, diameter 0.4cm and length 1.0 cm and a $Cr\text{-}Cr_2O_3$ reference electrode, height 1.0 cm, are build into the Al_2O_3 insulation tube (wall thickness 0.05 cm), these dimentions are described as follows:

$$l_{(Al2O3)} = 0.05$$
$$l_{(ZrO2)} = 1.0$$
$$d_{(ZrO2)} = 0.4$$
$$l_{ref} = 1.0$$

The requirements set by equation [B] are satisfied when these dimensions are used in the calculation ($0.002 < 0.01$) and therefore the height of the Cr/Cr_2O_3 reference electrode should be less than 10mm to minimize polarization.

© University of Pretoria

UNIVERSITEIT VAN PRETORIA
UNIVERSITY OF PRETORIA
YUNIBESITHI YA PRETORIA

REFERENCES

1. J.P. Schade: *Stahl und Eisen*, 1989, vol. 109, pp. 539-42.

2. E.B. Pretorius: *Ph.D Thesis*, The Pennsylvania State University, U.S.A, 1989.

3. K.P. Abraham, M.W. Davies and F.D. Richardson: *Jnl. Iron Steel Inst.*, 1960, vol. 196, pp. 82-89.

4. S.R. Mehta and F.D. Richardson: *Jnl. Iron Steel Inst.*, 1965, vol. 203, pp. 524-28.

5. N.Y. Toker: *Ph.D Thesis*, The Pennsylvania State University, U.S.A., 1978.

6. H.T. Tsai: *Ph.D Thesis*, The Pennsylvania State University, U.S.A, 1981.

7. D. Janke: *Arch. Eisenhüttenwes.*, 1983, vol. 54, pp. 250-66.

8. M. Iwase, E. Ichise, N. Yamada and K. Nishida: *Trans. ISS/AIME*, 1984, vol. 4, pp. 47-53.

9. M. Iwase, N. Yamada, K. Nishida and E. Ichise: *Trans. ISS/AIME*, 1984, vol. 4, pp. 69-75.

10. M.J.U.T. Van Wijngaarden and R.J. Dippenaar: *J. S. Afr. Inst. Min. Metall.*, 1986, vol. 86, pp. 443-53.

11. M.J.U.T. Van Wijngaarden, R.J. Dippenaar and P. M. van den Heever: *J. S. Afr. Inst. Min. Metall.*, 1987, vol. 87, pp. 269-78.

12. D. Janke and H. Richter: *Arch. Eisenhüttenwes.*, 1979, vol. 50, pp. 93-99.

13. A.R. Romero, J. Härkki and D. Janke: *Steel Res.*, 1986, vol. 57, pp. 636-44.

14. M. Iwase and A. McLean: *Solid State Ionics*, 1981, vol. 5, pp. 571-74.

15. M.J.U.T. Van Wijngaarden and R.J. Dippenaar: *Iron and Steelm.*, 1988, vol. 15, pp.49-56.

© University of Pretoria

UNIVERSITEIT VAN PRETORIA
UNIVERSITY OF PRETORIA
YUNIBESITHI YA PRETORIA

16. M.J.U.T. Van Wijngaarden, J.M.A. Geldenhuis and R.J. Dippenaar: *Iron and Steelm.*, 1988, vol. 15, pp. 35-44.

17. M.J.U.T. Van Wijngaarden, J.M.A. Geldenhuis and R.J. Dippenaar: *Jnl. Appl. Electrochem.*, 1988, vol. 18, pp. 724-30.

18. M.J.U.T. Van Wijngaarden, J.M.A. Geldenhuis and R.J. Dippenaar: *J. S. Afr. Inst. Min. Metall.*, 1988, vol. 88, pp. 265-71.

19. R.J. Fruehan: *Trans. AIME*, 1969, vol. 245, pp. 1215-18.

20. M. Heinz: *Ph.D Thesis, Universität Clausthal*, West Germany, 1987.

21. C. Wagner: *Z. Physic. Chem.*, 1933, Abt. B, vol. 21, pp. 25-41.

22. H. Schmalzried: *Z. Physic. Chem.*, Frankfurt, 1963, vol. 38, pp. 87-102.

23. H. Schmalzried: *Z. Elektrochem.*, 1962, vol. 66, pp. 572-76.

24. J.F. Elliott and M. Gleiser: *Thermochemistry for Steelmaking*, Addison Wesley Publishing Co., 1969, vol. 1.

25. D. Janke: *Stahl und Eisen*, 1983, vol. 103, pp. 29-30.

26. M. Heinz, K. Koch and D. Janke: *Steel Res.*, 1989, vol. 60, pp. 246-54.

27. T. Oishi, T. Goto, Y. Kayara, K. Ono and J. Moriyana: *Metall. Trans. B*, 1982, vol. 23B, pp. 423-30.

28. J.E. Stukel and J. Cocubinsky: *Jnl. of Metals*, 1954, nr. 3, pp. 353-56.

29. E.T. Turkdogan: *Jnl. Iron Steel Inst.*, 1956, vol. 182, pp. 74-79.

30. S.R. Simeonov and N. Sano: *Trans. ISIJ*, 1985, vol. 25, pp. 1116-21.

31. B.E. Vassiliou: *Trans. Brit. Ceram. Soc.*, 1957, vol. 56, pp.516-18.

32. N. Toker and L.S. Darken: *Geochim. Cosmochim. Acta*, 1975, vol. 39, pp. 847-52.

© University of Pretoria

UNIVERSITEIT VAN PRETORIA
UNIVERSITY OF PRETORIA
YUNIBESITHI YA PRETORIA

33. A. Muan: *Mintek 50, Proc. of the Int. Conf. on Mineral Science and Technology*, Ed. L.F. Haughton, Council for Mineral Technology, Randburg, South Africa, 1985, vol. 2, pp. 897-904.

34. H. Chen and J. Chipman: *Trans. ASM*, 1947, vol. 38, pp. 70-113.

35. L. Coudurier, D.W. Hopkins and I. Wilkomirski: *Fundamentals of Metallurgical Processes*, Pergamon Press, New York, 1985, p. 94.

36. R.J. Fruehan, L.J. Martonic and E.T. Turkdogan: *Trans. TMS/AIME*, 1969, vol. 245, pp. 1501-09.

37. W.A. Fischer and C. Pieper: *Arch. Eisenhüttenwes.*, 1973, vol. 44, pp. 251-59.

38. C. Wagner: *Thermodynamics of Alloys*, Addison Wesley Publishing Co., Reading, Mass., 1962. (Cited from ref.39).

39. C.H.P. Lupis and J.F. Elliott: *Trans. Am. Inst. Min. Metall. Engrs.*, 1965, vol. 233, pp. 829-30.

40. G.K. Sigworth and J.F. Elliott: *Metal Science*, 1974, vol. 8, pp. 298-310.

41. C.H.P. Lupis and J.F. Elliott: *Acta Met.*, 1966, vol. 14, pp. 529-38.

42. I. Barin and O. Knacke: *Thermochemical Properties of Inorganic Substances*, Berlin/Heidelberg/New York and Düsseldorf, 1973.

43. N.Y. Toker, L.S. Darken and A. Muan: *Metall. Trans. B*, 1991, vol. 22B, pp. 225-32.

44. F.P. Glasser and E.F. Osborn: *Jnl. Am. Ceram. Soc.*, 1960, vol. 43, pp. 132-40.

45. R.C. Weast (Ed): *Handbook of Chemistry and Physics*, 1983, vol. 64, CRC Press, Inc.

46. F.P. Glasser: *Am. J. Sci.*, 1958, vol. 256, pp. 398-412.

47. H. Jehn and E. Olzi: *Jnl. Less-Common Metals*, 1972, vol. 27, pp. 297-309.

© University of Pretoria

UNIVERSITEIT VAN PRETORIA
UNIVERSITY OF PRETORIA
YUNIBESITHI YA PRETORIA

48. T.B. Massalski (Ed): *Binary Alloy Phase Diagrams*, Am. Soc. for Metals, Metals Park, Ohio, 1987, vol. 2.

49. D. Janke: *Private Communication*, 1991.

50. M. Iwase: *Scand. J. Metallurgy*, 1988, vol. 17, pp. 50-56.

51. M. Iwase, E. Ichise, M. Takeuchi and T. Yamasaki: *Trans. Japan. Inst. Metals*, 1984, vol. 25, pp. 43-52.

52. H. Nakamura and T. Moriya, *Solid State Ionics*, 1983, vol. 9/10, pp. 1257-62.

53. D.L. Porter and A.H. Heuer: *Jnl. Am. Ceram. Soc.*, 1979, vol. 62, pp. 298-305.

54. K. Schwerdtfeger: *Trans. AIME*, 1967, vol. 239, pp. 1276-81.

55. J. Pappis and W.D. Kingery: *Jnl. Appl. Ceram. Soc.*, 1961, vol. 44, pp. 459-64.

56. D. Janke and W.A. Fischer: *Arch. Eisenhüttenwes.*, 1977, vol. 46, pp. 311-18.

© University of Pretoria

UNIVERSITEIT VAN PRETORIA
UNIVERSITY OF PRETORIA
YUNIBESITHI YA PRETORIA

VITA

Jacobus Marthinus Andreas Geldenhuis was born in Alberton, Republic of South Africa, on April 28, 1961. He graduated from Pretoria Tuine High School in 1979. He was awarded a Bachelor of Engineering degree from the University of Pretoria in June 1985. In January of the following year, he was awarded a Bachelor of Engineering Honours degree in the Department of Materials Science and Metallurgical Engineering at the same University.

In May 1988, he earned a Master of Engineering (Metallurgical) degree at the University of Pretoria, and then began his studies leading to the Ph.D degree. From November 1986, he has been employed by Iscor Ltd. He is a registered professional engineer at the South African Engineering Council, and is a member of both the South African Institute of Mining and Metallurgy, and the Iron and Steel Society of AIME.

© University of Pretoria